Disturbed soil properties and geotechnical design

Frontispiece

$q/p = \eta$ Stress obliquity

$\eta = 3$ Open cracking $\sigma'_a < \sigma'_r$

$v_\lambda = v + \lambda \ln p'$

Herrick's liquefaction; fluidised rubble, hydraulic fracture, and piping

Watertight slip planes

Critical states
$\eta = M$
C

Plastic compression of original Cam Clay paste

Optimum compaction

Over-compacted

High liquidity

Low pressure   Dense Γ v_λ Loose   High pressure

$(\lambda - \kappa)$

Hazen's liquefaction

$\eta = 1.5$ Spalling $\sigma'_a < \sigma'_r$

'Dry' side ⟵ Critical states ⟶ 'Wet' side

(v_λ, η) *map of disturbed saturated soil behaviour*

Disturbed soil properties and geotechnical design

Andrew Schofield

Dedication

For Margaret

Foreword

In my final year as an undergraduate at Oxford University, I undertook a project on the warping of asymmetrical steel beams with Dr Edgar Lightfoot. I took no formal lectures on soil mechanics, although Dr Lightfoot also gave a few lectures on slip lines and bearing capacity within an optional 'speciality' paper on civil engineering. He also gave me career advice along the lines that 'there is this new theory called critical state soil mechanics, which seems to be worth investigating'. I duly bought a copy of Schofield and Wroth's (1968) book on that subject, and so began my education in soil mechanics. I subsequently studied for my PhD with Professor Peter Wroth, and cut my teeth as a lecturer at Cambridge University in the group then headed by Professor Andrew Schofield. It is therefore with humility, and a sense of the wheel having turned full circle, that I find myself writing a foreword to this 'retrospective' new book by Andrew; indeed, I have a sense of being back under examination, wondering what grade my former professor will assign.

Much of this book describes the developments leading to the original Cam Clay model, focusing on fundamentals of the shearing of soil. The aim is to lay the groundwork of understanding that should form the basis of geotechnical design, guiding engineers towards the class of behaviour to be expected under different combinations of effective stress and water content. There are a few equations, but simple ones; much greater challenge rests in the arguments put forward regarding soil behaviour and the intellectual effort needed to keep pace with the author. After the Special Lecture that he delivered at the 2001 International Society of Soil Mechanics and Geotechnical Engineering in Istanbul, he commented that it was 'heard without comprehension'. The lack of comprehension was not to do with the complexity of concepts or algebra, but with grasping the underlying message and appreciating the gap between the understanding that many experienced academic and practising engineers do indeed have, and the misleading language and teaching that pervades much education in soil mechanics.

The book is divided into six chapters, which progress from the simple planar sliding of soil towards plastic design in geotechnical engineering. But Andrew Schofield is not constrained by sequence, and rather than write a conventional textbook, he had in mind the sort of book that 'engineers might read on a flight and leave on their office coffee tables'. The 'coffee table' image came from a reviewer of the proposed book, perhaps meant as disparaging, but is excellent advice here: the book *invites* reading at a single sitting, both because it is intensely interesting, and because of the author's global approach, with much cross-referencing – across the centuries as well as between chapters. After reading, it is a book to be left readily available for frequent dipping, both for the pleasure in

the historical anecdotes spread across the last 400 years and to reinforce the fundamental understanding of soil behaviour conveyed in the book.

The frontispiece illustration is the lynch-pin to the ideas the author wishes to convey, and is referred to throughout this book. Heroes (Coulomb, Hvorslev and Taylor) and villains (Terzaghi in particular) are identified in Chapter 1, with detailed discussion of the nature of friction, the role of interlocking, and the misinterpretation of Hvorslev's empirical envelope of peak strengths as indicating true cohesion. The second chapter focuses on the critical state, correcting Casagrande's critical void ratio to allow for the effective stress level, and liquefaction, contrasting extreme forms related to ultra-high void ratio, or to near-zero effective stress. Historical anecdotes replace the usual glossy pictures of a coffee table book, and suitably leaven the technical arguments, and one of the many rewards for those who read the book will be the connection described here between the latter form of liquefaction and the 17th-century poet Herrick.

There are frequent (positive) quotations from Terzaghi's writings in the literature, but inevitably for someone so fond of dogma it is not difficult to find negative examples. His assertion of cohesive bonding between soil grains, and rejection of the usefulness of Rankine's limiting stress states, are two such examples that are discussed at some length in Chapters 3 and 4. In defence of his (c, ϕ) strength model, Terzaghi did advocate that clay should be tested 'under conditions of pressure and drainage similar to those under which the shear failure is likely to occur in the field'. However, that caveat seems to have been overlooked and, even today, the c–ϕ strength model is taught widely and used inappropriately. Current teaching is littered with calculations where the effective stress differs significantly from the conditions under which the strength measurements used to generate the c–ϕ fit were derived. Modern teaching often applies such a model to bearing capacity analyses on sand, without adjustment for the resulting high stresses, or to the stability of slopes and cuts, where pore pressure dissipation would destroy any apparent c. Students who understand soil strength according to Andrew's approach are wise to these dangers. A modest ambition for the present book might be to see the words 'cohesion' and 'adhesion' excised from our soil mechanics vocabulary, replacing them with, respectively, 'shear strength' (at a given water content and effective stress level) and, on the rather rare occasions where it is appropriate, 'cementation'.

The basis of the original Cam Clay model, including its background in the theory of plasticity and the experimental evidence for the internal plastic work, is described in Chapter 5. Limitations of this simple model in terms of anisotropy, soil sensitivity and cyclic loading are readily acknowledged. As a basic framework for teaching, however, the model still has much to offer, and it is refreshing to be taken through the careful experimental data on reconstituted clays on which it is based, and the (now classic) examination questions from the Cambridge Tripos of nearly 40 years ago. Once armed with the simple concept of wet and dry of the critical state line, students will understand whether a sample will wish to contract or dilate, whether pore pressures generated during undrained shearing will tend to the positive or negative, and conditions where ductile plastic deformation might change to brittleness and fracture. The ability of the model to quantify these states is immediately appealing to modern students, rather than them having to digest purely qualitative explanations.

Andrew Schofield deserves to be regarded as one of the geniuses of soil mechanics of the latter half of the 20th century. His Fellowship of the Royal Society is based on his two remarkable contributions of original Cam Clay and the promulgation of centrifuge modelling in geotechnical engineering beyond its origins in Russia. It is appropriate, therefore, that the final chapter in this book is devoted to the application of the principles of critical state soil mechanics by means of centrifuge experiments conducted under conditions of stress similitude.

This is a rewarding book, full of insights, both technical and personal. It reinforces ideas described in the original Schofield and Wroth book *Critical State Soil Mechanics*, and in Schofield's 1980 Rankine Lecture. For the unconverted, it is an invitation to re-examine your basic understanding of soil behaviour. For the converted who might be tempted to dismiss the book too lightly, it is a call to ensure that our teaching, and the vocabulary and nomenclature we use in describing strength models for soil, reflect accurately the underlying concepts.

Professor Mark F. Randolph
The University of Western Australia, Perth

Preface

This book originated with seminars that I gave in November 1999 at Georgia Institute of Technology in Atlanta. I outlined their intended content in the following three paragraphs:

> *There is a fundamental error in the Mohr–Coulomb equation. The proposition that opens Coulomb's 1773 Essay supposes that a pier is cut by an inclined plane in such a way that the two portions are connected at the cut by a given cohesion, while all the rest of the material is of perfect strength. The pier is loaded by a weight, which makes the upper portion of the pier slide along the inclined plane. Coulomb resolves the load components along and normal to the inclined plane and determines the inclination of the plane for which cohesion and friction combine to give the greatest load. The same result is obtained if Mohr's circles have a limiting envelope with constant cohesion and friction. The error in this simple analysis is that it omits a component of strength that is due to 'interlocking'.*
>
> *Taylor in 1948 reported shear box tests on dense Ottawa standard sand. When the upper part of his shear box was displaced laterally by dx it rose up vertically by dy as his dense sand dilated. This is the phenomenon that he called 'interlocking'. Peak strength τ in dense sand occurred at a point where dy/dx was a maximum. Taylor calculated what happened to the work $\tau\, dx$ at peak strength. Part went into friction $\mu\sigma'\, dx$ and part went to lift the weight $\sigma'\, dy$ on the normal load hanger. This led to friction and interlocking components in the peak strength of dense sand $(\tau/\sigma') = (\mu + (dy/dx))$. The Mohr–Coulomb equation omits interlocking. After the 1948 publication of Taylor's book, Terzaghi should have reviewed his interpretation of data of load-controlled drained tests of saturated reconstituted clay soil in a shear box. Terzaghi and Hvorslev had fitted peak strength data to a line with 'true' friction and 'true' cohesion, but there was an increase of water content in the region of failure and hence a volume increase. This effect is found both in laboratory shear box tests, and in slickenside gouge material in failure planes in the field. Terzaghi and Hvorslev did not have a component of peak strength due to interlocking, hence part of the strength they attributed to bonds among fine soil grains was not due to 'cohesion' but to the high relative density of stiff clay soil.*
>
> *The title to Coulomb's Essay considers static problems that have solutions by calculus (which he calls 'the rules of minimum and maximum'), but which take no account of strain boundary conditions. The error is not that a straight Mohr–Coulomb envelope should be curved but that it contradicts the test data that Coulomb himself published in his 1773 paper; for him, clay such as Hvorslev*

tested can have no cohesion. The original Cam Clay (OCC) model is just dust and water with no chemistry and it shows the 'apparent cohesion' of clay. Many other soil models have been proposed and used in code calculations, and geotechnical centrifuge model test data are used to validate them.

In January 2000 I made a proposal to the publisher Thomas Telford for a book as described in the following three paragraphs:

My experience of attempting to explain Terzaghi's 'Mohr–Coulomb' error, Schofield (1998a, b and c, 1999), shows that a simple, short and readable book is needed. This proposal is for a 150-page book introducing and updating critical state soil mechanics, the original Cam-Clay model, and geotechnical centrifuge testing. Fundamental soil mechanics needs review because Coulomb (1773) made a simple fundamental error. When he considered failure on an inclined plane he assumed that the slip direction was the same as the direction of the plane. This is true only if shear failure takes place at constant volume, as in undrained shear tests, but in general there is a volume change during shear strain of any aggregate of hard particles. Taylor (1948) tested dense sand in a drained shear box and in addition to slip by an amount x in the direction of the plane found what he called 'interlocking'. Dense sand grains rose up to pass each other, and the distance y between the upper and the lower halves of his shear box increased. Taylor's analysis showed that the peak strength of the sand was equal to a combination of an angle of friction (the angle of repose), plus a term (dy/dx) for interlocking which Coulomb never considered. When Hvorslev (1937), working as Terzaghi's research student, made shear box tests on stiff clay in a drained shear box, he found an increase in water content in the vicinity of the slip plane, as is also found on slickenside failures in the field. The thickness of a slickenside increases, so there is interlocking. Terzaghi and Hvorslev analysed their data in terms of Coulomb's 'true cohesion and friction' without considering interlocking. Mistaking interlocking for cohesion, they attributed peak strengths of their stiff reconstituted clay soil to surface chemistry among clay soil grains.

I conceived an ideal soft cohesionless soil that I called Cam-Clay, Roscoe and Schofield (1963), as a paste of frictional interlocking fine cohesionless soil grains. It behaves like data of reconstituted soil on the wet side of critical states; hence no cohesion need be considered in any newly disturbed soil, including the dry side either. Terzaghi failed to appreciate that peak strength is due to soil compaction. The physical phenomenon of peak strength is not chemical but geometrical. Values of soil 'cohesion and friction' cannot characterize disturbed soil compacted in road formations or in embankment dams or in fill behind retaining walls. Coulomb himself in his earth pressure calculation states in three places in his Essay that newly remoulded soil has no cohesion and so avoids this error.

Schofield and Wroth (1968), though widely quoted, is little understood. What was described in 1968 as 'the inter-relation of concepts, the capacity to create new types of calculation, and the unification of the bases for judgment' was extended in Schofield (1980) and there is no book available anywhere that correctly clarifies Terzaghi's fundamental error.

The Shorter Oxford English Dictionary has several definitions of what is meant by the word *genius*, of which the earliest, dated 1513, is '*the tutelary god or attendant of a place, institution etc.*' and the latest, dated 1749 is '*a native intellectual power of an exalted type*'. About the time of my seminars and of my proposal for a book, Goodman's (1999) biography of Terzaghi was published, with an opening chapter titled 'The Roots of Genius' that considers the roots of Terzaghi's genius. His insight into the effective stress principle and his founding of the International Society of Soil Mechanics and Geotechnical Engineering (ISSMGE) made Goodman and Skempton and many others see him as the genius of 20th-century soil mechanics. He taught that soil has Mohr–Coulomb strength (c, ϕ) on slip planes, and that drained shear box tests of clay in Vienna by his research student, Hvorslev, had found true (c, ϕ) values under well-defined effective stress conditions. However, I was surprised by an anecdote that Goodman related, that, as a Harvard professor, Terzaghi prevented and delayed publication of a textbook by Taylor, an assistant professor at MIT, until his own textbook could be published (Terzaghi and Peck, 1948, referred to below as T&P, and described by Goodman as '*the main pillar of geotechnical education*'). Goodman's anecdote, and my high regard for Taylor's insight that part of the peak strength of dense sand called *interlocking* is due to volume increase during shear distortion, led me to reassess Harvard soil mechanics teaching and to offer to give the Istanbul ISSMGE Special Lecture (Schofield, 2001), which is the basis for this book. In preparing that lecture I learned that I was wrong to suppose that Coulomb did not consider interlocking. Indeed, at the start of the 18th century (300 years before Goodman's book), Amontons (1699) proposed a theory that rough asperities on a slip plane are the cause of sliding friction. Since slip planes are observed at failure of soil, Coulomb's soil mechanics started with a reasonable suggestion that the strength of soil on such planes must involve a combination of Amontons' friction plus some cohesion. Although the asperity theory of friction was discarded early in the 19th century, the 18th-century slip plane approach was retained in Mohr–Coulomb strength theory; however, slip plane friction became linked with energy dissipation in sliding rather than with work done to surmount asperities. The theory is universally taught as the basis of geotechnical design and of studies that range from earth science and rock mechanics to bulk solids handling and powder technology. This book will explain how Mohr–Coulomb theory is in error; an Istanbul lecture slide made a statement that I justify in this book, that

> *Terzaghi and Hvorslev wrongly claimed that true cohesion and true friction in the Mohr–Coulomb model fits disturbed soil behaviour. Geotechnical practice using Mohr–Coulomb to fit undisturbed test data has no basis in applied mechanics. Critical state soil mechanics offers geotechnical engineers a basis on which to continue working.*

Roscoe, Schofield and Wroth (1958) took an approach to soil that treated it as an aggregate of stressed grains in which energy is dissipated during shear distortion by *internal friction*. Our critical state (CS) hypothesis has stressed aggregates of grains yielding on test paths, with changes of stressed packing that lead to ultimate steady CS shear flow. Roscoe and Schofield's original Cam Clay (OCC) model saw soil approaching CS as contractive material with a combination of plastic compression

and distortion. Cambridge undergraduates studied the OCC model while studying structural plasticity, and before using slip planes in geotechnical analysis. In this book, I will reinterpret dense clay strengths as the sum of internal friction and Taylor's interlocking (Schofield, 1998a, 1999), rather than Terzaghi's sum of true friction and cohesion, and I will reassess Casagrande's liquefaction. The error of Harvard soil mechanics teaching on Mohr–Coulomb failure criterion and on contractive soil has been plain to see for 40 years in Figs 52 and 63.

I met plastic design of structures in lectures by Professor J. F. Baker in the first year of my Cambridge University course in 1948, and I met soil mechanics in final-year lectures by Roscoe in 1950. After graduating in 1951, I worked as a junior engineer of Scott & Wilson, consultants to the Nyasaland Protectorate (now Malawi), on low-cost road design and pavement materials location (Schofield, 1957), under a partner, Henry Grace, who had been a pupil first at Bristol University under Baker and then at Harvard University. Roscoe wrote to ask me to become his research student at Cambridge University. I returned from Africa in 1954 with confidence both in plastic design methods and in T&P soil mechanics. My studies led me to OCC, to geotechnical centrifuge model tests, and to ideas on cohesion and liquefaction that differ from Terzaghi and Casagrande, two acclaimed professors at Harvard University. I have tried to write this book using few equations, in such a way as to explain to Henry Grace (were he still alive) how Taylor's insight at MIT changes soil mechanics. A reader can find more words and equations in my Roscoe and Schofield (1963) paper and in my book (Schofield and Wroth, 1968), published with my colleagues and friends nearly 40 years ago.

While I am entirely responsible for the views expressed here, many students and colleagues with whom I worked have helped me to understand soil mechanics over these years, and in particular I thank Dave White for reading through a final draft of this book, and Mark Randolph for writing a foreword to it. Stuart Haigh (2002) (who as a student heard my final lectures) stayed to test models as a research student, and has worked from a desk next to mine in the final months of my work on this book. He not only read through the book but also worked out the examples in Chapter 5 and drew Figs 56 to 60, so a special thank you is due to him.

Since our marriage in 1961, my wife Margaret has continued to encourage me over 44 years in which I have developed OCC and centrifuge tests, into the present years of retirement in Cambridge in which (with her support) I have completed this book. I dedicate this book to my beloved wife.

<div align="right">

Andrew N. Schofield
http://www2.eng.cam.ac.uk/~ans/ans1.htm

</div>

Nomenclature

Abbreviations

ANS&A	Andrew N. Schofield & Associates Ltd
BRS	Building Research Station (now Building Research Establishment, BRE)
CS	critical state at which an aggregate of grains can flow steadily
CVR	critical voids ratio (an early name for CS)
ESB	Empire State Building
FE	finite element, in a computation to solve a problem
ISSMFE	International Society of Soil Mechanics and Foundation Engineering (now International Society of Soil Mechanics and Geotechnical Engineering, ISSMGE)
LCPC	Laboratoire Central des Ponts et Chausées
NCL	normal compression line
OCC	original Cam Clay
OCR	over-compression ratio
PPT	pore pressure transducer
SOED	*The Shorter Oxford English Dictionary*
SRC	Science Research Council
SSA	Simple Shear Apparatus
T&P	Terzaghi and Peck (1948)
TC2	Technical Committee 2 of the ISSMGE
USACE	US Army Corps of Engineers
WES	Waterways Experimental Station
WWII	World War II

Notation

A	thickness of a marsh clay layer (Fig. 64)
B	height of a levee on a marsh (Fig. 64)
A, B	Skempton's pore pressure parameters in Eqn (25), $\Delta u = B[\Delta\sigma_3 + A(\Delta\sigma_1 - \Delta\sigma_3)]$
B'	Skempton's pore pressure parameter in Eqn (26b), $\Delta u = BA\,\Delta\sigma_a = \bar{B}\Delta\sigma_a$
C	thickness of a sand layer below clay (Fig. 64)
c	cohesion; strength property (Fig. 1(b) and Eqn (2))
c'	Hvorslev's true cohesion (Fig. 27)
e	ratio of the void volume to the solid volume in a grain aggregate
G_s	mass of a unit volume of a solid soil grain, about 2700 kg/m^3

g	the acceleration of Earth's gravity field, about $10\,\text{m/s}^2$
I_L	liquidity index, $I_L = (w - w_L)/(w_L - w_P)$
l	length of a triaxial test specimen (Fig. 2(b))
l	Coulomb's equation has a constant $l = 2c\tan(45 - \phi/2)$ (Eqn (5))
m	Coulomb's equation has a constant $m = (\gamma/2)[\tan(45 - \phi/2)]$ (Eqn (5))
n	porosity of an aggregate, $n = e/(1 + e)$
n_0	Casagrande's (1937) critical porosity
n_1, n_2	porosities (Fig. 17)
P_A	the minimum force on Vauban's wall in Coulomb's equation (Eqn (5)), $P_A = mh^2 - clh$
p'	mean normal effective pressure $p' = (\sigma_a + 2\sigma_r)/3 - u = (\sigma'_a + 2\sigma'_r)/3$ (Fig. 2)
p'	effective pressure at CS point C (Fig. 55)
p'_B	the pressure at B (Fig. 18(b))
p'_K	the pressure at K (Fig. 18(b))
q	deviator stress; $q = [(q_1^2 + q_2^2 + q_3^2)/2]^{1/2}$ (Eqn (23))
q	$q = \sigma'_a - \sigma'_r$ (Fig. 2)
s	in Eqn (19) and Fig. 31, $s = (\sigma_1 + \sigma_2)/2$
t	in Eqn (19) and Fig. 31, $t = (\sigma_1 - \sigma_2)/2$
u	water pressure (Eqn (1))
V	a point on the right of Fig. 61
v	specific volume of aggregate $v = 1 + e$ (Fig. 2(a))
v_λ	in Eqn (10), $v_\lambda = v + \lambda \ln p'$; in Fig. 55(a) at CS, $v_\lambda = \Gamma + \lambda - \kappa$
w	water content ratio of the mass of pore water to the mass of solids in an aggregate
w_L	water content at the liquid limit
w_P	water content at the plastic limit
x	shear box displacement (Fig. 1(a))
y	shear box rise (Fig. 1(a))
α	slip plane angle, $\alpha = \phi_d = 45°$ (Fig. 4(a))
Γ	CS soil constant, $\Gamma = v + \lambda \ln p'$
γ	weight of a unit volume of soil, $\gamma = \gamma_w(G_s + e)/(1 + e)$
γ_w	weight of a unit volume of water
ε	strain
$\varepsilon_{x,y}$	strain components (Fig. 30(f))
$\varepsilon_{\alpha,\beta}$	strain components (Fig. 30(g))
η	generalized stress obliquity in a triaxial test, $\eta = q/p'$; at CS, $\eta = M$
κ	slope of inclined single lines (Fig. 18(b))
λ	slope of double lines (Fig. 18(b))
M	CS friction constant (Eqn (9))
μ	friction coefficient (Eqn (2))
σ	total stress normal to a plane (Fig. 1(a))
$\sigma_1, \sigma_2, \sigma_a, \sigma_b$	total stress components on planes (Fig. 33)
σ_i, σ_j	generalized stress components (Fig. 51)

σ' effective stress (Eqn (1))
$\sigma'_f, \sigma'_g, \sigma'_a, \sigma'_r$ effective stresses (Fig. (11))
τ shear stress on a plane (Fig. 1(a))
τ_1, τ_2 shear stresses near and on a slip plane (Fig. 11(a))
ϕ angle of friction (Fig. 1(b))
ϕ_d drained angle of friction (Fig. 4(c))
ϕ' angle of friction (Fig. 10(c))

Contents

1 Slip plane properties

Coulomb was taught Amontons' asperity theory of friction on slip planes and Musschenbroek's cohesion theory, but simple experiments led him to question these 18th-century theories for the strength of soil and rock.

1.1 Maps of soil behaviour

For 300 years, since 1700, engineers have defined disturbed soil behaviour by slip plane strength properties. Coulomb applied the slip plane model to both disturbed and undisturbed soil and rock in an Essay that he wrote in French, *On an Application of the Rules of Maximum & Minimum to Some Statical Problems, Relevant to Architecture* (Coulomb, 1773). That Essay was on limiting states of masonry construction. Heyman (1972) made the Essay accessible in an English translation, with a study of Coulomb's place in the history of civil engineering. George Washington and Charles Coulomb were very much of an age. American geotechnical engineers who have read Goodman's book and were interested in the historical context of Terzaghi's work may also find it interesting that Washington was born in 1732 and Coulomb 4 years later; Washington died on 19 December 1799 at the very end of the 18th century, and Coulomb died 6 years later. Washington came from a well-born Virginia planter family, and pursued two intertwined interests: military arts and Western expansion. At 16 he helped survey Shenandoah lands for Thomas, Lord Fairfax. Commissioned a lieutenant colonel in 1754, he fought in the first skirmishes of the French and Indian War. In the War of Independence that followed, he became US Commander in Chief, taking command at Cambridge, Massachusetts, on 3 July 1775. The British gun batteries defending Boston and New York against French ships had great military importance to the armies. Heyman tells of Coulomb's experience of construction of similar fortifications as a young French Royal Engineer in Martinique, where major French fortifications were needed against possible attack by the British Navy. Coulomb's posting there was accidental. A ship was sailing from Brest in February 1764, and the engineer who had been posted originally fell ill. Coulomb, aged 28, was drafted in his place. He was put in charge of the work in Martinique. In finding the earth pressure in the ramparts using the slip plane model, he developed a new calculation that improved on what he had been taught in France. When he got back to France (in broken health after 13 years of overseas service on a fever-stricken island) he included his new earth pressure calculation in the 1773 Essay on admission to the Academy.

Figure 1(a) sketches a shear box containing soil. In a soil shear test the total pressure σ on the mid-plane is held constant. Any water pressure u in the pores of soil or rock is subtracted from the total stress σ to give the effective stress σ'

(a)   (b)
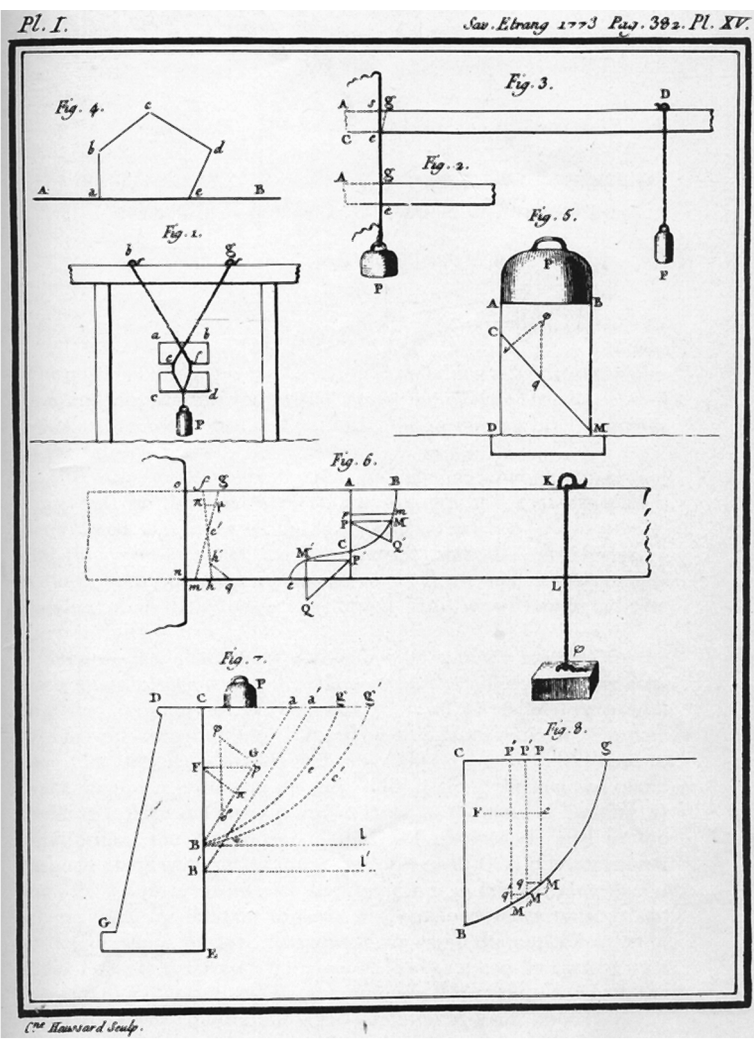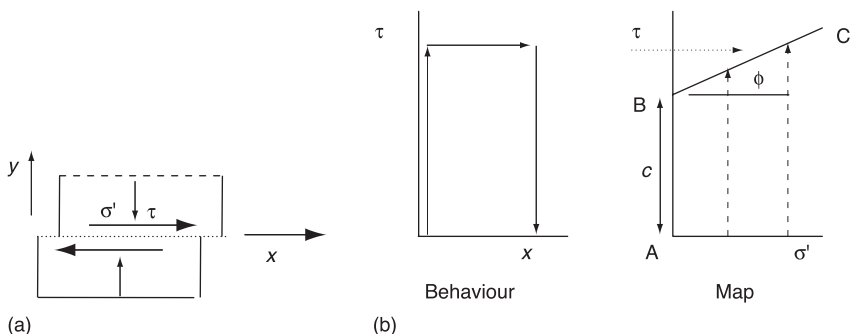
Behaviour   Map

(c)

Fig. 1 Coulomb's 1773 Essay. (a) Shear box. (b) Shear box test data plots. (c)
Coulomb's Plate 1 (French Academy of Sciences, prior to the French Revolution)

normal to the slip plane (Eqn (1)). In the slip plane model (Eqn (2)), when a vector of effective stress (τ, σ') across the mid-plane reaches a limiting value there is a slip displacement $+x$ (Fig. 1(b)). The 18th-century definitions of friction and cohesion were symmetrical, and supposed that soil and rock had properties called *friction* and *cohesion* where:

- friction depends on σ' but is independent of the plane area;
- cohesion depends on the plane area but is independent of σ'.

If a set of drained tests at various values of normal stress σ' gives a set of peak strength points that lie on a line BC in Fig. 1(b), then the slope ϕ and the intercept c of that line will give the friction angle ϕ and cohesion c soil strength properties in Eqn (2):

$$\sigma' = \sigma - u \tag{1}$$

$$\pm\tau = c + \mu\sigma' = c + \tan\phi\,\sigma' \tag{2}$$

Terzaghi and Hvorslev regarded the intercept c in Fig. 1(b) as true cohesion due to the close approach of clay grains to each other. If that were so, the same cohesion would apply at all σ' values. Alternatively, in Fig. 5(d), dense clay strengths are reinterpreted without any cohesion at all as the sum of internal friction (on the line AC) and interlocking (bringing peak strengths up to BC). Coulomb gave an example of the design of a high rampart such as the one that he built in Martinique with a masonry wall that retained well-drained soil. Although the soil was well compacted, his design assumed that it had zero cohesion, and he wrote words that the reader should re-read several times:

> *Supposing that the coefficient of friction is unity, as for soils which take a slope of 45° when left to themselves and that the cohesion is zero, as for newly disturbed soils:*

> *(Si l'on suppose que le frottment soit égal a la pression, comme dans les terres qui, abandonées à elles-mêmes, prennent 45 degrés de talus; si l'on suppose l'adhérance nulle; ce qui a lieu dans les terres nouvellment remuées:)*

The critical state (CS) concept agrees with what Coulomb puts forward here. Engineers should still learn to design for newly disturbed soil with zero cohesion, and to link internal friction with the observed slope at repose of an aggregate of disturbed soil grains. The matrix of soil grains in mechanical contact gives soil its elastic stiffness. I will calculate soil plastic strength from the dissipation of energy in shear distortion of a unit volume of the aggregate of solid soil grains. I will use the word *grain* rather than *particle* (a word better used in the context of basic physics). The Frontispiece map considers soil bodies that exhibit other mechanisms of behaviour, as well as slip on planes.

Maps give information about what is supposed to be known, and where to look for what is not yet known. The limiting states of incipient slip plotted on the line BC in Fig. 1(b) can be seen as mapping slip displacement soil behaviour at points on the map with stress state coordinates (τ, σ'). Each dashed arrow in Fig. 1(b) shows the succession of stress states on a test path that ends in slip plane
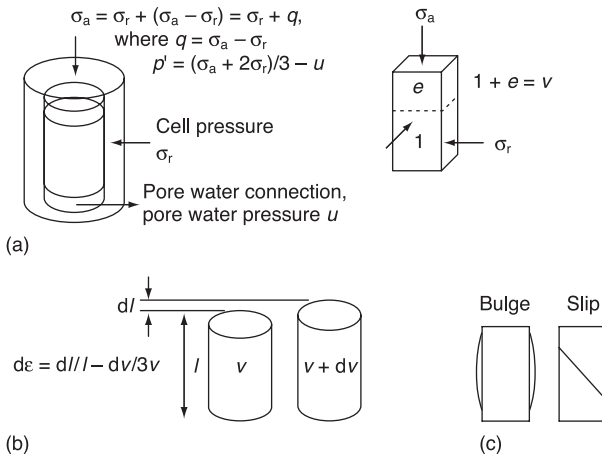
$\sigma_a = \sigma_r + (\sigma_a - \sigma_r) = \sigma_r + q,$
where $q = \sigma_a - \sigma_r$
$p' = (\sigma_a + 2\sigma_r)/3 - u$

Cell pressure σ_r

Pore water connection, pore water pressure u

(a)

$1 + e = v$

$\mathrm{d}\varepsilon = \mathrm{d}l/l - \mathrm{d}v/3v$

Bulge   Slip

(b)   (c)

Fig. 2 Triaxial test stresses and strains

formation. If a test shows new behaviour not predicted by the slip plane model state, points on a new map can record this, just as old maps were revised with explorers' new findings. The shear box allows only simple soil behaviour, with slip in one direction or the other depending on the sign ±. The triaxial cell (Fig. 2) is less constraining. It lets some specimens fail with inclined slip planes and lets other specimens exhibit axial compression and bulge laterally (Fig. 2(c)). The geotechnical centrifuge allows even more freedom for soil bodies to exhibit failure mechanisms and unexpected behaviour. My Rankine Lecture (Schofield, 1980) on geotechnical centrifuge modelling showed a map of soil behaviour like the Frontispiece, with coordinates relating to triaxial test states.

There must be stress at boundaries, and forces at grain contacts, if innumerable small soil grains without cohesion are to aggregate together and form a solid body. When stresses change we do not see all grain movement in the aggregate in a specimen. We see and measure displacements of boundaries that are caused by integrated effects through the aggregate. The slip plane model does not predict all the successive forms of a specimen. A body can divide into separate blocks with slip displacement on planes, or crack with blocks moving apart from each other, or bulge and flow. The behaviour of a solid body that deforms under load but returns to its original form when the load is removed is called *elastic*; the word *plastic* describes the behaviour if the body is left with permanent deformation. *The Shorter Oxford English Dictionary* (SOED) tells us that the word 'plastic' in the English language is derived from the Greek word 'πλασσειν' (*plassein*) for forming clay paste into a pot or a figure. One difference between soil and metal is that soil paste saturated with water shows permanent changes not only in shape but also in volume and water content. Volume change in an aggregate of grains in a soil paste shows up as a change in soil water content. If soft water-saturated soil paste is allowed to dry in the air and is remoulded between the fingers, changes of behaviour are observed with the change of water content. At a water content called the liquid limit w_L the paste has the consistency of clotted cream. At what is called the plastic limit w_P the paste has dried to the

point at which it breaks into crumbs when we try to roll it into a thread. Casagrande called the range $w_L - w_P$ of water contents over which soil paste exhibits plastic ductility the plasticity index I_P. The liquidity index $I_L = (w - w_L)/(w_L - w_P)$ expresses the current water content w of a paste relative to the liquid and plastic limits w_L and w_P. There are great differences between the materials and pore water chemistry in different soil pastes, but pastes with the same liquidity index have similar mechanical behaviour. A point in the Frontispiece map defines a soil state in terms of two parameters (v_λ, η), where $v_\lambda = v + \lambda \ln p'$ is a measure of the effective liquidity and packing of a stressed grain aggregate and $\eta = q/p'$ is a measure of the stress obliquity in that aggregate. Words on the map record the behaviour seen in soil in states in various zones. This book will discuss types of behaviour that are indicated on the map. I will argue that soil liquefaction is not a phase transition from solid to liquid throughout an aggregate but a failure mechanism in which a soil body near to zero effective stress cracks and crumbles and is fluidized by seepage forces. In a zone on the left in the Frontispiece the catastrophic transition from a solid body to flowing rubble and hydraulic fracture and piping events are all linked under my heading *Herrick's liquefaction*.

It is another difference between soil and metal that geotechnical engineers can break up soil by hand in water into slurry that is washed through a nest of sieves in their site investigation. The innumerable clean solid grains left on the sieves are weighed to give a grading analysis. The mechanical behaviour of the disturbed soil that this book discusses depends on the behaviour of the aggregate that would be formed if all those grains were mixed together. Drained heaps of aggregate (whatever the height) usually have slopes at the same drained angle of repose ϕ_d; this angle was taken to define the internal friction in soil in the 18th century. Increased effective stress does not usually reduce the internal friction in an aggregate. Aggregates in which increased stress reduced ϕ_d would be unusual; in such aggregates, deep-seated slip failure would reduce the slope angle of high heaps. The angle ϕ_d and the Greek letter M (capital mu) in the original Cam Clay (OCC) model will be linked in Eqn (44).

Figure 1(c) is Plate 1 from Coulomb's Essay; in it, his Fig. 7 shows that he considered very small slips on many parallel slip planes, as well as localized rupture on discrete slip planes. He extended the slip plane model of behaviour that he had been taught to include continuous shear, but not to include another aspect of deformation that needed consideration, spherical compression of soil paste under an increase of triaxial cell pressure. The OCC model of plastic behaviour of triaxial test specimens that will be discussed later in this book does include plastic compression. It recognizes that when stressed grains slip in an aggregate they can pass or move towards or away from one another, or rotate. In Fig. 2(a), many soil grains that all together have a unit volume form an aggregate in solid-to-solid contact, with a pore volume e. The *specific volume $v = 1 + e$* defines grain-packing density; v varies from one specimen to the next. In saturated soil with a solid grain specific gravity of G_s the weight of the solid grains and of the water in the pore space together is $G_s + e$, and the saturated unit weight of the soil is $(G_s + e)/(1 + e)$. If a saturated soil specimen is weighed, dried in an oven and reweighed, the specific volume v can be calculated.

In a shear box the slip plane measure of *stress obliquity* in cohesionless soil is $\tau/\sigma' < \tan\phi$ (Eqn (2)); as the obliquity of a vector of stress acting on a potential slip plane increases, more and more friction is mobilized; slip occurs when friction is fully mobilized. In a triaxial test (Fig. 2(a)), the effective stress parameters, mean normal pressure $p' = (\sigma_a + 2\sigma_r)/3 - u$, and shear stress $q = \sigma_a - \sigma_r$, and specific volume v define an isotropic stressed aggregate stress state (q, p', v). The triaxial test stress ratio $\eta = q/p'$ in the Frontispiece is a measure of the triaxial stress obliquity.

A shear box has rectangular corners that make it difficult to prevent pore water from leaving the test specimen. A triaxial test cylinder of soil is encased in a rubber sheath that is clamped tightly to the top cap and the pedestal by rubber rings so that the volume of pore water dv that leaves the specimen is controlled. In drained triaxial tests the drainage dv is measured at the pore water connection (Fig. 2(a)). In an undrained test, changes of the pore water pressure u are measured, and the effective stress is calculated (Eqn (1)). Later, in Fig. 22(b), we will come to a simple representation of the cylinder of soil as a compression spring, but here a general measurement of deformation involves both a volume change dv and a distortion dε of the specimen. The length of the specimen is l, the axial strain in the test is dl/l, and the volume strain is dv/v. Compression with no distortion produces an axial strain $\frac{1}{3}$ dv/v. If there is both volume change and distortion in a deformation, d$\varepsilon = $ d$l/l - \frac{1}{3}$ dv/v is the pure distortion (Fig. 2(b)).

A state of a triaxial test specimen is defined by two parameters (η, v_λ); the stressed-aggregate packing parameter $v_\lambda = v + \lambda \ln p'$ combines effective pressure and specific volume. The ratio $\eta = q/p'$ is the stress obliquity. The stressed grain aggregate packing in triaxial test specimens changes during distortion. As a test progresses, state points follow a path that moves across the map in the Frontispiece. CS flow satisfies the equations $v_\lambda = \Gamma$ and $\eta = M$, where Γ and M are the soil constants that give the CS point in the Frontispiece. Schofield and Wroth (1968) discussed steady-state CS flow with no cohesion between grains as follows:

> *Consider a random aggregate of irregular solid (grains) of diverse sizes which tear, rub, scratch, chip, and even bounce against each other during the process of continuous deformation. If the motion were viewed at close range we could see a stochastic process of random movements, but we keep our distance and see a continuous flow. At close range we would expect to find many complicated causes of power dissipation and some damage to (grains); however we stand back from the small details and loosely describe the whole process of power dissipation as 'friction', neglecting the possibilities of degradation or of orientation of (grains).*
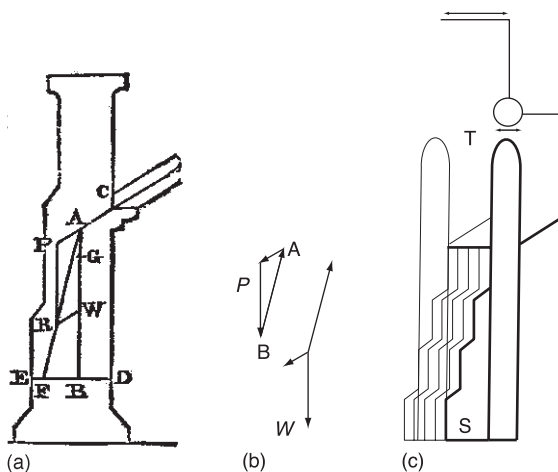
The OCC straight line in the Frontispiece follows the gradual mobilization of internal friction; CS plastic shear flow occurs with an increase of stress obliquity and decrease of specific volume that ultimately reaches the CS value $v_\lambda = \Gamma$. In the zone shaded with vertical lines in the Frontispiece, where stress ratio values are $\eta/M = q/Mp' < 1$, friction is not fully mobilized in soil (e.g. at rest below slopes of a heap at repose). The deformation behaviour of a stressed aggregate of random disturbed solid grains of all shapes and sizes is mapped in the Frontispiece. In general, it is at rest at (v_λ, η), but at the CS point where $v_\lambda = \Gamma$ and $\eta = M$

the grains flow as a frictional fluid. Energy is dissipated in shear distortion of a stressed aggregate. Analysis of the data of a series of triaxial tests at Cambridge University in 1962 led to a simple equation (Eqn (33)) for the dissipation of energy both in yielding and in continuous flow, as a function of effective stress and plastic strain in the aggregate. The OCC hypothesis that a frictional aggregate yields with small stable plastic deformation increments led to equations that, when integrated, defined the strength of the ideal OCC soil (Roscoe and Schofield, 1963; Roscoe *et al.*, 1963a).

In states in the Frontispiece on the straight OCC line the aggregate yields as paste. In states on the 'watertight slip plane' curve, a soil body fails with deformation becoming localized in layers where what is called *gouge material* softens to a CS paste on the slip plane. If a body such as an embankment dam deforms as a whole with a mechanism of slip planes and zones of plastic yielding without interconnected open cracks, it remains watertight. Strength on slip planes has a plastic component that is due to CS friction, and another peak component due to interlocking. While CS friction usefully dissipates damaging load energy, the peak component that is due to interlocking dissipates no energy. In *over-compacted* states above CS density $v_\lambda < \Gamma$ the dense aggregate of lightly stressed soil grains can have high stiffness, but a body is unsafe if it depends on interlocking peak strength components for stability; in brittle failure mechanisms high loads impart kinetic energy to soil masses, and their motions subsequent to failure cannot be predicted. The Frontispiece contrasts compaction to a density at which soil is strong but ductile and safe, with unreliable high compaction to states with $v_\lambda \ll \Gamma$ of soil that is so dense and stiff that stress obliquity can rise to values as high as $\eta = 3$. Water-retaining structures of such soil can fail by cracking or piping, causing high secondary permeability. Both Coulomb and Rankine relied only on fully disturbed CS strength. It was safe for Coulomb to use his low safety factor of 1.25 if his construction retained ductility, but the over-compacted soil that was used to build the Los Angeles, Division of Water and Power reservoir in the Baldwin Hills, or the US Department of the Interior, Bureau of Reclamation dam on the Teton River would not have been made safe by a 1.25 safety factor.

1.2   Masonry in Coulomb's Essay

At this point a digression is needed about masonry, as lightly cemented heavily over-compacted soil that cracks into discrete block rubble behaves rather like random masonry. When large rough blocks of stone were brought by river in the 15th century to construct King's College Chapel in Cambridge (illustrated on the front cover) they were sawn up and chiseled into shape on site. As construction progressed in successive bays along the length of the chapel, each block of rock had faces squared to fit against the faces of adjacent blocks, all to the original design. In the work that halted on Henry VI's death the masons left a saw cut in one large block that they did not complete until Henry VII restarted the work. The early part of the work had the austerity appropriate to the pious Henry VI. The later part was decorated with proud emblems, the rose of the Tudors and the portcullis of Lady Margaret Beaufort, mother of Henry VII. Masons erected

Fig. 3 Masonry. (a) Thrust lines in a buttress (from Rankine, 1874). (b) Chord with weight W. (c) Plan and elevation of King's College Chapel

formwork high in the air, and lifted the heavy blocks with ropes to assemble them on the formwork. When wedges at points in the formwork were knocked away, all the blocks descended together under gravity. As an arch settles, it reacts on the abutments. A heavy keystone in the centre of an arch makes a line of force pass from one block to the next from abutment to abutment. If one block crushes when the full load bears on it, every block in an arch will settle safely on the form-work. Masons then replace that defective block and repeat the process. All defec-tive material was detected and eliminated as every block survived the construction process.

Such masonry structures have no cement in their joints and are flexible. If a great gale of wind applies a force to the structure or if the ground moves, a joint in the masonry can open up, with a hinge along a line where two blocks make contact. As the structure then moves a little, forces find alternative paths but the thrust vectors in the masonry must remain in equilibrium (Heyman, 1995). The masons did not learn the graphics that engineers were taught in the late 19th century, but Heyman states that their use of models is well attested; they could learn a lot from diminu-tive models. Figure 3(a), from Rankine's 1874 textbook, shows a vertical section of a buttress supporting an inclined thrust P from the roof at C in the direction CA. The vector diagram APR represents the equilibrium of the masonry above section DE. If the line of thrust CAR through the masonry is inverted, it has the form that a string CR would have with W as a weight hung from the string. It has been known from early times that a catenary form as adopted by a string hanging under self-weight would, if inverted, be the perfect form for an arch; a Parthian brick arch near the Tigris 20 miles from Baghdad at Ctesiphon exemplifies this. In Fig. 3(a) the height of the buttress above C has been increased to increase the weight W and make P and W have a resultant R that acts within the section DE of contact in the masonry. This principle is evident in the pinnacles at the corners of King's College Chapel (Fig. 3(c)).

In the 15th century the Earth was considered flat; *up* was good and *down* was bad. In Gothic Perpendicular style, an ideal structure should rise vertically to heaven without a sloping line of props or flying buttresses that were thought ugly. The King's College Chapel vault inevitably required lateral support, provided along the length of the chapel by triangular buttress slabs, projecting out at each side (Fig. 3(c)). Between these slabs at their base there are closets, some of which form side chapels S. The resultant of the thrust from the vault and the weight of the slab is a vector that falls within the base of these buttresses. At each corner of the chapel there is less lateral thrust of the vault than along a side, but the increased weight of each high tower T combines with these thrusts to make thrust lines that fall within the small circular bases of the towers. The masons of the chapel thus created an illusion of ideal Perpendicular construction without any ugly sloping lines. From outside the side chapel walls the ugly slope of the buttresses cannot be seen against the strong vertical profile of the elegant soaring corner towers. They are unbelievably slender when compared with other famous Gothic towers that were completed at about the same time such as the leaning tower of Pisa. From inside the chapel all that can be seen are the edges of the buttress slabs in the wall of stained glass, thin lines that Wordsworth saw as lofty pillars supporting tens of thousands of stone blocks to

> . . . *spread that branching roof*
> *Self-poised, and scooped into ten thousand cells.*

Each builder who learns the skills of an older master-builder will in their turn teach the next apprentice. From very early times, men such as those who built Stonehenge had to understand static equilibrium to organize the erection of the large, heavy stone blocks in that structure. By the time of the East Anglian masons, such men probably used models to learn the effects of applied loads and the thrusts in stone skeletons. A line of thrust must pass through masonry blocks. No stone block is flexible, but hinges can open in a stone skeleton. If hinges close up so that blocks fit together again, the skeleton is restored to the form that it had when first built. It will be argued later that, because no energy is dissipated in the opening and closing of any hinge, a stone skeleton is less safe than a modern steel skeleton structure, but use of a model as a structural analogue made Gothic construction fairly safe. More was known about static equilibrium than about strength in the 15th century, but the formwork provided what was in effect a full-scale apparatus for testing material; the strength of all the material was tested by an observational method as construction progressed. Physics and mathematics have made slow progress. When peasants first made a tally, it was easy to make a scratch on a rock or a piece of slate for each beast; but scribes needed to read such scratches quickly, and taught men to form what we call Roman numerals. The five fingers on a hand are represented by two scratches for the letter V, and the ten fingers on two hands by two scratches for the letter X. Two scratches $<$ is read as the letter C for 100, and four scratches give the letter M to denote 1000. The Roman numerals were displaced by Arab numerals, but when I lifted floor boards in a first-floor room of my house in Cambridge (built in about 1650) I was intrigued to see chisel cuts making Roman numerals on each beam. I do not know if the 17th-century builder salvaged those beams from an
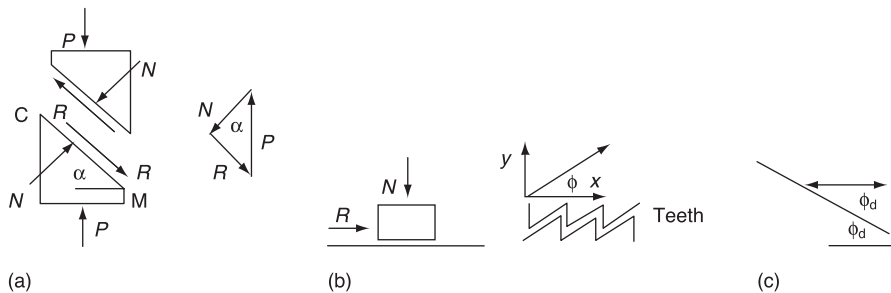
Fig. 4 (a) Coulomb's slip plane in rock. (b) Amontons' asperities. (c) Slope at repose

older building or if he made those chisel cuts himself, but I think if he had been asked then to mark today's date of 2005 in a stone in the face of the house he would quickly make ten cuts, forming MMV. That skill is lost. No builder today would be asked to chisel those three letters in oak or in stone.

I am not an expert on 17th and 18th-century engineering, and have read few papers of the period. Coulomb's Essay was one of the papers on slip and strength published by the French Academy of Science in the 18th century. Coulomb's Fig. 5 within his Plate 1 (shown in Fig. 4(a)) shows compression failure of a column of undisturbed rock with a slip plane CM inclined at α. The triangle of normal and shear forces R and N on CM shows that $R = N \tan \alpha$. Amontons tested surfaces of various solid materials sliding in contact and, in explaining his data, he suggested that asperities on sliding surfaces cause resistance to slip. This effect is what Taylor later called *interlocking*. If asperities act like teeth (Fig. 4(b)), with slip on smooth contact faces at an angle ϕ, interlocking causes a resistance to sliding of $R = N \tan \phi$ independent of the area of contact and proportional to the force N normal to the slip plane. It fits the 18th-century definition of friction, but an interlocking motion that surmounts smooth asperities does not dissipate energy, which is how friction was defined in the 20th century. Coulomb's 1773 paper accepted Amontons' friction as a first component of the internal strength of soil and rock. Eight years later, Coulomb (1781) reported subsequent friction tests with various sliding materials. Realizing that the asperity theory of friction cannot continue to apply after the first asperities have slipped past each other, he considered other suggestions for the physical causes of resistance to slip in the slip plane model of soil strength. In that later publication (p. 117) Coulomb questioned the friction, cohesion and interlocking components, and wrote of the need for new insights from further experiments as follows:

> *The physical cause of the friction opposing the slip of surfaces on each other cannot be explained by the engagement of surface asperities that do not disengage as they bend, or break, or as they surmount each other, or perhaps by the molecules of the plane surfaces in contact gaining a coherence that must be overcome to produce movement: only experiment can help us to determine the reality of these different causes.*

> *(La cause physique de la résistance opposée par le frottement au mouvement des surfaces qui glissent l'une sur l'autre, ne peut être expliquée, ou que par*

l'engrainage des aspérités des surfaces qui ne peuvant se dégager qu'en se pliant, qu'en se rompant, qu'en s'élevant à la sommité les unes des autres; ou bien il faut supposer que les molécules des surfaces des deux plans en contact contractent, par leur proximité, une cohérence qu'il faut vaincre pour produire le mouvement: l'expérience seule pourra nous décider sur la réalité de ces différents causes.)

Rupture planes through intact rock and slip planes through soil are rough and have asperities. The behaviour of loose granular aggregate such as sand or gravel (Fig. 4(c)) was explained by asperities that are teeth with smooth horizontal surfaces on which a smooth grain can move in either direction, as shown by the double arrow, hence $\phi = \phi_d$. All 18th-century writers took the angle of repose ϕ_d as the internal friction angle of soil. In Fig. 5(a), force components (N, R) normal to and tangential to the slope at repose are applied by a slab of soil to the slope on which it rests. In Fig. 5(b), points on a line AC with slope ϕ_d represent values of N, R at increasing depths in the slope: the same points are plotted as components of stress (force per unit area σ', τ) normal and tangential to the slip surface in line AC (Fig. 5(c)). A series of slabs of increasing thickness (Fig. 5(a)) gives limiting stress points (τ, σ') on a line AC in Fig. 5(c) with a slope ϕ_d. This was thought to be well known and not to need experiment.

An 18th-century physics textbook by Musschenbroek (1729) taught that the cohesion strength component that is independent of the normal force acts effectively on a slip area and depends on the slip area, and that this cohesion *resists direct separation of a solid body into parts*, with the same effect causing both the tension and the shear strength of solids. This was not obviously true, and needed experiment. Figure 1(c) depicts Coulomb's tests that showed the teaching not to be exactly true even though the strength values were close enough for practical purposes. Tests of stone slabs are shown in Coulomb's 1773 Plate 1 (Fig. 1(c)). To measure cohesion in tension, in his Fig. 1 he had a slab of limestone with two notches cut into it, with a weight hung on a loop of rope; it broke in tension across
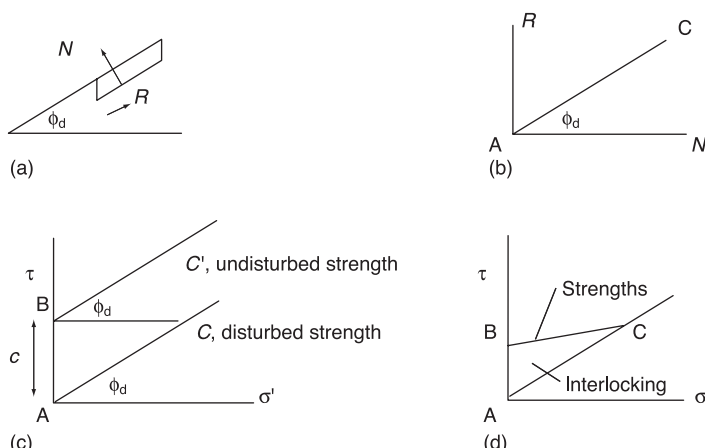

Fig. 5 Coulomb's soil strength theory. (a) Aggregate at repose in a drained heap. (b) Forces. (c) Stresses. (d) Hvorslev's peak strengths

the neck section ef. Other slabs were built into a wall. His Fig. 2 shows a short slab with a heavy weight hung from a rope round it to cause shear failure, and his Fig. 3 shows a longer slab with a smaller weight hung from it to cause the upper surface near the wall to fail in tension. His limestone strength data were that the notched square slab 1 inch thick with a neck 2 inches wide failed with a tensile adhesion of $215 \, \text{lb/in}^2$ and the short slab loaded with a force directed along the plane of shear by a rope that passed round it close to the clamped end failed with a cohesion of $220 \, \text{lb/in}^2$. These strengths were almost the same, but the strength in shear (cohesion) was usually slightly larger than the strength in direct tension (adhesion). His test results for limestone were repeatable; the results for brick were not. Musschenbroek was in error: tensile and shear strength are different; adhesion and cohesion are not identical physical effects.

Several questions arise here for geotechnical engineers today. Why do we not test soil in direct tension in the same way as Coulomb tested rock, and as structural engineers test steel? We can never be sure if cemented bonds between grains that formed in past times have been broken by subsequent disturbance, with failure both in shear and in tension. Coulomb and Rankine did not rely on cohesion; why are we less prudent than them? When engineers rely on cohesion to resist slip on new slip surfaces through undisturbed soil or on old slip surfaces that become bonded or cemented over time, do they appreciate that disturbed soil is only left with frictional shear strength? Coulomb's case of $\alpha = \phi_d = 45°$ is consistent with $R = N$ on the inclined rupture plane, and with Amontons' suggestion that interlocking is the cause of friction. If Coulomb had wanted to include any cohesion c' (Fig. 5(c)) in a calculation it would be a constant for undisturbed soil that is not altered by σ', the effective normal pressure. A line BC' (Fig. 5(c)) displaced by a constant amount c' above AC would define Coulomb's limiting stress in undisturbed soil. Hvorslev found data that fitted a line BC with $c = \text{constant}$ and $\phi < \phi_d$ (Fig. 5(d)), but his data did not support extension of the line to the right of C, where there is plastic compression ultimately at some point.

1.3   Marshal Vauban's fortress wall

Before the 18th century, a force in a fort with high ramparts was safe but could still sally out to engage attackers. After heavy cannon fire could bring down ramparts, the infantry who had to fight in the open field took heavy casualties from the fire of horse-drawn light cannon and from cavalry. Marshal Vauban (1633–1707) built many forts to defend France, and formed an army engineer corps (Corps Royale du Génie) to assist in the attack and defence of forts. He wrote books on this, and gave the cross-section for a masonry wall that could retain a rampart of compacted drained soil. If very heavy cannon fire dislodged masonry blocks so that the wall fell and the retained soil formed a slope at repose, an enemy could storm up the slope, over the rampart and into the fort (as in the fall of Constantinople in 1453). Vauban's *glacis* embankments stopped cannons from battering the masonry. A vertical wall retained the glacis. It faced the fort wall, inwards. These *escarpment* and *counterscarp* walls formed a ditch (Fig. 6) that could be swept by defensive fire from bastions. Defensive fire from the ramparts also swept the gradual
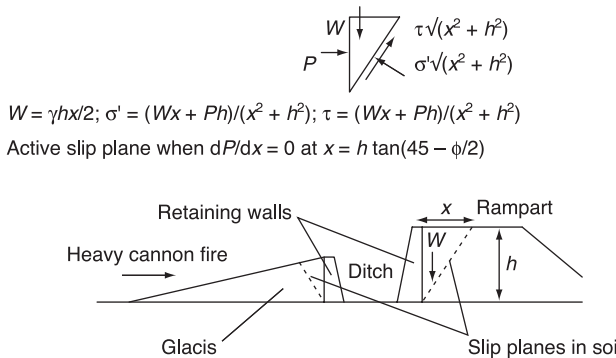
$W = \gamma hx/2$; $\sigma' = (Wx + Ph)/(x^2 + h^2)$; $\tau = (Wx + Ph)/(x^2 + h^2)$

Active slip plane when $\mathrm{d}P/\mathrm{d}x = 0$ at $x = h \tan(45 - \phi/2)$

Fig. 6 *A glacis protects a rampart from cannon fire*

outward glacis slope. Discreet sally ports in the wall of the fort let the defenders sally out into the ditch, where they could engage attackers at close quarters. An attacking regiment (in the Napoleonic war in the Iberian peninsular for example) had to climb the wall with ladders from the ditch, while their grenadiers supported their attack by marching up the glacis under fire to throw grenades at the men on the ramparts (grenadiers faced great danger, and children still sing the Grenadier Guards song '*Our leaders carry fuses and we the hand grenades. We throw them from the glacis about the enemy's ears*'). Great cities in the 18th and 19th centuries had star-shaped fortifications in plan view, with ramparts and bastions from which defensive cannon could fire at attackers. Old cities that were garrisoned and provisioned for 18th-century defence still have esplanades, ramparts and sally gardens. In the 21st century these are used as public spaces for leisure, and seen as quaint. Engineers today, unfamiliar with the reasoning behind the design and construction of these fortification details, do not learn why Coulomb thought a wall of Vauban's specified width at the top and with his specified batter of the face can stand up and retain soil, whatever the wall height.

For slip of a soil wedge in a fill behind Vauban's walls on a plane shown by the dashed lines in Fig. 6, Coulomb resolved the forces W and P due to the weight of the wedge and the lateral force applied by the wall to get average stresses on the slip plane. Introducing these stresses (τ, σ') into Eqn (2) gives an expression for P in terms of the length x of the horizontal face of the wedge. Calculus finds the least value of P. When a school for French Royal Engineers was opened in Mézières in 1749 the teaching included the design of ramparts with high masonry walls under the lateral pressure of a wedge of retained soil. Coulomb had graduated from that school. His Figs 7 and 8 (in Fig. 1(c)) show slip plane and circle failure mechanisms behind a wall. His Fig. 5, redrawn here as Fig. 4(a), shows a drained test of a column of rock under an axial load P with failure on an inclined plane CM; at this point the reader should note in passing that when solid bodies are displaced to either side of a slip line such as CM in Fig. 4(a) there is no change of their dimensions, and later will need to recall that a slip line keeps a constant length during slip. There are two soil constants c and ϕ in Eqn (2). Coulomb regarded strength in tension as a safe approximation to shear strength c due to cementation in the absence of friction, and he regarded the angle ϕ_{d} of the slope

at repose as a safe value for friction in the absence of cohesion. With these values of the c, ϕ constants, Coulomb could use Eqn (2) in design. The slip plane model is still in use today, and design standards and codes are still written in terms of cohesion and friction but with other values of cohesion and friction. The engineers who use Eqn (2) today have heard different lectures to Coulomb about soil strength; no student today hears that friction derives entirely from interlocking.

Coulomb used Eqn (2) in a calculation of lateral earth pressure on Vauban's wall, as shown in Fig. 6 with a rampart of height h. Coulomb's Fig. 7 in Fig. 1(c) shows slip plane and slip circle failure mechanisms behind such a wall; in his calculation he assumes that he knows the failure mechanism; he appeals to experience, and writes '*I assume first that the curve which gives the greatest thrust is a straight line; experience shows that when retaining walls are overturned by earth pressures, the surface which breaks away is very close to triangular*'. Significantly, he speaks of experience of a single slip line that is straight like aB in Fig. 1(c) rather than a curve like gB, but in both cases he draws a second parallel line a′B′ or a second parallel curve g′B′ on which limiting stress conditions also apply, thus considering volumes of soil (so Terzaghi was wrong to write '*in contrast to Rankine, Coulomb never attempted to investigate the state of stress within the backfill*'; Coulomb did explicitly consider a soil continuum when he wrote about slip surfaces through soil bodies). The force vectors in Fig. 6 show the weight W of the triangular wedge, for a unit weight γ of the earth, supported by lateral force P from the wall and by friction and cohesion force on the plane slip surface. If the normal and shear stress on the slip plane given in the equations in Fig. 5 are substituted into Eqn (2) they lead to Eqn (3):

$$P = [W(h - x\tan\phi) - c(x^2 + h^2)]/(x + h\tan\phi) \tag{3}$$

What Coulomb called the *rules of maximum and minimum* today we would call differential calculus. An engineer today can differentiate Eqn (3) to find the slope of aB for the least soil resistance and get

$$dP/dx = 0 = (c + \gamma h\tan\phi/2)(x^2 - h^2 - 2cxh\tan\phi) = 0$$
$$\text{giving} \quad x = h\tan(45 - \phi/2) \tag{4}$$

This slip plane slope does not depend on c. Equation (3) leads to a minimum lateral earth pressure value, the *active earth pressure*, that occurs with this slip plane:

$$P_A = (\gamma h^2/2)[\tan^2(45 - \phi/2)] - 2ch\tan(45 - \phi/2) = mh^2 - clh \tag{5}$$

The constants $l = 2c\tan(45 - \phi/2)$ and $m = (\gamma/2)[\tan(45 - \phi/2]$ in Eqn (5) depend on the soil properties; for example, the case where $\phi = 30°$ has $\tan(45 - \phi/2) = 1/\sqrt{3}$, and if we introduce these values in Eqn (4) we get values of $l = 2/\sqrt{3}$ and $m = 3\gamma/2$, so ϕ affects both l and m, but c only affects l. The slip plane is inclined at an angle of $45 - \phi/2$ to the vertical. The earth is active with this force on the wall, as indicated by the suffix A for P_A in Eqn (5) as the wall moves outwards and the earth slips. With a variable h in Eqn (3), Coulomb's pressure has a triangular distribution. His whole mass slips on many parallel slip lines aB, a′B′ as shown in his Fig. 7 in Fig. 1(c). When he also considered soil-resisting movement of a wall into the retained soil he stated that a (curved) surface
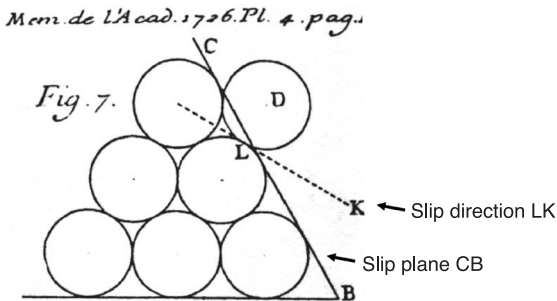
must be sought for which the lateral thrust is a maximum. The suffix P denotes this *passive* lateral force P_P on the wall. Coulomb noted that if c and ϕ are zero the lateral thrust becomes that for retained fluid, $P_A = P_P = \gamma h^2/2$.

> *Thus it follows that the difference between forces in fluids for which friction and cohesion are zero and those for which these quantities cannot be neglected is that for the former the (vertical) side of the vessel containing them can be supported only by a unique force while for the latter there is an infinite number of forces (P) lying between the limits $P_A > P > P_P$ which will not disturb equilibrium.*

Coulomb wrote Eqn (5), and to check this equation he confirmed that a retaining wall with Vauban's dimensions could resist the overturning moment of the calculated thrust with a factor of safety of at least 1.25, writing that '*it is desired to increase the mass of the masonry by a quarter above that which would be needed for equilibrium*'. Coulomb did not write Eqn (2).

1.4 Soil properties in Coulomb's Essay

Coulomb began his Essay with clear propositions on friction (quoting the tests of Amontons) and on cohesion (quoting his own test data). Amontons' friction law can be written as $R = \mu N$ for the normal force N and the tangential force R that are effective at an interface between sliding solid bodies, where μ is a supposed material constant called the coefficient of friction. Amontons' paper concerned friction in machines. In his time, scientific observations of the motions of the planets had accurately confirmed calculations of the orbit of planets (mechanics in space without friction) but engineers made machines that had friction. Amontons found that for slip of a wooden skid on soft earth the resisting force R was about $\frac{3}{4}$ of the weight N on the skid, but there was much less frictional resistance on any hard plane surface lubricated with old oil; the coefficient $\mu = \tan \phi'$ fell from $\frac{3}{4}$ to as little as $\frac{1}{3}$. For such lubricated hard plane surfaces he found that this low friction coefficient value did not depend on whether the sliding material was wood, iron, copper or lead. He explained that only an ideal plane surface is truly flat; real surfaces seem flat, but machining leaves small asperities. He speculated that the friction coefficient depends on the asperities that are left by whatever types of tools are used in the machining of hard plane surfaces. His asperity theory was reasonable if sliding friction did not depend on the material. It explained the 18th-century friction component (dependent on σ' pressure normal to the plane surface but independent of the plane area). The energy input by the force R in his slip displacement $y = x \tan \phi_d$ is conserved in the energy output to the force N (this differs from the later definition of friction where energy is dissipated in slip). If this asperity theory is applied to slip through a stack of spheres (Fig. 7), local asperity contact angles of ϕ_d give a slip direction different from the slip plane and a friction coefficient of $\mu = \tan \phi_d$. Displacements may be so small that they are invisible. Coulomb learned the accepted theory in France in the 18th century, that the resistance R on the slip plane in Fig. 4(a) has two components: friction force due to asperities is independent of the area of the slip surface and is proportional to the pressure normal to the surface, and force due to
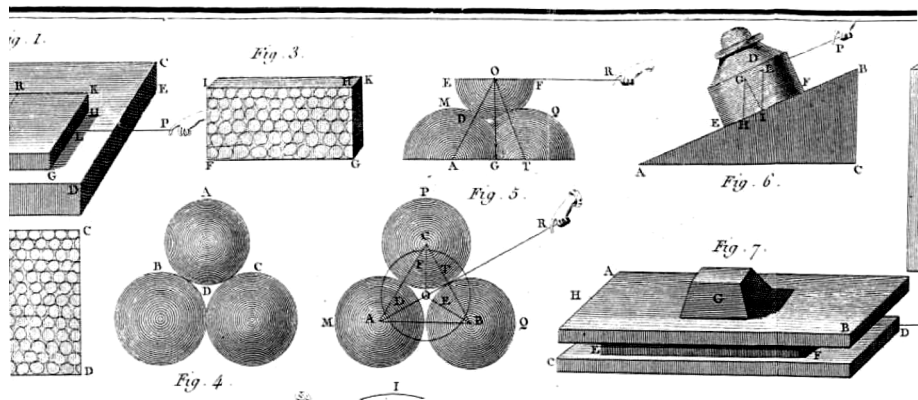
Fig. 7 Slip plane and slip direction (Couplet, 1726)

cohesion is proportional to the area of the slip surface and is independent of the pressure on that surface.

Under Professor Bossut (1772) in Mézières, Coulomb studied a physics textbook by Musschenbroek (1729) and a textbook by Bélidor (1737) that postulated (Fig. 8) that the asperities on a pair of slip surfaces are smooth hemispheres; it calculated a value of $\mu = \frac{1}{3}$ from the slip angle geometry of hemispherical contacts. The Mézières school was closed by the French Revolution, but the same teaching was continued at the École Polytechnique in Paris. Professor Navier in the early 19th-century École Polytechnique created an annotated 1819 edition of Bélidor's book, in which he wrote his own footnote on asperities as follows:

> *Amontons' experiments on friction of which Bélidor speaks were published in the Memoirs of the French Academy of Science (1699). That author concludes that the resistance provided by friction is independent of the size of the area of contact, as has since been confirmed; that it is more or less the same for wood, iron, copper, lead, etc., when these various substances are lubricated with old oil, and is about one-third of the pressure: we will show later that this result requires some corrections. I need not say if the supposition of hemispherical asperities with which Bélidor tries to explain Amontons' data merits attention, nor need I delay any more here to burden these notes with useless remarks on the geometry on which his hypothesis rests, which is quite wrong.*

Fig. 8 Slip over spherical asperities (Bélidor, 1737)

(Les expériences d'Amontons sur le frottemont, dont Bélidor vient de parler, se trouvent dans les Mémoires d' Académie des Sciences pour 1699. L'auteur conclut que la résistance provenant du frottement est indépendante de la grandeur des surfaces en contact, ce qui a été confirmé depuis; qu'elle est à-peu-près la même pour le boix, le fer, le cuivre, le plomb, etc., quand ces diverses substances sont enduites de vieux oing, et environ le tiers de la pression: on va voir plus bas les rectifications don't ce dernier résulat est susceptible. Il n'est pas besion de dire combine la supposition des demi spheres hérissant la surface des corps, sur laquelle Bélidor veut appuyer le résultat expérimental d'Amontons, merite peu d'attention. Je ne m'arrêterai pas non plus, pour ne point charger ces notes de remarques inutiles, à la demonstration géométrique fondée sur cette hypothèse, demonstration qui est très-fautive.)

The American War of Independence had profound effects in all of Europe. In France at the end of the *Ancien Régime*, prominent intellectuals such as Voltaire and lawyers such as Robespierre considered the possibility of changes in the Catholic Church and in the French Monarchy. Similar intellectual views led to a Scottish Enlightenment in Edinburgh, where David Hume was a leading figure. One young Scot there was John Leslie (1766–1832), who later became Professor of Physics at Edinburgh University. He considered heat transfer from the Sun through space, and generation of heat by friction. He knew of the French asperity theory and he queried it. In his book, Leslie (1804, pp. 299–305) expressed his doubts about it as follows:

> If the two surfaces which rub against each other are rough and uneven, there is a necessary waste of force, occasioned by the grinding and abrasion of their prominences. But friction subsists after the contiguous surfaces are worked down as regular and smooth as possible. In fact, the most elaborate polish can operate no other change than to diminish the size of the natural asperities. The surface of a body, being moulded by its internal structure, must evidently be furrowed, or toothed, or serrated. Friction is, therefore, commonly explained on the principle of the inclined plane, from the effort required to make the incumbent weight mount over a succession of eminences. But this explication, however currently repeated, is quite insufficient. The mass which is drawn along is not continually ascending: it must alternately rise and fall: for each superficial prominence will have a corresponding cavity; and since the boundary of contact is supposed to be horizontal, the total elevations will be equaled by their collateral depressions.

Coulomb may well also have had this doubt, but my deduction from the quotations of Leslie and Navier is that the asperity theory of friction was generally accepted in France when Navier himself taught it in 1819, objecting only to Bélidor's geometry. When Bowden and Tabor (1973) wrote their book on friction they quoted Leslie's criticism, but they developed another theory for sliding friction of metal surfaces in which welded junctions grow between asperities under load. In their theory of friction, work is dissipated due to plastic damage at welded junctions. They argued that the total area and total strength of local welds is proportional to the pressure normal to the surface, so for them sliding

friction is due to metallic bonds with what Coulomb would have called *coherence*. Their junction growth theory is accepted today in mechanical engineering, and has been validated by experiments on metal surfaces. In their book, Bowden and Tabor showed the saw tooth slip plane of Fig. 4(b) but they did not discuss aggregates of grains; they wrote that Leslie's criticism of asperity theory

> . . . *remains unanswered. Of course one can say that work is used in dragging a body up a slope and when it gets to the top it falls with a bang, bending and denting the surface, so that all the work done on it is lost as deformation work during impact. If we adopt this view we have gone a long way from the dragging-up-the-roughness model. We are really talking of a deformation mechanism.*

This passage hints that the elastic bending energy in transient deformations is dissipated on unloading. Leslie envisaged an ultimate steady slip process without dilation in which the space between the sliding surfaces is constant. With almost invisible asperities such a process begins after very small displacement. Bélidor's identical asperities are all perfectly in phase, but if the asperities are both very small and irregular then high loads are applied to successive prominent asperities with successive local elastic deflections. If energy stored in elastic asperities is not recovered in Leslie's steady sliding, that could explain what he called *a waste of force*. Coulomb wrote of the molecules of the plane surfaces in contact gaining coherence, but such welding could not explain all the data, for example for slip of wood on wood. While friction, cohesion and interlocking were all thought of as possible components of resistance to slip, Coulomb in 1781 wrote that '*only experiment can help us to decide the reality of these different causes*'. Coulomb published no more on friction or cohesion after 1781, but we cannot conclude that he thought that Eqn (2) had been fully established by scientific experiment. Coulomb, like Washington, had lived and continued working through a time of revolution.

Heyman (1972) tells us that Coulomb held the army rank of Capitaine en Premier de la Première Classe when he was elected to the French Acadamy of Science in 1781. He invented and used a torsion balance for experiments on magnetic forces that were published by the academy. He wrote seven papers on electricity and magnetism that were published between 1785 and 1791, describing his own experiments and putting forward the case for an inverse square law for action at a distance between electrical charges that was similar to Newton's law of gravitation. In his 13 years of military service in Martinique his health had been ruined by fever (much the same happened to 20th-century engineers constructing the Panama Canal). He did not resolve the problem of Amontons' asperity theory, but it is no surprise that he wrote no more on friction and soil strength. His skill in experimental mechanics had won him recognition as what would be called a *scientist* in the 19th century. In Paris, revolutionary activity increased. The Bastille was stormed on 14 July 1789. Coulomb resigned from the army in 1790. William Wordsworth, as a Cambridge undergraduate sympathetic to revolution, went to France in the 1790 summer vacation. He went back the following year, and became friendly in Orleans with a Captain Beaupuy who was in a group fighting for the lost royalist cause. On 4 August 1792 the Legislative

Assembly voted for the abolition of all privileges and feudal rights of the Church and King, and for equality of all in France. A Jacobin mob attacked the Tuileries Palace and killed the Swiss Guards. Royalists were massacred in Parisian prisons; the danger on Paris streets in September 1792 is described in Charles Dickens' *Tale of Two Cities* and in *The Scarlet Pimpernel* by Emmuska, Baroness Orczy. When the Academies were suppressed, Coulomb went to his house in Blois in 1793 to live outside Paris and make scientific experiments. Washington proclaimed the neutrality of the USA in respect of European wars in 1793. After the consolidation of power in France under Napoleon began, Coulomb was elected in December 1795 to the Institut de France that replaced the former Academy of Sciences. In Coulomb's final years between 1802 and 1806 he was Inspector General of Education under Napoleon, and was active in setting up the system of *lycée* schools across France. He had clearly stated his educational intentions 30 years earlier:

> *J'ai tâché autant qu'il m'a été possible de render les principes don't je me suis servi assis claires pour qu'un Artiste un pue instruit pût les entendre & s'en servir*

> *(I hope that it is possible for me to make the principles that have served me clear enough for a builder without higher education to understand and to follow them.)*

1.5   Coulomb's law

The slip plane model dominates soil mechanics, but no other branch of continuum mechanics considers the vector of stress on any plane to be important. Coulomb's notable achievement in using calculus to find Eqn (5) and to explain how friction and cohesion together affect lateral earth pressure did not discover a law of nature that makes soil an exceptional continuum. What civil engineering students should learn as Coulomb's law rather than Eqn (2) or (5) is the truth in his Essay in the repeated words '*Cohesion is zero in the case of newly disturbed soils*'. They should learn to reconcile soil mechanics with the theory of plasticity. The apparent cohesion of soil is behaviour due to solid-to-solid contact of interlocking grains, not to electrochemical bonds that make grains *cohere* when they are close. If an aggregate of solid grains has become cemented together to form a solid body and then is broken up, it at first forms lumps that act as soft rubble, and is freely draining while it has large connected voids. Coulomb's workers excavated soil by pick and shovel, wheeled soil lumps in a barrow and tipped them into place in fill behind a retaining wall. Since the lumps formed a slope at an angle of repose when tipped into the fill, they would seem to an 18th-century engineer to have friction but not cohesion. The introduction to Coulomb's 1773 Essay says that it was originally meant only for his own use in the different tasks in which he was professionally engaged. Presenting it to the Academy as a subject of practical use he wrote

> *the Sciences are memorials dedicated to the public good, with each citizen contributing to them according to his capabilities. While great men, installed in the roof of the building, design and build the upper stories; ordinary workmen, scattered in the lower stories, or hidden in the darkness of the foundations, only try to perfect that which more capable hands have created.*

He did not report new test data supporting a law of slip plane strength. He considered the static equilibrium of masonry, and gave an improved lateral earth pressure calculation that other engineers might use for backfilled walls.

Coulomb invented an accurate torsion balance with which, as a scientist, he got data that clarified the physics of interaction at a distance between electrostatic charges. As an engineer he knew that construction engineers who select materials carefully, and are vigilant as their work progresses, can rely on simple serviceable principles even though these do not have the authority of physical law. Disturbance breaks cemented bonds in an aggregate of grains until, as more bonds are broken, it forms a soft paste of silt-size grains. Ultimately, when mixed into water each grain can act separately and be dispersed so that it settles with a velocity related to the small grain diameter, or small grains can aggregate in *flocs* that settle at a terminal velocity in water related to the size of the floc. At various stages of disturbance as the size of the aggregated lumps or grains and of the pores in the aggregate gets smaller the disturbed soil becomes less permeable, and if there is air in some pores the soil behaviour will be too complicated to discuss in this book.

By the 20th century, elastic solids were no longer explained by Young's modulus of elongation of a fibre normal to a particular plane but as a combination of a bulk and a shear modulus. Friction was no longer explained as work done in surmounting asperities but in terms of the energy dissipation in damage to surfaces. The OCC model is defined in terms of the energy dissipation in a volume of grains. Possible forms of damage are the crushing of a soil grain or one grain scratching a face of another grain. Terzaghi taught that strength depends on effective stress. The slip plane model has remained in use, but engineers do not discuss dissipation or study interlocking or use the slope angle ϕ_d of a heap of loose granular aggregate to define friction. Both cohesion and friction are obtained from tests of soil in a shear box or a triaxial cell. If pore water with a pressure u saturates the pores in the soil specimen in the shear box in Fig. 1(a), or if part of the total load P across CM in granular rock body in Fig. 4(a) is carried by pore fluid pressure u, the total load divided by the slip plane area gives the total stress σ normal to the slip plane. Equation (1) is used to find stress components (σ', τ) normal and tangential to the slip plane, and these effective stresses are used in the slip plane model of the strength of rock and soil (Eqn (2)). These components apply in drained tests in a shear box such as is sketched in Fig. 1(a). Figure 9(a) (Section 2.1) plots Taylor's data of paths to peak strengths τ in two tests in drained equilibrium at two different aggregate packing densities (Taylor, 1948). The slip plane model of soil strength (Eqn (2)) with cohesion c and coefficient of friction $\mu = \tan\phi$ is plotted in terms of effective stress in Fig. 9(b) (Section 2.1). The line with slope ϕ through peak strength data points has cohesion c, given by the intercept of the line with the τ axis. Stress paths in Fig. 9(b) rise to a peak and then fall to an ultimate value on the CS double line. Coulomb and Rankine designed for the case of soil with zero cohesion (states on the CS line AC in Fig. 5(c)), but by the early 20th century the use of the Mohr–Coulomb model of strength generally included cohesion; in this model, no shear stress component τ on any possible slip surface through rock and soil may exceed a limiting value in Eqn (2). Terzaghi and Hvorslev proposed a modification by

which in Fig. 5(d) the peak strengths on the line BC are regarded as the sum of *true cohesion c* and *true friction* (given by the slope of BC). Skempton at Imperial College regarded Terzaghi's theories as fundamentally true, and advised Roscoe to base research at Cambridge University on Hvorslev. My view is different, that drained slopes of heaps of aggregate at repose at an angle ϕ_d give the basic friction coefficient $\mu = \tan \phi_d$, and that peak strengths result from adding Taylor's interlocking to this basic friction.

2 Interlocking, critical states (CS) and liquefaction

Where Amontons had proposed that interlocking caused friction, Taylor found experimentally that ultimate steady friction and interlocking must be summed to give the peak strength on slip planes in dense sand. This work led to the CS concepts of the Frontispiece, and leads to questions on liquefaction.

2.1 An interlocking soil strength component

Volume 6 of *Géotechnique* includes an obituary of D. W. Taylor, who at his death in 1955 was an associate professor at MIT. Shear box experiments on dense and loose sand (see Fig. 9(a) and Taylor, 1948) gave him an insight into energy dissipation in soil. In the sketch in Fig. 1(a), a dashed line shows the piston, and a dotted line shows the mid-plane of the box. Figure 10(b) sketches development of the shear stress τ on the mid-plane in a shear box with what Taylor called *interlocking* as the shear displacement x increased in a test at constant effective normal stress σ'. Figure 10(a) shows volume change with piston movement dy for a dense sand aggregate. Figure 10(b) shows that the shear strength τ reaches a peak. Taylor saw that interlocking is a maximum at peak strength; at the point with a maximum gradient dy/dx (although his book does not give Eqns (6), (7) and (8) below). The terms $+\tau\,dx$ and $-\sigma'\,dy$ in Eqn (7) relate to work that is done by stresses during boundary movements that are in the direction of the force with which they are associated; the term $\mu\sigma'\,dx$ relates to the work that is dissipated in friction; and the displacement dx is not in the direction of the force that is associated with the stress σ'. In Eqn (8) the ultimate CS strength at Taylor's large strain constant friction of Fig. 9(a) gives the coefficient μ on the mid-plane at the maximum peak strength.

$$\tau\,dx = \mu\sigma'\,dx + \sigma'\,dy \tag{6}$$

$$\tau\,dx - \sigma'\,dy = \mu\sigma'\,dx \tag{7}$$

$$\tau = \mu\sigma' + \sigma'\,dy/dx \qquad \text{so} \qquad \tau/\sigma' = \mu + dy/dx \tag{8}$$

Taylor also saw that an increase in the effective pressure reduces the interlocking, so that above a critical effective pressure there will not be an increase of volume but a reduction. A different book might embark at this point on a review of published data of tests on various soils in various different shear test apparatus, but here it is more important to consider logically the consequence of the equations. I assume that at large displacement the ultimate strength falls to a CS value, and I have sketched curves in Figs 10 and 11 that resemble Taylor's data in Fig. 9(b). In
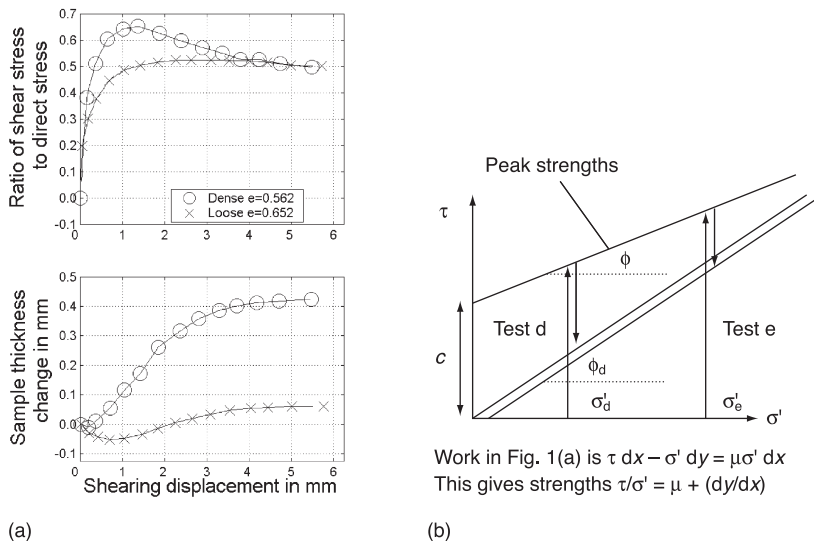
Fig. 9 Shear box tests. (a) Taylor's sand data. (b) Drained shear box test peaks

Fig. 11(b) the peak strength on BC is the sum of friction ($\mu\sigma'$) and interlocking ($\sigma' \, \mathrm{d}y/\, \mathrm{d}x$) as shown in Fig. 10(c) with peak strength point P plotted on BC. Figure 10(b) gave one test d under constant effective normal stress σ'_d; Eqn (7) and Fig. 11 led me to sketch curves of shear stress versus displacement for more shear box tests e, f and g at constant effective normal stresses $(\sigma_e, \sigma_f, \sigma_g)$.

The sketched paths d, e, f and g between peak and ultimate strength in Fig. 11 follow the logic of Taylor's data. After high peak strengths (P_d, P_e) on line BC in
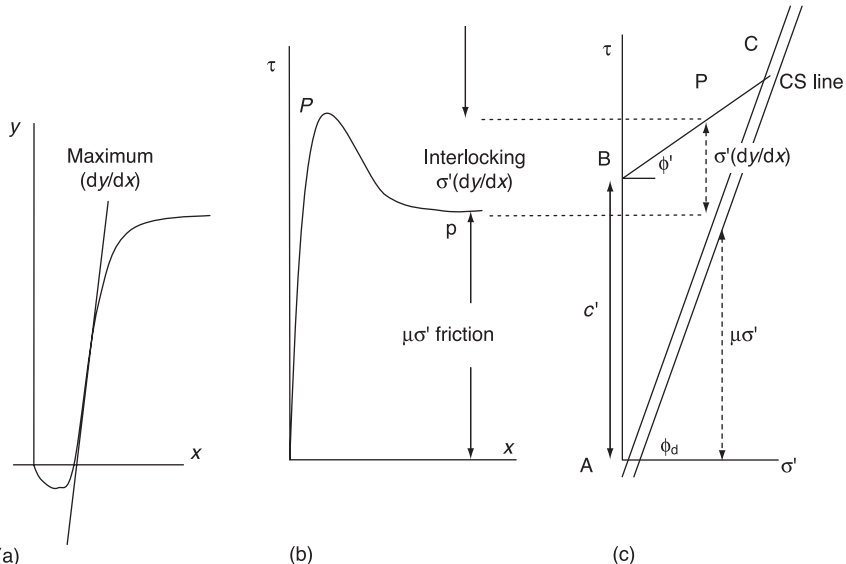
Fig. 10 The interlocking component of strength in a drained shear test
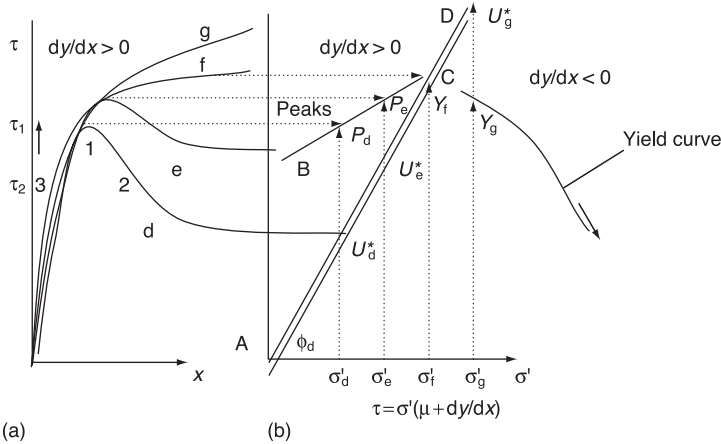
Fig. 11 Interlocking decreases as pressure increases

Fig. 11(b), the test strength at large displacement falls ultimately to (U_d^*, U_e^*) on the CS line AC. Work enters the shear box as the shear stress τ moves through the shear displacement dx; work leaves as the normal stress σ' on the sand rises through the vertical displacement dy. Taylor assumes that the difference between these amounts of work is dissipated in internal friction and equals a quantity $(\mu\sigma'\,dx)$ found by multiplying the normal stress by the shear displacement and by a friction coefficient. He assumes no work is dissipated in volume change. Figure 9 shows Taylor's piston movement before and after peak strength. Equations (6), (7) and (8) are consistent with four supposed test paths sketched in Fig. 11(a); in tests d and e the piston rises; in test f it does not move; in test g it falls. In Eqn (6) the work input from vertical and shear movements are added together to provide the dissipated work. Taylor only considered the work dissipated at peak strength, but, in Cambridge, Thurairajah (1961) found a dissipation function by calculating the work done in every step along a path, before, at and after peak strength. To the right of C, work still came in both from the pressure σ' on a falling piston, and from the applied shear stress τ. The yield stress strength Y_f in test f has a value greater than all the peak strengths along line BC. Beyond C a drained test g in Fig. 11(b) at constant effective pressure $\sigma_g' > \sigma_f'$ follows the dotted path with yielding at a strength $Y_g < Y_f$, but ultimately reaches an even higher strength $U_g^* > Y_f$. The drained test at a normal stress σ_g' slightly higher than σ_f' yields with a lower yield stress Y_g, but this is followed by drained hardening, as shown on the dotted path from Y_g to U_g^*.

Taylor showed dense sand samples with brittle interlocking and loose contractive sand with yielding behaviour. The changing state of any aggregate (at peak strength and on test paths through states before and after peak) is mapped in Fig. 12. In Fig. 12(b) the state of a test specimen gives coordinates (v, σ') of one point. Every state shown in Fig. 12(b) falls into the interlocking I or contractive C zones or on the CS line where the zones meet. In Fig. 12(a) the CS double line has a constant stress ratio $\tau/\sigma' = \mu$, so this corresponds to states with $dy/dx = 0$. In zone I in Figs 12(c) and 12(d), peak strength states on the dotted

Key:
C   Contractive ductile soil $\tau/\sigma' > \mu$ dashed lines
I   Interlocking brittle soil $\tau/\sigma' < \mu$ dotted lines
CS Steady flow of soil $\tau/\sigma' = \mu$ double lines
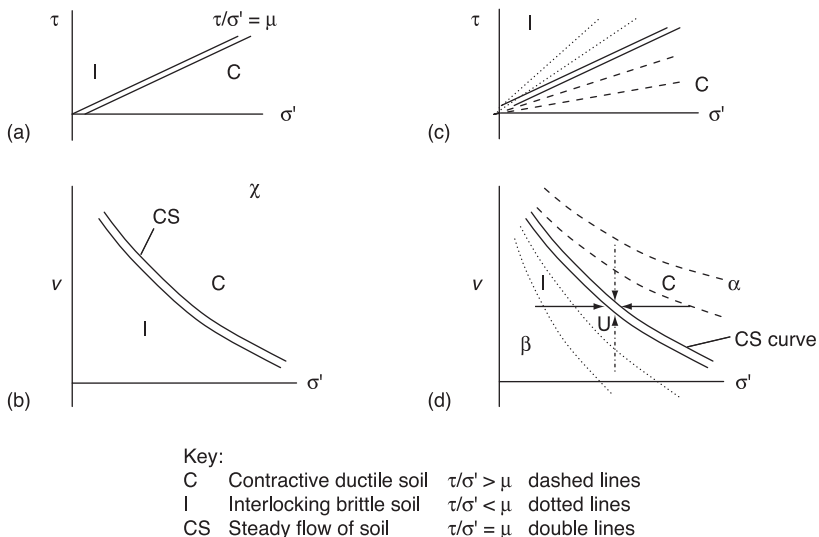
Fig. 12 Variation of interlocking with soil state (v, σ')

lines with $\tau/\sigma' > \mu$ must be for tests with $dy/dx > 0$; zone I has v increasing in drained shear as the piston rises in the shear box. Zone C of contractive soil has decreasing v in drained shear as the piston falls in the shear box, with yielding at stress states $\tau/\sigma' < \mu$ on each dashed line. Three possibilities exist: (i) $\tau/\sigma' > \mu$ in zone I, (ii) $\tau/\sigma' < \mu$ in zone C and (iii) at the curve where zones I and C meet in Fig. 12(b) at $\tau/\sigma' = \mu$ there are states with steady CS flow. The existence of the CS curve follows from Eqns (6), (7) and (8). The form of the CS curve can be found by experiment.

The double lines in Figs 11(b) and 12 should apply to any aggregate of grains that flows with steady deformation at steady pressure and density and forms heaps with a slope at a constant angle of repose for all heap heights. For this class of aggregate we can represent CS strength by a straight double line in Fig. 12(a). Each point on that straight line shows a state below a sliding block in Fig. 5(a), and represents aggregate states at various depths in a heap. The paragraph above explains that a CS curve in Fig. 12(b) must represent constant states (v, σ') of steady CS flow of a grain aggregate. Figure 12 shows zones C and I beside the CS line. Zone C contains contractive soil states; we will later find yielding of soil as a ductile frictional solid with the OCC model in this zone. Coulomb's slip plane rupture occurs in zone I, of interlocking soil behaviour. The argument given above suggests that aggregates that have an angle of repose should have some form of CS line. Roscoe *et al.* (1958) found from test data for fine grain and coarse grain soil that the CS line is a straight line on a $(v, \ln \sigma')$ plot with the equations

$$q = \mathrm{M}p' \tag{9}$$

$$v + \lambda \ln p' = v_\lambda = \Gamma = \text{const.} \tag{10}$$

In the Frontispiece the CS line with equations $v_\lambda = \Gamma = \text{const.}$ and $q/p' = \eta = \mathrm{M}$ is reduced simply to a point, C.

The existence of a peak strength shows the failure of interlocked soil to be unstable. In Taylor's shear box, failure was not instantaneous. Perhaps the large sand grain size relative to the small dimensions of the box delayed localization of failure and caused a gradual fall of strength in Fig. 9 after peak strength rather than sudden instability. In interlocking aggregate, slip planes result from a localization of interlocking that arises as follows. In Fig. 11(a) curve d of τ against x applies to a drained shear box test at constant σ', and the peak strength is marked as point 1, where the shear stress is τ_1. If I consider three neighbouring volumes, peak stress τ_1 must apply to all three. If more strain occurs in the middle volume and the strength in it falls to τ_2, the increase in strain corresponds to movement from point 1 to point 2 on curve d in Fig. 11(a). This reduced stress τ_2 now applies to the two neighbouring volumes to either side, where a fall in the shear stress from τ_1 to τ_2 will correspond to unloading from point 1 to point 3 on curve d; however, strain in the middle volume will run ahead of strain in the neighbouring volumes; both have been unloaded, and no further shear strain is possible during unloading. These blocks to either side are displaced as rigid blocks to either side of a weak localized slip surface where disturbed CS clay sucked in water and has softened. A fall in strength after the peak in an interlocked aggregate localizes progressive failure in an inclined slip plane as sketched in Fig. 2(c); it did not exist before the instability occurred. Contractive soil displacement is quite different and tends to be homogeneous. Small volumes of grains that contract will stop yielding and will form harder volumes beside neighbouring generally softer volumes. Figure 2(c) sketches a ductile test specimen of contractive soil C bulging in compression.

The 18th-century slip plane model was inspired by the observation of slip planes in the field. The instability in a disturbed grain aggregate model continuum explains the development of such planes, and Skempton and Petley's study (1968) of localization of failure in a slip plane will be mentioned later. An increase in the effective pressure σ' and a decrease of the specific volume v will both reduce interlocking (dy/dx). Drained test paths, shown in Fig. 12(d) by two chain-dashed lines with arrows, approach an ultimate critical state U, across dashed and dotted curves in contractive or interlocking zones. The drained test paths in Fig. 11 are sketched to show volume change rates that correspond to the appropriate behaviour at these crossing points, whether the gains are sand size or clay size. Far on the dry side of the CS, over-compaction makes soil so stiff and brittle that cracks open, with undesirable high secondary permeability in the rubble. The optimum most desirable degree of compaction for soil is just to the dry side of the CS in the Frontispiece, where gouge material on a slip plane allows a body to deform with pore water suction, but the body of the ground as a whole remains watertight. Problems of large slow consolidation deformations with yielding and plastic compression make soil states on the wet side of the CS less desirable. In the CS model, local softening or hardening follows changes of specific volume $v = 1 + e$, as the fall from peak to ultimate strength in Figs 10 and 11 is seen as local instability on a plane through an interlocking granular aggregate. When a large body of stiff fissured clay breaks up into a body of rubble it interlocks or slips. The ultimate strength will depend on the CS strength in layers of gouge material on contact surfaces between blocks of dense soil with interlocked grains

sucking water into the gouge material. Henkel (1956) discussed the phenomenon of slip planes in softening stiff fissured London Clay, showing water contents in the gouge material on slip surfaces higher than in undisturbed clay beside the slip surface. According to CS theory the strength falls only from peak strength points on BC to points on the CS line (Figs 10 and 11), and design for fully softened strengths on the CS line instead of for peak strength is safe. Strength on the slip surface is seen as due to CS friction and suction in soil paste, rather than in terms of Mohr–Coulomb cohesion and friction.

An alternative to the CS explanation might be a theory that any plate-like grain within the gouge material that happens to be longer than the layer thickness rotates into the slip plane direction. If such an explanation were developed with plate-like grains rotating to align themselves in the slip plane direction, the localization of failure would be a process that depended on the chance that a grain was in a position where this rotation could advance a progressive failure. In this view of the grain aggregate, continued displacement on such a slip plane could lead to a fall to less than CS strength; it might explain why failure of clay in Hvorslev's shear box was sudden. Clay soil grains are small, and localization of displacement in incipient slip planes is delayed only by the time taken to suck a small quantity of water into the voids of a few interlocked grains as the specific volume increases.

Equation (2) (with Mohr–Coulomb soil strength properties of friction and cohesion) can be contrasted with Eqns (6), (7) and (8) (which relate to work dissipated in distortion). Equations (6) and (7) lead to Eqn (8), where the peak stress (τ) for dense sand is seen in Figs 10(b) and 10(c) to be the sum of two strength components: a friction component ($\mu\sigma'$) and an interlocking component ($\sigma' \, dy/dx$). If the cohesion c' in undisturbed rock or soil is independent of the effective pressure σ', then Mohr–Coulomb undisturbed peak strengths lie on line BC$'$ that is parallel to AC in Fig. 5(c) and at a constant distance c' above it. Figure 10(c) draws a line BC to fit peak strengths in the way that Hvorslev interpreted his data, supposing that peak strength is the sum of a large true cohesion c' (constant as normal stresses increase), and a friction component $\mu\sigma' = \sigma' \tan \phi'$ (less friction because Hvorslev's $\phi' < \phi_d$ is less than the angle of repose). Figure 10(b) sketches friction and interlocking components of strength for one specimen in a drained shear test under constant normal effective stress σ'. Figure 11(a) sketches curves of τ against shear displacement x for three specimens d, e and f, all initially at the same specific volume but under different effective normal pressures σ_d, σ_e and σ_f. The curves of τ against x in Fig. 11(a) represent successive uniform states on test paths, in a shear box that imposes uniform conditions in an aggregate of grains in shear, while a specimen is free to change volume and pressure is held constant. If we think of soil as an elasto-plastic solid, then in test g before stress Y_g the soil is elastic and at Y_g it yields. If we had an unloading cycle after Y_g we would find that it had yielded with plastic deformation. The curves sketched in Fig. 11(a) show how an increase in pressure σ' will reduce interlocking (dy/dx). The strength on line BC in Fig. 11(b) is the sum of a CS friction component $\sigma'\mu = \sigma' \tan \phi_d$ and an interlocking component that is large at low stress at B and decreases from B to C. The strengths at first increase along the line BC in Fig. 11, but to the right of C as effective normal stresses on the set of soil specimens increases above σ_f' their ultimate strength increases along the line CD to values $\tau = \sigma' \tan \phi_d$. The

contribution of power input from the contractive effect suppresses the brittle peak strength along line BC and makes it easy for soil to yield to the right of C. High effective stress makes brittle dense aggregate become ductile. In both Figs 10(c) and 11(b) the double lines of fully disturbed CS strengths $\tau = \mu\sigma' = \sigma' \tan \phi_d$ apply to loose soil as in a heap at repose. The CS double line represents the ultimate strength of a disturbed soil specimen at large deformation under effective normal pressures σ_g. In a set of several different specimens the soil behaviour becomes contractive as the effective normal stress increases from σ_f' to σ_g'. The interlocking effect is replaced by contraction. A *contractive* component $\sigma'(dy/dx)$ is subtracted from the frictional component $\mu\sigma'$, giving yield strengths that are on a curve below the CS double line and also below the extension of line BC. A grain aggregate is brittle at low pressure but above the pressure denoted by point C it becomes increasingly ductile; the high effective pressure makes contractive soil very slippery.

Displacements dx and dy in Fig. 2(a) are associated with the horizontal shear force τ and the vertical effective normal force σ'. The peak power $\tau(dx/dt)$ is equal to the rate of working $\sigma'(dy/dt)$ at the peak rate of volume change plus the power dissipated in friction, $\mu\sigma'(dx/dt)$. The displacement dx is not recovered when the shear force τ is removed. The normal force σ' is held constant in a drained shear test by a constant load on a loading hanger, and the work done by the shear force τ to lift the hanger load during dilation dy is recovered, not dissipated. The work dissipated in the sand sample is the difference between the work done by the shear force $(+\tau\,dx)$ and the work on the rising piston $(-\sigma'\,dy)$. When Eqn (6) is rearranged in the form of Eqn (7), then the term on the right in Eqn (7) is called Taylor's dissipation function for internal friction in the aggregate of grains:

$$\tau\,dx - \sigma'\,dy = \mu\sigma'\,dx \tag{7 bis}$$

Equations (2) and (7) can be checked if the alternative components of shear box test data at different σ' pressures are compared. The contrast between them is clear. Equation (2) predicts that the cohesion component of strength is unaltered by pressure, whether to the left or the right of point C in Fig. 8(b). Equation (7), applied through the shear displacement x, predicts the strength τ both of interlocking and of contracting soil. During shear displacement, dense sand expands. The term dy/dx in Eqn (7) is positive, with τ/σ' greater than μ. Loose sand contracts; the term dy/dx is negative, and Eqn (7) predicts that τ/σ' will be less than μ in Fig. 11(b) to the right of point C. Test data confirm the predictions of Eqn (7) rather than of Eqn (2).

Equation (7) and Fig. 12 have further implications. Taylor himself interpreted the interlocking component of peak strength in soil at peak stress as if it were an increase in the angle of friction $\phi > \phi_d$, giving $\tau/\sigma' = \tan \phi < \mu = \tan \phi_d$ with lines (dotted in Fig. 12(c)) that have steeper slopes than the double CS line at the angle of repose. In the Frontispiece the stress ratio value $\eta = M$ at point C represents the whole of the CS line. In Fig. 12(d) the straight chain-dashed arrows represent drained test paths that approach a state U on the CS line. The straight solid arrows represent undrained test paths that also approach U. At a point at which an arrow in zone D crosses a dotted curve in Fig. 12(d) the rate of change of the volume in a drained test or the rate of change of the pore water

pressure in an undrained test has a particular value corresponding to the dotted lines in Fig. 12(c). Taylor showed curves like those dotted in Fig. 12(d). In Figs 12(c) and 12(d) each dashed line in zone C relates to a certain rate of soil contraction in shear. As the behaviour depends on the distance from the CS line in this way, data at the end of tests approaching CS should show one group of test paths in which the specific volume increases in drained tests or the pore water pressure decreases in undrained tests, and another group of paths where the specific volume decreases or the pore water pressure increases; this effect was found by Parry (1959).

2.2 Frictional dissipation of energy and the CS

Hvorslev's thesis had already shown that CS soil behaviour applies both to clay soil and to sand 10 years before Taylor published his data of interlocking in sand in 1948. When the data of triaxial tests on clay began to be studied in 1950 and the work associated with volume changes of test specimens at peak strength was calculated, Bishop (1954) introduced the term *boundary energy correction* for what he envisaged as a small contribution to be added to cohesion and friction to allow for the effect of interlocking on the peak strength of dense clay. We (Roscoe *et al.*, 1958) referred to this correction in our *Géotechnique* paper 'On the yielding of soils'; we had a misprint where '*boundary error commission*' was unfortunately printed, which should have read '*boundary error correction*'. I did not understand at that time that the whole strength of disturbed soil can be found by combining Taylor's interlocking (*boundary energy correction*) with CS friction in the CS model of soil behaviour. Understanding that apparent cohesion is due to interlocking is more important than introduction of a small correction to triaxial test data. When we (Roscoe *et al.*, 1958) proposed the CS interpretation of triaxial compression test data we wrote these words:

> Hvorslev's equation for the shear strength of clay (defines) a surface in a space of three variables σ', e, τ. The progressive yielding of a sample defines a loading path in this space, and the paths taken by samples in differing tests can be correlated if a boundary energy correction is applied. The final portions of all paths then lie in a unique surface, and the paths end at a unique critical voids ratio line. At the critical voids ratio state unlimited deformation can take place while σ', e and τ remain constant.

We considered an isotropic grain aggregate in terms of a *void ratio e* or the *specific volume* $v = 1 + e$ in Fig. 2(a), the volume of space in which a unit volume of solid grains is packed. In an undrained triaxial test in Fig. 2(b) the pore water pressure u is measured at the pore water connection in the pedestal on which the specimen stands. In a drained test, pore water can drain out and give the volume change of a specimen. The mean normal pressure that acts effectively between the grains in an aggregate is denoted as $p' = (\sigma'_a + 2\sigma'_r)/3$, and $q = \sigma'_a - \sigma'_r$ is an isotropic invariant measure of shear stress. The state (p', q, v) of soil changes during soil deformation. We considered the ultimate steady CS flow of test specimens. Schofield and Wroth (1968) taught that ultimate fully disturbed-soil grain aggregate strength is predicted by the CS steady-state Eqns (9) and (10) below,

and that only this CS strength is reliable in a plastic design. We expressed the CS concept as follows:

> *The kernel of our ideas is the concept that soil and other granular materials, if continuously distorted until they flow as a frictional fluid, will come into a well defined state determined by two equations*
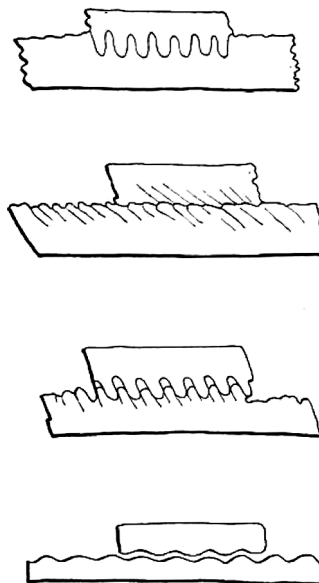
$$q = Mp' \qquad\qquad\qquad (9\ bis)$$

$$\Gamma = v + \lambda \ln p' \qquad\qquad\qquad (10\ bis)$$

> *The constants M, Γ, and λ represent basic soil material properties and the parameters q, p' and v are defined in due course. The equations of the critical states determine the magnitude of the 'deviator stress' q needed to keep the soil flowing continuously as the product of a frictional constant M with the effective pressure p'. Microscopically, we would expect to find that when inter-particle forces increased, the average distance between particle centers would decrease. Macroscopically the second equation states that the specific volume v occupied by unit volume of flowing particles will decrease as the logarithm of the effective pressure increases.*
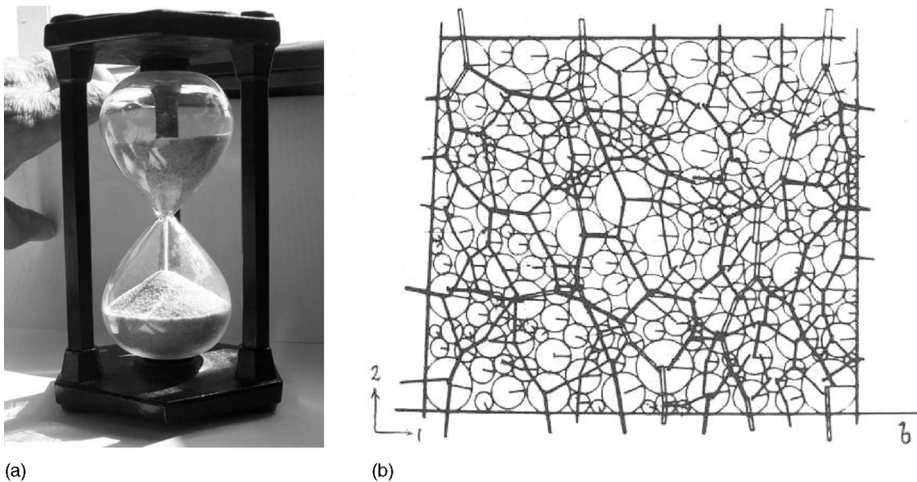
The friction coefficient is denoted by the lower-case Greek letter μ in Eqn (2) and by the Greek capital letter M in Eqn (9). The function on the right side of Eqn (8) gives the dissipation of energy in internal friction in distortion of soil. The CS definitions above do not state what local physical phenomena cause power dissipation in CS flow, but I assume that the same phenomena that cause internal friction in a grain aggregate also make a loose heap stand with a constant angle of repose. Coulomb in 1781 suggested that one cause of friction is dissipation of stored elastic energy, as follows.

   Coulomb made tests on lubricated sliding friction in a French naval dockyard (naval constructors have a problem if ship's hulls, constructed on land, stick on the slipways and cannot be launched into the fitting-out basin). He used many materials, with slip at different speeds, both when surfaces stick, and when slip restarts. His report on the tests won a double prize of the French Academy. It noted variations of resistance to slip of wood on wood unlike slip of metal. His explanation was that when wood slides on wood, stubby brushes of flexible fibres bend and store energy as they brush against each other (Fig. 13). When the end of a fibre slips past a restraint it springs free, and the stored energy is not recovered. This suggestion for wood could also apply to successive prominent asperities on any slip plane that are elastically stressed and suddenly unloaded in slip, and to grains that are elastically stressed and suddenly unloaded in an increment of deformation of an aggregate of grains. Since Coulomb relied on ϕ_d he did need to develop this suggestion or give any further explanation of power dissipation in internal friction in soil. Schofield and Wroth's (1968) discussion of steady CS flow explicitly considered a process without degradation or orientation of grains. The back cover of this book and Fig. 14(a) show a conical heap of sand at repose in the bulb in the lower half of a time-glass. Tests of a plane model of a grain aggregate with stress-sensitive circular discs seen in polarized light showed lines of highly stressed grains, also found in a discrete numerical model

Fig. 13 Dissipation of elastic energy (wood fibre brushes) (Coulomb, 1781)

(Fig. 14(b)) (Cundall and Strack, 1979). This suggests an explanation that applies in the first instance to the very lightly stressed aggregate near the surface of a slope at repose where rough strong elastic grains form columns in compression. If three-dimensional frameworks of lines of highly stressed grains support the normal and shear stress in a loose aggregate below a slope at repose, then when a line buckles the aggregate will yield; new lines form from grains that were lightly stressed, and they then bear new high stress.

(a)   (b)

Fig. 14 (a) Sand in a time-glass. (b) Aggregate in plane stress (with highly stressed grain columns) (Cundall and Strack, 1979)

Site investigations classify disturbed soil samples broken up in water. A judgement is made about the degree to which friable grains or grain clusters may break up when soil flows as a paste in the expected failure. Wet sieving and sedimentation analyses determine grain sizes. The MIT soil grain size classification uses the words 'coarse clay', 'silts' and 'sand' for grains of 2, 60 and 200 μ size, respectively. I visualize an aggregate of grains as large blocks of more familiar sizes (a bicycle, a building, and a city block are 2, 60 and 200 m, respectively). In chaotic dumps of large blocks between the sizes of a bicycle or a building, forming heaps of aggregate at repose 100 m high over the area of several city blocks, it would be an impossible task at any scale to record the position and details of each surface of each block. A CS flow of grains is like such blocks in slow motion. It would be impossible to record the positions and sizes of flaws everywhere, and to find the forces at every contact of blocks where a load application might initiate fractures during chaotic motions. However in the slope at repose in Fig 14(a), each hard grain has survived innumerable highly stressed loadings and has developed a rounded grain shape that make fracture of any grain increasingly unlikely. Micro-mechanical models might envisage a frictional fluid flow of hard grains of random shapes and sizes with rounded corners and edges, and a CS law might result from repeated impact between elastic grains with conservation of linear and angular momentum and dissipation of energy in damped vibrations in a soil continuum. Aggregates can form heaps with a constant angle of repose, and be unable to slump further into a slope that is less steep; I think the limiting condition must be when the work done as grains fall further in the Earth's gravity field is less than the work that must be done in further distortion of the aggregate of grains. Discrete numerical models might well develop, at some future date, to a point where such reasoning is as reliable as that of the kinetic theory of gases, and statistical studies might explain the way that grains of widely dispersed sizes and shapes move relative to each other in CS flow. However, without having to analyse the micro-mechanics of CS flow at the grain scale, CS theory has made progress with a grain aggregate law for energy dissipation in shear flow that is like a gas law. In the Frontispiece, CS frictional dissipation in disturbed aggregates of grains is assumed to apply at all stages of yielding on test paths, as well as when the soil state reaches the CS line (Eqns (9) and (10)).

2.3   Reynolds' dilatancy and Hazen's liquefied soil

Amontons published his paper on friction at the turn of the 18th century. His thought, that friction resulted from what Reynolds (1885) called *dilatancy* and Taylor (1948) called *interlocking*, does not seem to have been the subject of clear discussion or of good experiments until Taylor's work. In a Rede Lecture in the Senate House of the Cambridge University, *On an Inversion of Ideas as to the Structure of the Universe*, Reynolds (1902) demonstrated dilation with two rubber balloons, each full of coloured water that his audience saw standing in a tube above each balloon. One balloon contained only water. The other contained a dense aggregate of small solid grains with water in the voids. He squeezed each balloon in turn. The audience saw water rise in the tube from the water-filled balloon but, when he squeezed the balloon that held grains, they saw with surprise

that, although he squeezed the balloon, the water moved down the tube into the enlarging voids as the aggregate dilated. He repeated what he had said in 1885, that this explained something that they might have seen at the seaside:

> *A well-marked phenomenon receives its explanation at once from the existence of dilatancy in sand. When the falling tide leaves the sand firm, as the foot falls on it the sand whitens, or appears momentarily to dry round the foot. When this happens the sand is full of water, the surface of which is kept up to that of the sand by capillary attraction; the pressure of the foot causing dilatation of the sand, more water is required, which has to be obtained either by depressing the level of the surface against the capillary attraction or by drawing water through the interstices of the surrounding sand.*

Reynolds predicted that study of the property of dilatancy *would place the theory of earth pressure on a true foundation*, but he did not discuss earth pressure problems (he left them for engineers to solve). He wanted in his 1902 lecture to resolve the cause of electromagnetism, a problem unresolved by Cambridge physicists. Maxwell had died in Cambridge in 1879. In 1865 he had related electromagnetic waves and electrostatic displacement curves, and Gibbs had rewritten Maxwell's relations as vector equations in 1884, but no-one had given a physical explanation of the equations linking electricity and magnetism. It was not surprising that Reynolds should feel confident in his proposal; the vortex effect in fluid flow had been an unresolved problem until he made experiments. Kelvin (well known for his self-confidence) had published a paper sketching granular ether with no experimental data. From his experiments, Reynolds suggested that dilation '*places a hitherto unrecognized mechanical contrivance at the command of those who would explain the fundamental arrangement of the universe*'. He thought of the '*luminiferous ether*' as an aggregate of very small spheres with cyclic transverse shearing (electromagnetic waves) causing cyclic dilation (electric *displacement* currents). Cyclic dilation could explain the oscillation of electrical charge in Maxwell's displacement current, with electromagnetic waves propagating in the proposed granular ether. Reynolds' 1902 lecture followed 17 years of personal study (including study of how energy dissipation in the granular ether of his universe could explain why the night sky is dark). Cambridge University Press published his monograph on the structure of the universe, but demonstration of dilation failed to make his ideas credible to a Cambridge audience that probably included one of his own Manchester students, J. J. Thompson, who had been elected in 1884 at the age of 28 to follow Maxwell as Cavendish Professor of Physics in Cambridge. In 1897, Thompson's experimental study of conduction through gases in Cambridge had led him to the epoch-making discovery of the electron. He respected Reynolds as his former professor, but he rightly thought the ether dilatancy concept to be flawed. Nobody discussed Reynolds' granular ether after 1902, but he had not been entirely foolish to pin his hopes on changes in length with dilation. We can read in Feynman's 1963 lectures (Feynman *et al.* 1965) that, as a distribution of moving electrons oscillates to and fro, transient shrinkage of space-time geometry (Lorentz' contraction of space-time) causes transient changes of charge density and hence changes in the electrostatic forces on nearby static electrons. Lorentz' idea was even more fantastic than Reynolds' link
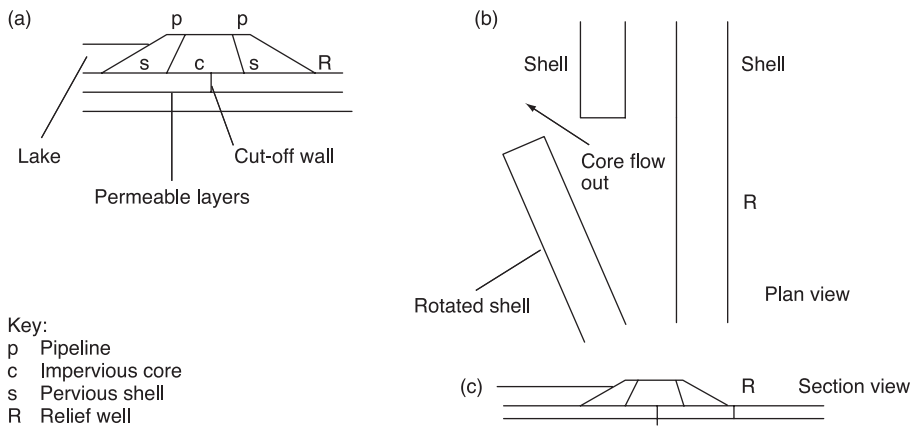
Fig. 15 The Fort Peck Dam failure, 22 September 1938

of electromagnetism with dilation of his supposed granular ether, but a relativistic contraction of space is now accepted as the cause of electromagnetic waves.

However, Casagrande (1936) recalled Reynolds' volume change in aggregates when he introduced the critical voids ratio concept to explain the liquefied soil that Hazen (1920) had mentioned in a paper on hydraulic-fill dam failures. Hazen wrote that the hydraulic-fill method of dam construction grew out of the process of hydraulic mining that moves slurry in pipelines at very low cost. Figure 15(a) illustrates the method of construction, with points p showing a pair of pipelines. The discharge of the slurry deposits gravel and sand on an upstream and a downstream beach near to each pipeline, while fine soil grains are carried into the pool (c) between them. As each deposit rises, it forms what Hazen calls a *toe* dam, but Fig. 15(a) calls a *shell* (s). Hazen notes many failures during construction because fine-grained materials '*that have not consolidated to the point of stability ... remained in almost liquid form, dividing the (toes) and tending to disrupt them ... [The] core material is so fine in grain size that it is incapable of drainage ... within a reasonable length of time*'. Hazen notes that in the core very fine solid grains '*settle down and consolidate while the water moves upward between them to the top ... [The core] acts essentially as a heavy liquid ... and exerts the full lateral pressure corresponding to its height*' on the two shell banks. Hazen refers to the '*Calaveras Dam near San Francisco Cal. which slipped as it was approaching completion on March 24th 1918 (in which) the weight of material pushed forward in the up-stream toe was five times as great as the pressure of core material against it*'. From this he estimates a friction coefficient of only 0.2 between the dam and its foundation.

Figure 15(b) shows a plan view of a later but similar slide that occurred on the upstream face of Fort Peck Dam on the Missouri river in north-eastern Montana; Fig. 15(c) shows the cross section of this dam. The slurry discharge forms the beaches that create the pervious banks upstream and downstream of the core pool; they hold the fine soil grains in the core pool. After this fine soil consolidates it forms the soft impervious core to the dam, but while the fine grains are in suspension in the core and remain fluidized with no effective stress at any depth

the total core pressure acts as a pore fluid pressure. High hydraulic pressure at the base of the core, transmitted down the sides of the cut-off wall sheet piles (Fig. 15(c)) entered the horizontal permeable layers, and was transmitted laterally. During construction, water issued from pressure relief wells *R* at the downstream toe of the dam, and a corresponding uplift pressure must have acted (unseen) below the upstream bank. As the reservoir filled, the effective vertical stress below the upstream shell was reduced to only the buoyant weight of the soil. Piles were used to support the hydraulic pipelines. Every time a pipe was moved, new piles had to be installed. Piling proved hard, and engineers employed water jetting to assist penetration. That increased the pore pressure in the region of failure. The uplift pressure below the upstream embankment slope reduced the friction resisting the lateral pressure of the fluidized core. Aerial photographs of the failure on 22 September 1938 (Fig. 15(b)) shows that a length of the upstream shell rotated as a rigid body (swung open like a 'barn door') and let core material flow upstream into the lake. When the lake was drained after the failure, the soil that had flowed from the core lay as a horizontal layer across the lakebed.

The condition in the hydraulic fill as solid grains *settle down and consolidate while the water moves upward between them to the top* is no different from that described by Terzaghi and Peck (1948) (T&P) when an upward seepage gradient causes sand to boil in the floor of an open excavation. Chemical engineers achieve this condition in fluidized beds; and they have a body of research dealing with it. T&P distinguish between this and the condition of a small group of very fine and very loose sands when they become 'quick' even without a critical hydraulic gradient. Casagrande and T&P both pick up a suggestion with which Hazen ends his paper on quicksand conditions in dams. He discusses the possible effect of a sudden blow or shock that crushes the edges and points of contact between grains to liquefy a certain volume and make quicksand (for a few seconds until the surplus water can get out). Hazen then writes:

> *The thought has occurred to the writer, in looking at the material that slid in the Calaveras Dam, that something of this kind may have happened on a large scale – 800,000 cu.yd. of fill flowed for a brief space, and then became solid . . .*

He continues:

> *It may be that after the first movement there was some readjustment of the material in the toe which resulted in producing temporarily this condition of quicksand, and which destroyed for a moment the stability of the material and facilitated the movement that took place . . . This will not account for the initial movement; but the initial movement of some part of the material might result in accumulating pressure, first on one point and then on another, successively, as the early points of concentration were liquefied and in that way a condition comparable to quicksand in a large mass may have been produced.*

2.4   Hazen's liquefaction and Casagrande

In order to write the word *liquefaction* at a point on the Frontispiece map I must know what the behaviour is and the state of the aggregate in which that liquefaction event occurs. At Hazen's points of concentration a sudden reduction of forces

at contact between grains results from a shock pressure, crushing points and edges of grains, but the total stress still has to be carried after the shock has passed. The sudden fall in the aggregate stress is replaced by a sudden rise in pore water pressure. Pore water cannot drain away instantly. High transient positive pore pressure eliminates positive effective stress that could have generated frictional resistance. Hazen wrote of a sharp blow that '*makes quicksand for only a few seconds until the surplus water can find its way out*', so in an instant a body of water-saturated contractive sand liquefies in a rapid flow of loose sand at constant volume. Casagrande equated this event with an instability (like the buckling of a strut) that occurs in a shear test path. His explanation (Casagrande, 1936) sketched the data of a shear box test of an aggregate of irregular hard soil grains (Fig. 16). The distance between an upper and a lower metal plate will increase if the aggregate is initially dense (Figs 16(a) and 16(b)); the distance will decrease if the aggregate is loose (Figs 16(c) and 16(d)). Figure 16(e) indicates the sort of test path to be expected from sand in a shear box if displacement increases steadily. Casagrande explained that a grain aggregate that is subject to shear distortion has one *critical density* at which it can be distorted without volume change. If it is more dense than critical, the specific volume of interlocked grains must increase in a drained test, and water is sucked into pores that enlarge during distortion. In undrained distortion this pore enlargement is prevented by incompressible pore water that develops suction; as the pore water pressure u in Eqn (1) is reduced, the effective pressure σ' in the grain aggregate will increase, which, Casagrande says, will increase the frictional strength so that '*the mass seems to be bracing itself, to become temporarily more stable*'. On the other hand, in an undrained distortion when the porosity is higher than critical there will be a positive pressure u in incompressible pore water, and a fall in the effective pressure σ'.

Casagrande proposed that all saturated soil without cohesion was at risk of liquefaction if in a contractive state. He began his 1936 paper with a section on '*the meaning of the term stability*', contrasting stable settlement of a building when clay consolidates, with unstable bearing failure when soil stress reaches the peak shear strength. The stable case is like a flexible beam on two supports bearing a central load; his analogue of instability is an attempt to stand a pencil upright on its pointed end. He gave curves of shear stress in drained shear tests versus shear box displacement (Fig. 16(e)). When he compares liquefaction of contractive sand to the instability of a pencil stood on its point, the energy that the pencil gains as it falls in the Earth's gravity gives the pencil increasing momentum. Casagrande once saw a rock rotate as it entered a hydraulic-fill pipe, which led him to think that grain rotation can change an interlocked grain structure to a *flow structure*. To describe the way that he thought of his special flow structure spreading through a loose aggregate under high effective stress he used the words *chain reaction* (echoing words used to describe propagating nuclear reactions). Casagrande expected an uncontrolled flow of energy in contractive soil to cause a *phase transition,* like the change when a crystalline solid melts and becomes a liquid. He made a laboratory experiment with a loose sand model in a tank. He struck the tank with a hammer. It caused liquefaction flow. The aggregate of loose grains had been a rigid solid until, all in an instant, the effective stress fell to a value near zero as a high transient pore pressure was generated. In this view, liquefaction
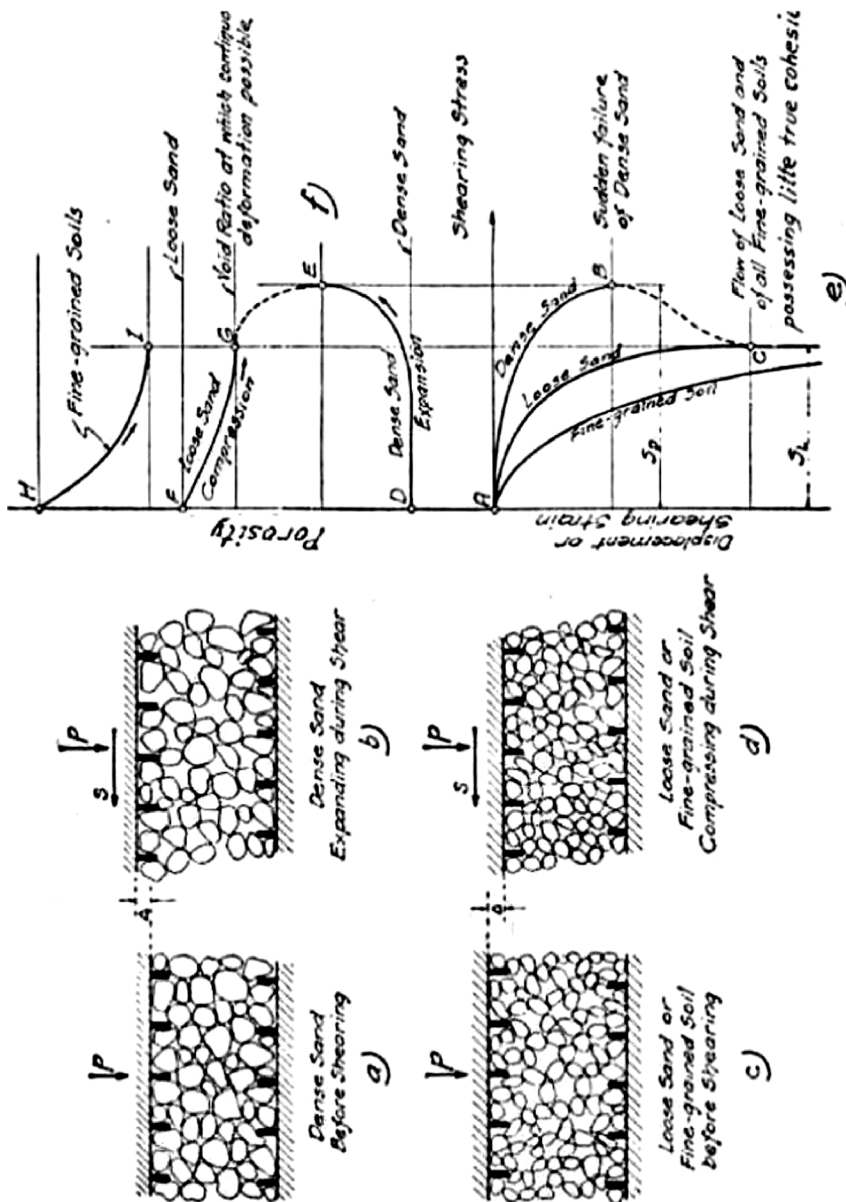
Fig. 16 Casagrande's (1936) explanation of liquefaction

of soil is rather like the collapse of a house of cards. When playing-cards are built up into a fragile house, some cards stand on edge as walls and others are laid across them to form a floor of the house. When the area of one floor is large enough, another floor can, with skill, be built on it. The house may be built up to have several floors, but ultimately the placing of one last card will always lead to an unexpected sudden collapse of the whole card house. This theory of Casagrande was fully accepted in 1937 when the United States Engineer Office in Boston, Mass. confronted the need to construct a large earth dam for flood control purposes at Franklin Falls, N.H. out of fine silty sand. The safety of such an embankment was thought to deserve special consideration, since Casagrande had shown that a large mass of fine-grained soil is inherently unstable unless it is compacted below the critical void ratio. The question immediately arose as to how densely this material should be compacted to be safely below the critical void ratio and triaxial compression tests were used to study this; extensive investigation by means of direct shear tests did not lead to a satisfactory solution.

Casagrande explained pore pressure changes during shear in detail as follows. In shear at constant effective normal stress (Fig. 16(e)) as shear stress on dense sand increases to a peak strength point B the sand expands; loose sand shows a fall in porosity. After large displacement, both loose and dense sand ultimately reach a critical porosity n_0 where sand flows at constant shear stress. His critical porosity n_0 was independent of the effective pressure; loose sand at a porosity higher than n_0 was potentially unstable, like the pencil standing on end. Casagrande proposed that silty sand, if compacted to a porosity lower than n_0, would not be at risk of liquefaction. He showed compression by static pressure following curves such as AB and FG in Fig. 17. His curve ABE for static compression of very loose sand goes from point A under zero pressure and porosity n_1 to a point B at porosity n_2 under pressure p_1. Further pressure increase in a drained compression to p_3 takes the sand to porosity n_0 in a state at point E, where the risk of his liquefaction is eliminated. He then considers a combination of compression and shear distortion. Figure 17 shows pressure increase compressing the loose sand to E, but he writes that static compression is relatively ineffective in reducing the volume, compared with compression combined with drained shear. He supposes that drained shear at constant pressure takes the sand from a state at B to a state C at what he calls the curve of *compression with large deformation*. When this 1936 theory is re-plotted in Fig. 18(a) on axes of $n, \ln \sigma'$ a drained test gives a chain-dashed path from B to C and an undrained test gives a solid path from B to D.

Casagrande supposed in Fig. 17 that there is a particular grain structure at C, and an undrained test reaches an ultimate state point D where a flowing aggregate has the same flow structure at D as at C. Here and in Fig. 18(a), for the sake of simplicity, the double line is for the critical void ratio concept as published by Casagrande in 1936. In Fig. 18(b) the double line is the CS theory, published in 1958. The difference between CS theory and Casagrande in 1936 is that *compression with large deformation* curves will depend on the initial state, but in CS theory after large deformation an aggregate of grains does not retain any record of any initial structure; we sent him a copy of the theory but he made no comment. The curves in Fig. 17 become straight lines when plotted on a log stress base in Fig. 18(a). Curve DC in Fig. 17 becomes the inclined dashed line through C in
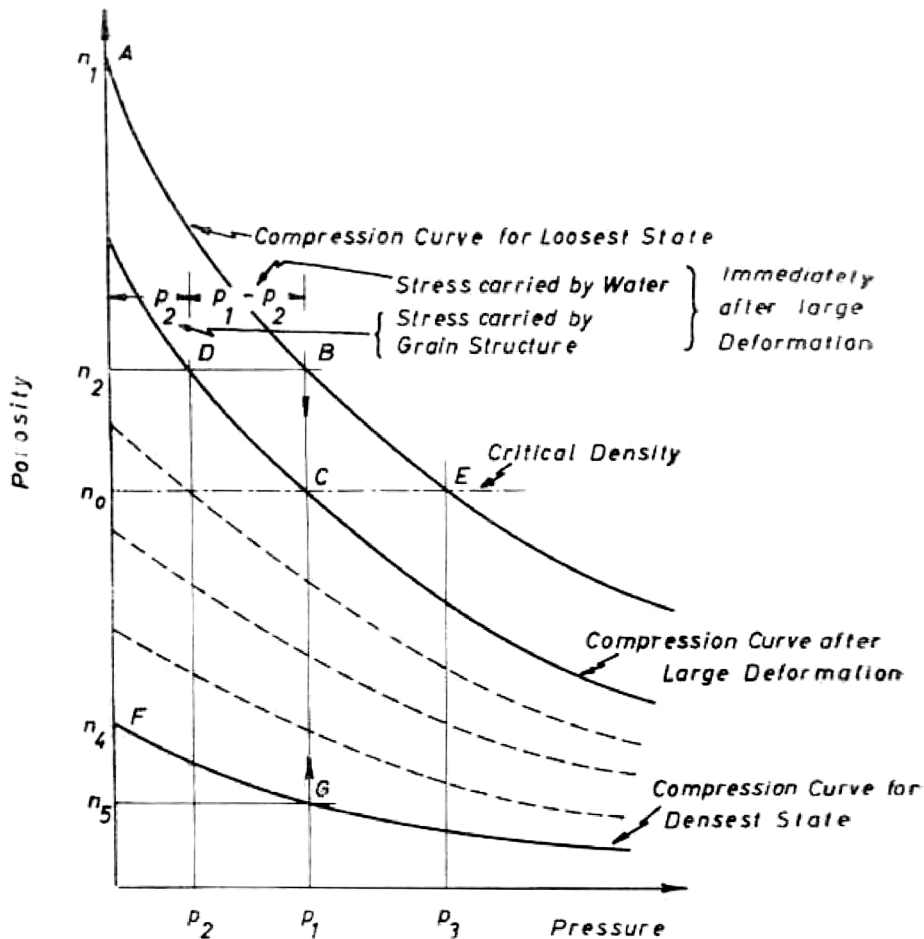
Fig. 17 Pressure–density relationship for sand (Casagrande, 1936)

Fig. 18(a). If Casagrande's curve of *compression with large deformation* is ulti-
mately reached by the soil initially at a state point B in Fig. 17, then in Fig.
18(a) the chain-dashed arrow of a drained test path at constant normal stress σ'
takes the soil from B to C, and the solid arrow of an undrained test path takes
it from B all the way to a point D on the dashed line. States on Casagrande's
curve differ from those predicted on the CS line AH in Fig. 18(b). Our solid
arrow ends at state point K on the CS line and does not continue from K to D.
Casagrande had constant critical porosity in 1936. CS theory combines the specific
volume v and the effective pressure p' in Eqn (7) in a variable $v_\lambda = v + \lambda \ln p'$.
Equation (9) gives $v_\lambda = v + \lambda \ln p' = \Gamma$, for a critical CS line in Fig. 18(b). Casa-
grande (1975) revised his theory of liquefaction and adopted this CS line, as will
be discussed later.

Inclined solid and dashed lines in Fig. 17 become elastic swelling and compres-
sion lines in Fig. 18(b). Roscoe *et al.* (1958) theorized that a large CS deformation
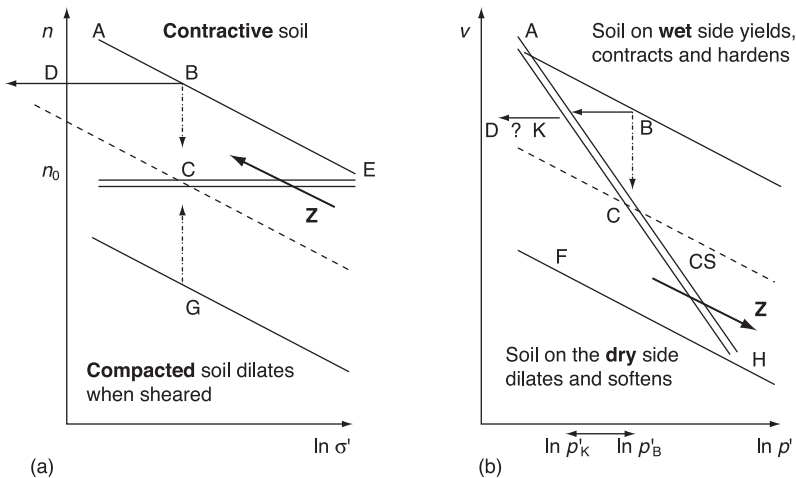
Fig. 18 *Critical porosity n_0 and CSs $(v, \ln p')$. (a) Casagrande constant n_0. (b) Cambridge CS line*

of soil (drained or undrained) destroys any initial structure that the aggregate had in a state such as B. By this CS prediction all test paths ultimately reach chaotic fully disturbed states on a CS curve, and not states on one of Casagrande's original curves of *compression with large deformation*. In Fig. 18(b) the slope of the dashed line DC is less than the slope of the CS double-line AH. Where Casagrande predicted that the stress carried by the water after undrained large deformation is shown in Fig. 17 as the difference, $p_1 - p_2$, between the pressures at B and at D, a CS prediction $p_B - p_K$ is of a pore water pressure that is only the difference between the pressures at B and at K in Fig. 18(b). Casagrande in 1936 had constant critical porosity, as shown in Fig. 18(a) by a flat double line, and he predicted that sand with this void ratio will not change in void ratio or pore water pressure when subjected to shear distortion. He contrasted the instability in a body of contractive sand (caused by a positive pore water pressure during liquefaction) with the strength of a body of dense sand at less than critical porosity (in Fig. 18(b) on the dry side of CS) where shear creates tension in the pore water, and an increase of shear resistance. In Fig. 18(b) the CS double line has a slope that is greater than the slope of the elastic compression lines. The solid bold arrows with the letter **Z** show a striking difference between Figs 18(a) and 18(b). In Fig. 18(a) the arrow shows that a *reduction* of effective pressure is unsafe as the aggregate of grains swells slightly from a *safe dilative* state to an *unsafe contractive* state. Casagrande warned of a risk of the behaviour that Hazen called liquefaction (flow in a critical state) if an aggregate is contractive. Figure 18(b), where the slope λ of the CS line is greater than the slope κ of the elastic swelling and compression lines, has the arrow **Z** showing an increase of effective pressure that carries an aggregate from a *safe dilative* state to an *unsafe contractive* state, that led Casagrande in 1975 to advise his readers that even dense sand, if heavily loaded, can liquefy. This (alarming) advice is discussed later.

2.5 Herrick's liquefaction

Florin and Ivanov (1961) used the word 'liquefaction' to describe the behaviour of a horizontal layer of loose sand when compacted by blasting. If the pores were full of air that could flow out quickly, the layer would quickly settle. If the pores are full of water, that flow takes time. In that brief period the soil grains are suspended in an upward flow of pore fluid, like an upward seepage flow fluidizing sand in the floor of a cofferdam. Chemical engineers use fluidized beds for example in some heat transfer processes. It is worth discussing carefully a difference between the two words *liquefy* and *fluidize* in order to clarify two separate issues. First, did a usage in the English language give the word liquefaction another, better meaning before Hazen? Second, does Hazen's concept of a shock transition in aggregates of highly stressed grains explain observed liquefaction events?

Hazen's use of the word *liquefied* may be questioned. In the SOED the word 'fluid' means '*having the property of flowing; consisting of particles that move freely among themselves, so as to give way before the slightest pressure*', and the word 'liquefaction' means '*the reduction to a liquid state; also the 'melting' of the soul (1711)*'. The words fluidization and liquefaction have about the same meaning, but of the two words liquefaction is used less commonly. A possible reason for the English to prefer to use the word 'fluidization' rather than 'liquefaction' is to avoid any embarrassing reference to the soul and religion. Christian believers in the Middle Ages who saw blood flowing from the wounds on a statue of Christ in a shrine would describe that miracle by the word 'liquefaction'. But a Cavalier poet (1591–1674) famously used the word 'liquefaction' in a secular sense with another precise meaning. Robert Herrick, an English country parson, was a graduate of St John's College in Cambridge. He put the idea of total absence of stress when a light silk dress floats in the air in a poem:

Upon Julia's Clothes

Whenas in silks my Julia goes,
Then, then, methinks, how sweetly flows
That liquefaction of her clothes.

Next, when I cast mine eyes and see
That brave vibration each way free;
O how that glittering taketh me!

Hazen adopted a meaning for *liquefied* that he thought right, unaware of, or ignoring, this earlier meaning. Herrick's secular use of the word 'liquefaction' conveys precisely the meaning that the SOED gives to the word 'fluidization'. In Herrick's use, a light silk dress moves to and fro in the air as Julia's movements cause transient motions. In Hazen's use of the word, his grains initially carry a high stress that (in an instant) is transferred to the local pore water so that the soil body flows as a liquid. In Hazen's use, separate solid grains bearing stress are initially held together as a single body by that stress until, like the fall of a house of cards, an unstable chain reaction is propagated, causing unstressed grains to flow away in suspension in the pore water, as if the aggregate had melted. However, if a buried water main fractures, the escaping water will fluidize the trench fill as it rises in the trench. And similarly, if an oil tank with an area of

$500\,\text{m}^2$ on a layer of saturated sand settles $200\,\text{mm}$ in an earthquake and displaces $500 \times 0.2 = 100\,\text{m}^3$ of water, that escaping water will fluidize the ground around the tank, causing damage. I would then say that there has been settlement of the sand below the tank and liquefaction or fluidization of the sand around the tank.

At the University of California at Berkeley, Professor Seed, once a Harvard student under Casagrande, adopted *zero effective stress* as a criterion when applying finite element (FE) analysis to liquefaction in Californian earthquakes. FE analysis had been used (for example by Professor Ross at King's College London where Seed was once an assistant lecturer) to follow the stress history of each part of a reinforced concrete nuclear reactor container vessel during cyclic loading in service. The aim was to find if the history of cyclic loading would cause fatigue failure at some point in the concrete. Seed needed a failure criterion for soil liquefaction in order to apply this technique to Californian embankment dams in earthquakes. Observing that, as the pore water pressure rose in undrained cyclic triaxial tests of sand and the effective stress fell, there was failure of sand at zero effective stress, he suggested a criterion of failure under any loading that led to zero effective stress. The striking difference between the Harvard and Berkeley criteria was that in Harvard the aggregate state before the instant of liquefaction was at a point α in Fig. 12(d), very much on the wet side of CS, and in Berkeley it was at a point β, far on the dry side. Casagrande's 1936 paper noted that if small cycles of strain release the contact forces here and there between grains, state points approach the lower left hand corner in Fig. 12(a) and move to $v_\lambda \ll \Gamma$, but to achieve a large displacement such as in Fig. 15(b) there must be steady shearing distortion, and interlocking during continuing shear flow brings states back to $v_\lambda = \Gamma$. If a triaxial test specimen state arrives at curve FG in Fig. 16 (Casagrande's *compression curve for the densest state*), reaching zero effective stress $p' = 0$ in cyclic loading, the state has got to follow a path that crosses Fig. 17 to reach CE (Casagrande's *critical density*) before Casagrande's liquefaction flow state is reached. The disagreement between Casagrande and Seed was resolved by the introduction of the term *cyclic liquefaction* to describe an aggregate at zero effective stress with small oscillations rather than continuous shear flow. Herrick's zero stress is not a sufficient condition for flow; pore flow is needed. In a desert or on the seabed, a stress component normal to the free surface is zero, but grains stay put on that surface unless the wind blows across the desert and sand dunes form, or sea currents move across the bed and sand waves form.

CS theory also questions Casagrande's alarming prediction of a risk of liquefaction at high effective pressure. In Fig. 11(b), above the CS pressure σ'_f yield strengths fall, but the aggregate remains ductile and stable. A high effective pressure to the right of C in Fig. 12(b) or to the right of the CS line ACH in Fig. 18(b) makes it easier to cause plastic flow in an aggregate, but does not cause a liquefaction event. This is seen in triaxial tests of sand that begin at a state point to the right of Figs 12(b) and 12(d). Successive axial load increments cause a pore pressure increment that takes the undrained test path towards the CS line, with *stable yielding* on the wet side of the CS. The stable test path ends with flow only when friction is fully mobilized. When the behaviour of contractive soil is discussed later, the yield curve in Fig. 11 will become the inclined straight line of the OCC model in the Frontispiece. Points on the wet side of CS do not map the

states with the behaviour called liquefaction. At first, an increase of the effective pressure on the dry side of CS will improve ductility, but after the OCC line is reached the risk to the aggregate is the steady fall of strength, rather than sudden instability. Along the OCC line the stress ratio to cause hardening and yielding falls from the CS value of $\eta = M$ when $v_\lambda = \Gamma$. Under increased pressure as the aggregate approaches the state at which $v_\lambda = \Gamma + (\lambda - \kappa)$ it becomes so slippery and it yields so easily that test specimens cannot be brought into the state with a stress ratio $\eta = 0$ at the point where $v_\lambda = \Gamma + (\lambda - \kappa)$. An aggregate can only be held near that point by cementation.

2.6 Failure at low effective stress

Casagrande commented on the news of widespread flow slides in loess in China that, in this loess, trapped pore air pressures caused liquefaction flow slides. An undisturbed very loose aggregate is transformed into a soft rock if the grains are lightly cemented. Loess is made up from grains of rock flour washed out from below glaciers in an interglacial period. They are deposited as a silt outwash fan and then blown away by wind, to form lightly cemented very weak but firm deposits. One description of Norwegian quick clay is *sea loess*. When thick glaciers still rested on Scandinavian fells, silt washed out from below the glaciers was deposited in the sea on the bottom of fjords. When the ice melted and the load on the fells was less, the rock rose up, and the newly deposited seabed soil formed land beside fjords. The quick clays were formed in the following millennia as rainwater gradually leached salt out of the uplifted ground. Figure 12(b) maps undisturbed lightly cemented rock flour at a state point like χ with a fully remoulded CS line having moved away to the left. Such quick clay or loess makes a firm foundation for small buildings if undisturbed; if disturbed, it will be near zero effective stress. In quick clay regions a typical failure of the ground below farm buildings or a housing estate starts with small initial cracks in the level ground surface; they can be detected when pools of water on the surface are seen to drain into them. These cracks open up. Large blocks of ground then slip, taking trees and buildings with them. In the flow slide large blocks crumble, and as rubble flows down a valley, it turns into fluidized silt with zero effective stress. A visitor to an area that is well known for liquefaction flow slides will be surprised to find how strong the undisturbed soil is, with steep almost vertical escarpments beside small streams.

This type of failure is shown occurring at a state point with coordinates (v_λ, η) far to the left in the Frontispiece map, as pore pressures rise and the stress approaches zero. It also applies to densely compacted soil where the onset of micro-cracking causes an increase of permeability. If a body of soil near to zero effective stress crumbles into rubble in the presence of a high hydraulic gradient, the pore pressure gradients will fluidize the soil rubble, and this can also be called liquefaction failure. This same name and explanation will apply to a range of failures from hydraulic fracture of dams to sand boils behind flood levees, from upward hydraulic gradients fluidizing sand in the base of a cofferdam to water flow from a broken water main that fluidizes the trench fill in which the main is buried. When effective pressure on a dense aggregate is near zero, and

there is a high hydraulic gradient, cracking, piping, channelling, boiling and clastic debris flow occur. A sudden increase in permeability lets water flood into the crumbling debris, and fluidizes it. What was previously firm ground is liquefied. The Frontispiece maps the soil states in all these failures on the dry side of the CS line. I described how a seepage pressure gradient *unlocks* a densely interlocked aggregate on the dry side of the CS line as follows (Schofield, 1982):

> The word 'interlock' is helpful in thinking about this event. A lock is made with a sliding bolt which is mechanically secure even though it is unstressed. Any attempt to shear a pair of interlocked doors apart will generate resistance by the bolt. However if a pair of interlocked doors are pushed open their lock or bolt will offer no resistance as the doors swing apart. In the same way a hydraulic gradient across a soil body at very low effective stress will open cracks or channels in the soil. In the case of a pair of doors where the bolts are jammed tight, it may be possible to free a bolt by joggling it in different directions until the forces that hold the bolt are relaxed. In the same way cyclic loading on interlocked soil grains can reduce the effective stresses between them until even the closest fitting interlocked grains become free to slide apart... The opening within the body may be an extensive crack or a local pipe or channel. In the case of a local pipe being formed, the seepage forces of water following tortuous paths round interlocked grains may be able to dislodge grains in a direction perpendicular to the axis in which the pipe is developing: the hydraulic pressures transmitted along the pipe would form hydraulic gradients in these directions... So in general the dilative response, that makes interlocked grains brace themselves to resist shearing deformation in soil in dry state sand (makes them suck water in among themselves as they dilate) turns into a disintegrative response in soil in which effective stress components fall to zero. In some cases the cracks are self-healing with soil grains from the walls of cracks forming a mud which limits the sped of pressure transmission. In other cases there can be sudden transmission of pressures, and a body of crumbling soil can disintegrate into a sort of soil avalanche, or several pipes can break through a sand layer and vigorous sand boiling can occur.

The report on the flow slide of Fort Peck Dam had made it clear that there was no sudden instability in the aggregate of soil grains such as Hazen envisaged, Thaddeus Merriman (1939) wrote

> The facts which have been presented disclose the cause of the slide. During the 60 days prior hereto, the difference in level between the core pool and the water in the reservoir had increased from 83 feet to 134 feet. Because of the open joints in the disintegrated and subfirm shale, a substantial part of this pressure head was transmitted through them by the drainage water from the core pool as it passed through both the core and the shell. This pressure acting as an uplift under the upstream portion of the dam reduced the effective weight of the toe so that finally, it was unable to restrain the slope upon it. Failure was thus initiated. The toe in the vicinity of station $US + 00$ and range $US + 00$ moved outward on the lubricated and disintegrated shale. The first motion was necessarily slow, but, once established, it rapidly became irresistible. All else happened as

a matter of consequence. The downstream shell carrying the paving moved smoothly outward, as though upon skids. As the bottom moved outward the plastic core subsided into the space thus made and the 'barn-door' began to open. The failure was distinctly in the disintegrated shale at depth under the dam. All of the observed facts are thus explained. As there is still evidence of pressure in the shale members, how much greater must that pressure have been before the slide!

Clearly, the liquefaction failure in Fort Peck Dam involved high pore pressure gradients in disintegrated shale near zero effective stress. It was not a phase transition occurring as a chain reaction in a granular aggregate as described by Hazen (and Casagrande). In Hazen's liquefaction, two sources of power drive chain reactions: elastic energy stored in highly stressed grains is released, and pressures on external boundaries move as high effective stress reduces the volume of a loose sand grain aggregate. In what I called Herrick's liquefaction, totally unstressed grains liquefy with no unstable release of energy, and the hydraulic fill flow described at the start of this section is powered by gravity. The criterion for liquefaction is not only that the grains are nearly at zero effective stress but also that they are subject to a hydraulic gradient and fluid flow. The Frontispiece has two axes (v_λ, η), where $v_\lambda = (v + \lambda \ln p')$, and liquefaction is written in a part of the Frontispiece that fits lightly stressed states reached by cyclic loading. As a path approaches $p' = 0$ it must leave the map; grains in an aggregate must always be held together by some small stress. Contractive soils on the wet side of the CS line are stable. Where Casagrande would plot liquefaction on the wet side of the CS line, the Frontispiece has a ductile plastic zone. As the OCC model yields, the energy input in volume reduction and the release of stored elastic energy both contribute to the plastic dissipation of frictional power in CS flow, $Mp' \, d\varepsilon/dt$, and cause the ductile plastic yielding of soft soil. To explain what happens when a soil body yields as a plastic body, I must clarify what *plastic* means.

3 Soil classification and strength

Terzaghi and Casagrande had a preconception that clay and sand soils must be very different types of material because of the surface chemistry of clay grains, but when their data of disturbed clay soil are re-assessed, mechanical concepts of plasticity and CS explain soil behaviour without chemistry.

3.1 Casagrande's soil classification and soil plasticity

Readers of soil mechanics literature are troubled with several papers asserting that the meaning that the word *plastic* now has in 20th-century solid mechanics does not apply to soil. It had another meaning for many centuries before it got the modern meaning. People who saw a potter forming a little figure and thought of man being formed from clay, or asked how the identical full-grown forms of many plants could come from a handful of small seeds, thought that all manner of creation of forms involves a *plastic principle* that applies both in art and in life. The SOED quotes a line from Sir Thomas Browne (a scientist and scholar who lived from 1605 to 1682): '*in what diminutives the plastick principle lodgeth is exemplified in seeds*'. Today we might write this as '*seeds are examples of the small dimensions needed to contain the plastic principle*'. The SOED states that the Greek derivation of the word 'plastic' alleges that a principle, virtue or force in nature causes the growth of natural forms of living organisms. It covers the growth of big recognizable plants from small grains. The solid mechanics of metal forming involves stress. The (τ, x) plot in Fig. 1(b) shows a cycle of (τ) loading and unloading that leaves a solid body with a plastic deformation (x), but the original definition of the word 'plastic' is wider than this. The plastic process in Fig. 1(a) gives a dimension x to a body. Unlike a fluid flow it covers any process in which a body acquires a form that persists when the process finishes. No stress need be involved. An example is finding the density of soil by digging a hole and pouring in loose sand to fill it. The ratio of the weights of the soil taken out and the sand put in gives the ratio of the densities of the soil and the sand. By the SOED definition, the ability of the aggregate of grains to adopt the irregularly formed form of the hole is correctly called a plastic property. The ductility of soil paste that lets a potter form it into pottery is the result of the mechanics of water-saturated fine-grained soil aggregates. The plasticity index I_p of a soil, in the *soil classification* system of Casagrande, is the range of water contents over which soil paste shows this plastic behaviour and can be moulded into different forms.

Engineers use soil classification to help to select some construction sites or soil materials, and to reject others. Classification begins with grading tests that break up soil specimens in water and wash the grains through sieves. Grains that crush when transported are called friable, and a size distribution that changes during

the handling of disturbed soil would have little meaning. In construction, strong grains are better than grains that easily crush because the form aggregates with predictable behaviour. The natural processes of transport and sorting can give soils a strong grain aggregate that dissipates power in distortion in the way that a loose grain aggregate dissipates energy in a slope at repose. When the CS theory was initially developed in 1955 the soil classification tests were thought to be only empirical, and Hvorslev's interpretation of shear box data and the Mohr–Coulomb failure criterion were thought much more fundamental than soil classification (both at Imperial College and at Cambridge University). But as developing CS concepts and the fundamental cause of plasticity in soil paste were discussed with soil mechanics' students making soil classification tests with remoulded water-saturated reconstituted soil paste that dried in the air, two explanations of the increase of the apparent cohesion strength were possible. I could repeat the (a) electrochemical explanation of forces that increase as clay grains became closer to each other, or (b) the explanation might involve surface tension in open pores on the paste surface, with curved water menisci that cause pore water suction and effective stress in the aggregate of grains. I preferred an explanation as follows. As a paste is remoulded, the air–water interface that envelopes it has innumerable menisci hanging like spider's webs from grain to grain across every surface pore. A student squeezing soil with their fingers can think of the lump of paste as a small sack, with tension in the sack holding effective pressure in the grains. As water evaporates from soil paste, the consolidation by surface tension is as effective as consolidation would be in an oedometer. There is internal friction in a sand bag that can effectively stop shrapnel fragments; this is the same property that would give rise to a slope at an angle of repose if the sand bag broke and the grains formed a heap. In 1955 a soil science research unit of the Department of Agriculture in Cambridge had a laboratory that would consolidate small cylinders of soil paste on water-saturated suction plates, with fine pores giving high air entry suction; pore suction in the plate was in equilibrium with mercury in a u-tube. The water content of the paste decreased, and p' and the paste strength c_u (or s_u) increased as water slowly evaporated into the air from all surfaces. Unconfined compression tests gave data on the paste strength. A straight line was obtained when strength was plotted against suction. The pore suction was in equilibrium with the positive effective spherical stress p' in the soil grain aggregate. The data showed that soil paste had frictional strength. The mechanical explanation of the plasticity and friction in soil paste was better for our students than a chemical explanation; geotechnical engineers do not regularly make chemical tests of soil.

The same effect is seen if a small cup is filled with soil paste, a level surface struck across the cup, and the apparent cohesion is measured with a falling cone that is held with its tip at the surface of the paste and is let fall. The depth of penetration d is measured when the cone comes to rest. Figure 19 shows the data of tests on kaolin paste with two cones of 30° tip angle; one cone has mass of 80 g and the other has mass of 240 g (Lawrence, 1980). Both cones were used to test a series of specimens of paste with decreasing water content. As the paste strength increases, d decreases, and as the water content of the paste decreases, the logarithm of the depth d decreases. As strengths fit a logarithmic plot in Fig. 19,

the pair of lines confirm the proposal in Eqn (10) that soil paste in CS flow is in states (v, p') that fit $\Gamma = v + \lambda \ln p'$. Another deduction from Fig. 19 is that the spacing Δw between the two lines is a measure of the slope λ of the CS line in Eqn (10). In CS plastic compression an increase in p' by a factor of $240/80 = 3$ is linked with a reduction of water content by Δw. In Fig. 2 the specific volume is $v = 1 + e$. If the voids e are full of water and the unit volume of solids has a mass G_s, I can calculate that the water content is $w = e/G_s$. So the fall in water content $\Delta w = \Delta e / G_s = \lambda \ln 3 / G_s$, hence $\lambda = \Delta w\, G_s / \ln 3$. Hence, tests with two cones of different mass give λ, a basic CS constant for the disturbed soil. I introduced this form of plasticity testing in our laboratory teaching in 1964, measuring depths of penetration of cones of 80 g and 240 g mass into the surface of soil paste. For a series of paste samples of increasing water content this gave the pair of straight lines (Fig. 19) at a spacing Δw that showed what reduction of water content was needed to triple the clay paste strength. The test data gave students an I_P value.

I once heard Bishop relate how Atterberg developed his soil classification test with the knife and the spoon in the lunch box that he took with him in the field. He used the knife to mix up a pat of soil paste with some drinking water in the bowl of the spoon, made a simple cut in the paste, tapped the spoon on the back of his wrist, and counted the number of blows to make the knife cut close up. In Casagrande's refined test the spoon and knife became the falling bowl and the grooving tool for his liquid limits. The US Army Corps of Engineers took Casagrande's liquid limit test with them around the world as they constructed road and airfield pavements in World War II, to become the most frequently performed and least understood of all soil mechanics tests, but in CS theory it became the most significant of all tests. Makers of Casagrande's apparatus made significant differences between the beds onto which the bowl fell. Each time that Casagrande's bowl falls, a standard spike of impulsive deceleration causes a miniature slope failure at each side of the groove in the soil paste. A little more water is added again and again to the soil paste in a liquid limit test. As the water content increases and the paste strength c_u decreases, the duration of the brief period in which a side of the groove flows will increase. The groove width is fixed, so the number of blows to close the groove decreases. When a standard number of blows closes Casagrande's groove, his test has found the water content at which the soil paste has the standard undrained shear strength. The CS relationships between w and p' and c_u for disturbed soil paste give the linear relationship between w and ln (number of blows). The second soil classification test finds a water content called the *plastic limit* w_P at which it is impossible to roll a thread of soil paste that does not crumble. The difference $w_L - w_P = I_P$ gives the *plasticity index* of soil. Skempton and Northey (1953) suggested that I_P is the fall of water content needed to give a 100-fold increase in the soil paste strength. My research student Lawrence (1980) made tests of mixes of rock flour and coarse kaolin clay in different proportions as tabulated in Fig. 19, giving the fan of CS lines shown in Fig. 20. Skempton and Northey defined activity of the colloidal fraction of a clay paste as $I_P/(\% < 2\,\mu)$, and related I_P to the clay fraction, and Schofield and Wroth (1968) translated this into a fan of CS6 lines all passing through one Ω point.

Table 'A'

Mix	LL	PL	PI	Δ	PI⁴	Real strength factor
1	66	38	28	10.5	44	18.7
2	58	33	25	7.8	43	34.3
3	52.5	29.5	23	8.0	33.5	23.5
4	47	28	19	7.15	30	18.5
5	39	24	15	5.6	23	19.0
6	36	22	14	4.5	19	30.5
3*	48	29	19	6.2	26	28.9

Mean = 24.80

N.B. $PI^4 = \dfrac{\Delta \ln 100}{\ln(w_{jwz})}$
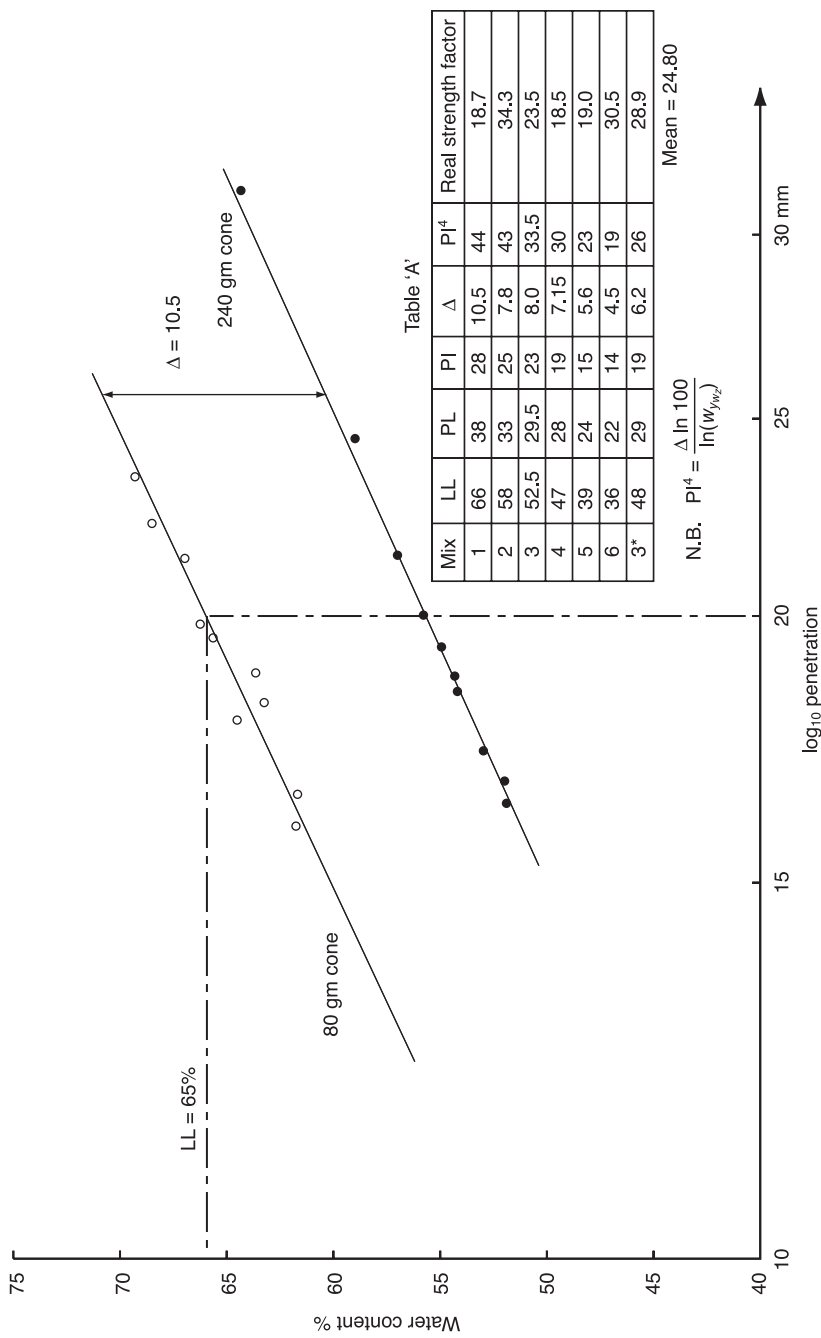
Fig. 19 Fall cone test data (Lawrence, 1980)
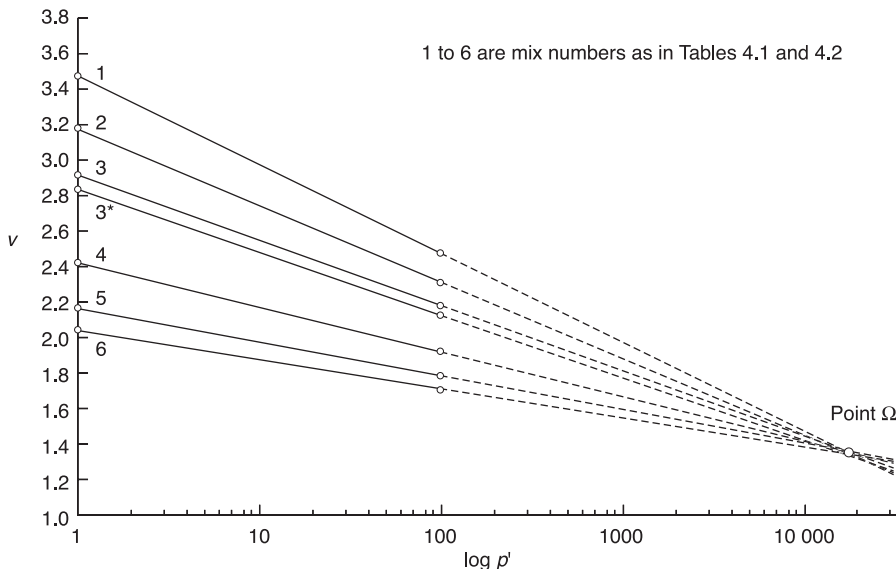
Fig. 20   A family of critical state lines (Lawrence, 1980)

The data of Lawrence's set of test specimens in Fig. 20 define a Ω point with more accuracy than Schofield and Wroth. Casagrande's soil classification system, Coulomb's dictum that disturbed soil has no cohesion and the CS model of its behaviour are all generally applicable to all types of soil throughout the world.

By the CS concept, undrained strength is due to internal friction. Aggregates of grains under effective spherical pressure dissipate energy as they flow. In a water-saturated soil paste the grains are held together at constant volume by pore water suction. Dry silt grains do not *cohere*; apparent cohesion is due to suction. The CS concept is in agreement with Rankine's mid-19th-century teaching. He had been involved as a civil engineer in the construction of railway cuttings in undisturbed stiff ground. Experience of construction in stiff clay taught him not to rely on the adhesion of soil. A slope failure in stiff soil initially has a small vertical face at the top of a slip, but in time that vertical face falls, leaving a slope at a constant angle ϕ_d. Evidence of slopes in stiff clay that stand at an ultimate angle of repose led him to believe that cohesion is unreliable and in the long-term only soil friction is reliable. His textbook (Rankine, 1874) states that '*friction is the only force which can be relied upon to produce permanent stability*'. The CS concept with zero cohesion agrees with him.

3.2   Hvorslev's clay strength data and the CS line of clay

At this point I can re-examine Terzaghi's interpretation of Hvorslev's tests. The tests were the culmination of a research programme with colleagues and research students in Harvard and Vienna. Terzaghi thought that they confirmed the role of effective stress (Eqn (1)) in the equation for soil strength (Eqn (2)), but when re-examined, his tests in shear boxes actually confirm the concept of the stable ductile yielding of frictional soil on the wet side of the CS. Hvorslev wrote that a definite
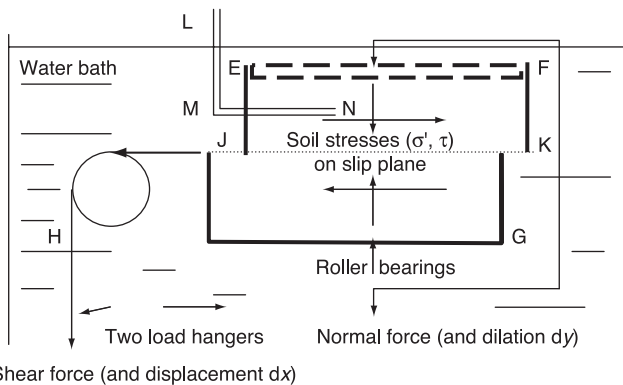
Fig. 21 Slip plane in saturated soil in a shear box

critical void ratio does not exist in the case of a cohesive soil, but any void ratio can become critical if it is produced by a critical consolidation procedure; he had confirmed the CS concept. Terzaghi's research on the strength of reconstituted clay used a type of direct shear test box that also acts as an *oedometer*, to consolidate samples for shear testing. Figure 21 shows the shear box in vertical section, immersed in a bath full of water; it is square in plan, with upper and lower halves. The lower half of the box is supported on roller bearings. Loading hangers apply horizontal and vertical forces on the upper half of the box and on the porous piston EF. The vertical load on the mid-plane is held constant. The lateral loading hanger is subject to successive load increments. Shear displacement of the lower half of the box is resisted by soil strength on the specimen mid-plane. In a test, average soil stress components (σ', τ) act on the mid-plane JK.

   A pipe shown by the double lines LMN is connected to a small porous stone that is in contact with pore water in the soil at N. The pore water pressure at all points in the soil and in the water bath is in equilibrium with the atmospheric pressure on the upper free surface of the water bath. If the water in the standpipe is seen to rise above or fall below the free surface level, then there is a positive excess pore water pressure or suction at N. In Terzaghi's analysis of the *consolidation* process, a load increment on a soil layer causes excess pore pressure gradients that make pore water flow across drainage boundaries. Steady application of a load eventually changes the effective stresses throughout an aggregate of soil grains. Terzaghi stated that any change of state such as elastic or plastic compression, all distortion and all change of shearing resistance of the aggregate depends only on changes of the effective stress σ'. A change in the volume of the soil will cause vertical displacement of the upper half of the box and of the forces on the vertical loading hanger. Figure 22(a) sketches shear test data for a work-hardening metal such as annealed copper. Compression from B' to B is called elastic; from B to C it is called elastic–plastic; swelling from C to C' is elastic. The same description is used for soil. Terzaghi analysed the consolidation of a horizontal layer under an increment of vertical load due to transient excess pore pressures. He treated the clay as a stack of elementary elastic coiled spring elements, each in a cylinder full of water with a piston applying a load to the spring and to the water (Fig. 22(c)). In Fig. 22(d), a vertical total stress σ that is applied to the piston causes an effective stress σ' in the spring below the piston
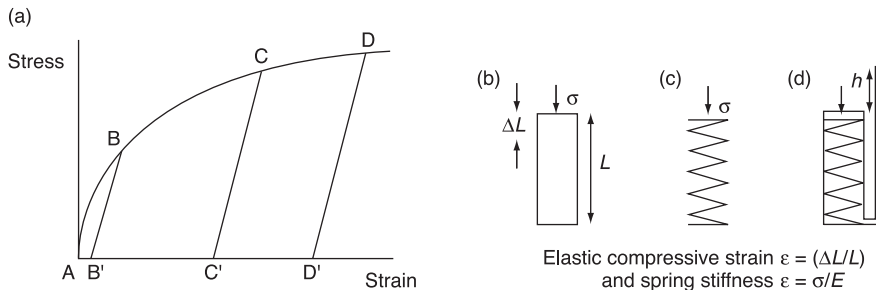
Fig. 22 *Elasticity, yielding and plastic strain*

and a pore water pressure u in the cylinder, as described in Eqn (1). If in Fig. 22(d) the excess pore water pressure in the cylinder below the piston is u, then in the stand-pipe, water with a unit weight γ_w will rise to a height $h = u/\gamma_w$ above the piston that rests on the water in the cylinder. His springs were elastic.

What is envisaged in the CS concept is an aggregate of fine grains, not a simple stack of springs. When disturbed, water-saturated soil is slowly compressed or swells in the box, and energy is dissipated in the transient process of consolidation and swelling, with flow of pore water through fine pores and channels among the grains. When this process ends, forces in grains resist all loads on the aggregate. If the load is removed very slowly, some of the energy stored in grains in compression can be recovered in swelling. The non-linear elastic compression and swelling curves $B'B$, $C'C$ and $D'D$ are as sketched in Fig. 23(a), following Taylor (1948). In Fig. 23(b) these elastic compression and swelling lines are idealized as straight lines. It is a simplification, as loops will result if grains slip during loading and unloading cycles. Terzaghi's model for the compressibility of a horizontal layer of soft water-saturated soil put a stack of springs and pistons in a vertical cylinder filled with water. A load increment causes a change of length of the springs in the water, and energy is dissipated by viscosity when water flows past a piston. The work done is small if the movement is infinitesimal. No viscosity is taken into
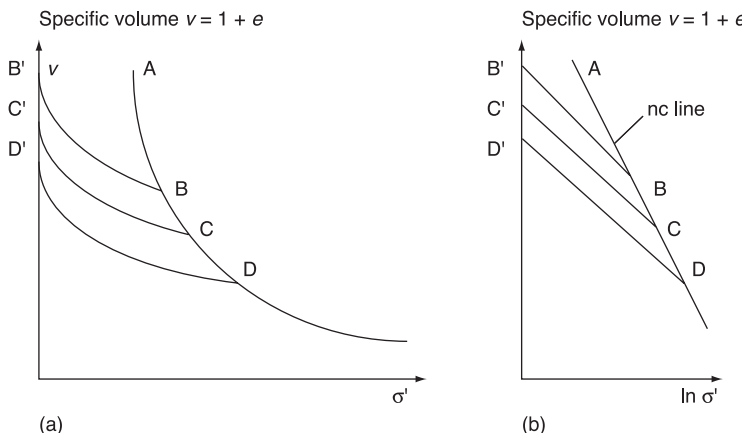
Fig. 23 *Elastic and plastic compression of soil. (a) σ' base. (b) $\ln \sigma'$ base*

account in the dissipation of power here, although viscous dissipation of energy in the transient flow of pore water must make a contribution to the stability of grain aggregates. All loading and unloading cycles will be idealized simply by straight lines such as are shown from D′ to D as non-linear elastic behaviour, and not with the loss of energy that there would be in loops. Geological processes involve loading and unloading of sediment layers being laid down in water and then uplifted and exposed by erosion. An undisturbed soil specimen that is brought into a laboratory for tests will have had over-consolidation similar to the path ADD′ in Fig. 23, but the effects of viscosity and creep in real soil specimens that creep under constant load must be discussed in other books – I only consider the idealized elastic–plastic behaviour of aggregates.

The box EFGH in Fig. 21 has two halves, divided on the mid-plane JK. Before shear, to eliminate sliding friction between these halves of the box, the upper and lower halves of the box are slightly separated by three lifting screws that pass vertically through the top half of the box and bear against the lower half of the box. When vertical movement of the piston has stopped, to ensure that the weight of the piston and of the top half of the box is carried entirely by the aggregate of grains on the mid-plane, the top half of the box is lifted a little, and a small screw that passes through the side FK is tightened to clamp the top half of the box on to the piston. The lifting screws are then removed. When shear force is applied in Fig. 21 the aggregate on the mid-plane resists slip. Whatever the grain size, if the soil grains are densely packed, shear distortion requires a loosening of the packing to let grains move past each other. As dense soil shears, the piston and the top half of the box in Fig. 21 rise; with loose soil they fall. The displacements are measured in both cases. In a stress-controlled drained test the shear load is applied by adding weight to a loading hanger. Initially a transient movement soon slows down, but as the hanger load is increased there will be an increment at which a steady load causes a steady or very slow shearing velocity. If that load is left on, there will be an ultimate failure on the slip plane. That failure load gives the peak strength. Coulomb did not rely on cohesion, but Terzaghi wanted to use accurate values that were found in laboratory tests of undisturbed soil in design practice. He wrote (Terzaghi, 1943):

> *The data for making a stability calculation pertaining to clays can at present be obtained only by means of the following purely empirical procedure. We test the clay in the laboratory under conditions of pressure and drainage similar to those under which the shear failure is likely to occur in the field . . . If we dig into a bed of dry or completely immersed sand, the material at the sides of the excavation slides towards the bottom. This behavior indicates the complete absence of a bond between the individual sand grains. The sliding material does not come to rest until the angle of inclination of the slopes becomes equal to a certain angle known as the angle of repose. The angle of repose of dry sand as well as that of completely immersed sand is independent of the height of a slope. On the other hand a trench 20 to 30 feet deep can be excavated in stiff plastic clay. This fact indicates the existence of a firm bond between clay particles. However, as soon as the depth of a trench exceeds a certain value, dependent on the intensity of the bond between the clay grains, the sides of the trench*

fail and the slope of the debris that covers the bottom of the cut after failure is far from vertical. The bond between the soil grains is called cohesion. No definite angle of repose can be assigned to soil with cohesion, because the steepest slope at which such a soil can stand decreases with increasing height of the slope. Even sand, if it is moist, has some cohesion.

In this passage, Terzaghi links cohesion with clay in which bonds formed after a long period of creep. He writes about total stress, not about frictional strength generated by positive effective stress and pore water suctions in stiff clay and moist sand. If he had made a vertically sided cylinder of newly remoulded clay by compaction or consolidation, 10 or 15 cm high, he could have left it standing on his laboratory bench with an air–water interface on all faces of the cylinder. With suction in the pores it would not have failed under self-weight because frictional strength would have been mobilized by effective stress. But tensile strength of pore water is not part of the strength of effectively stressed soil. If he had filled a sink in his laboratory with water, picked up that cylinder and immersed it in the sink, he could have left it under water for his students to observe. Before long the suction in the pores would have drawn water into the faces of the cylinder of soil, soil grains would begin to fall off the vertical faces, demonstrating Coulomb's law (that newly remoulded soil has no cohesion) to students who saw a heap of soil with fully softened clay soil slopes at an angle of repose.

In Terzaghi's research tests on disturbed saturated soil specimens in shear boxes, as a loading hanger applied weight to a square piston it slid freely down into the box (Fig. 21), and caused a vertical effective stress σ' through the depth of the clay in the box. Drained increase and decrease of the normal stress σ' caused both plastic and elastic compression, and elastic swelling of the clay. Plots of water contents w against $\ln \sigma'$ gave straight lines like AB and BB′ in Fig. 23(b), or DE and EB in Fig. 24, with slopes that define elastic and plastic compression properties of the clay. Casagrande and Albert (1932), in early shear box tests at Harvard University, prepared soft soil specimens under various normal loads σ' on line DE in Fig. 24. In slow fully drained shear tests at constant σ' they found that as each such specimen yielded, the specimen state moved from a state on the line DE to a state on the line AC. The final loss of water content of each specimen had the same value Δw. The ultimate shear strengths τ of normally consolidated specimens were proportional to the normal effective stress σ'. Such shear strength test data plotted as points on lines such as AC in Fig. 5 or 10(c).

Terzaghi's tests in Vienna of both normally consolidated and over-consolidated reconstituted clay specimens extended this Harvard work. Figure 24 sketches the elastic–plastic compression behaviour in the shear box as line DHE. The clay swells into equilibrium at states such as point B in Fig. 24. With the state at point B, Hvorslev began slowly to load the shear-loading hanger, to start a fully drained shear test at constant σ'. Figure 2(c) shows the compression of a cylinder of normally consolidated clay on line DHE causing general ductile bulging, and compression of over-consolidated clay causing localized brittle rupture on an inclined plane. Similarly in the shear box tests, Casagrande and Albert's specimens were ductile, but Hvorslev's heavily over-consolidated clay was brittle. The dense clay began to dilate as the shear stress increased, with the water content increasing
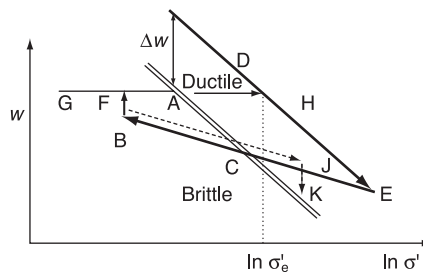
Fig. 24 Hvorslev's shear box test path DHECBF

from B to a point such as F. As Hvorslev's shear load τ on each such specimens increased, at first the shear creep rate decayed. The shear load then reached a value at which the creep rate began to accelerate. Hvorslev held that shear load steady and waited. Failure was sudden, on a thin shear plane, with shear and normal effective stress (τ, σ') at a state point F. After failure, Hvorslev cut out a slice of clay a few millimetres thick that included this thin slip plane to try to measure the water content at F, but slip planes are very thin. He mostly got clay from beside the slip plane as it was just before failure. According to the CS concept, water contents after failure in the slip plane would have given CS test data, but what he measured was the water content w as it was just before failure, and in Fig. 25 he plotted the data of (w, σ') and the peak strength data of (τ, σ') for a set of 12 specimens all consolidated to the same effective normal stress of about $5\,kg/cm^2$ (Hvorslev, 1937). The data on the dashed curves lie near to, but slightly above, the solid straight line of CS frictional strength. There is only a slight difference between the peak strengths of over-consolidated clay on the dashed curves, and the straight solid line of lightly over-consolidated peak strength points, but the slight difference contains the significant information about cohesion.

The explanation of this slight difference is as follows. In Fig. 24 the line GFA would represent a set of specimens that are all at the same water content when they fail. To get the set of specimens such that at failure all were at the same water content w as at point F, Hvorslev would have had to make many tests; a specimen at G would have to be heavily over-consolidated to a point on DHE beyond E, and swell back further than B, and dilate more than BF. He did not need this large set because, knowing values of (τ, w, σ') at points 1 to 12, he normalized those data as follows. From each value of w he found where the extended line GFA intersects line DE at an equivalent stress σ'_e. This point H in Fig. 24 is such that plastic compression under the effective normal pressure σ'_e would produce a water content w. To normalize the peak strength data in Fig. 23 he divided each shear and normal stress (τ, σ') by σ'_e. When he plotted τ/σ'_e against σ'/σ'_e in Fig. 26, he found that the normalized data lay on a straight line like BC in Fig. 27, so that peak strength depended on the water content w in the region of failure. Equation (10) fits line BC. It is like Eqn (2) but with a cohesion c' that depends on water content.

$$\tau = \sigma' \tan \phi' + c' \qquad \text{where} \qquad c' = c'(\sigma'_e) = c'(w) \qquad (11)$$
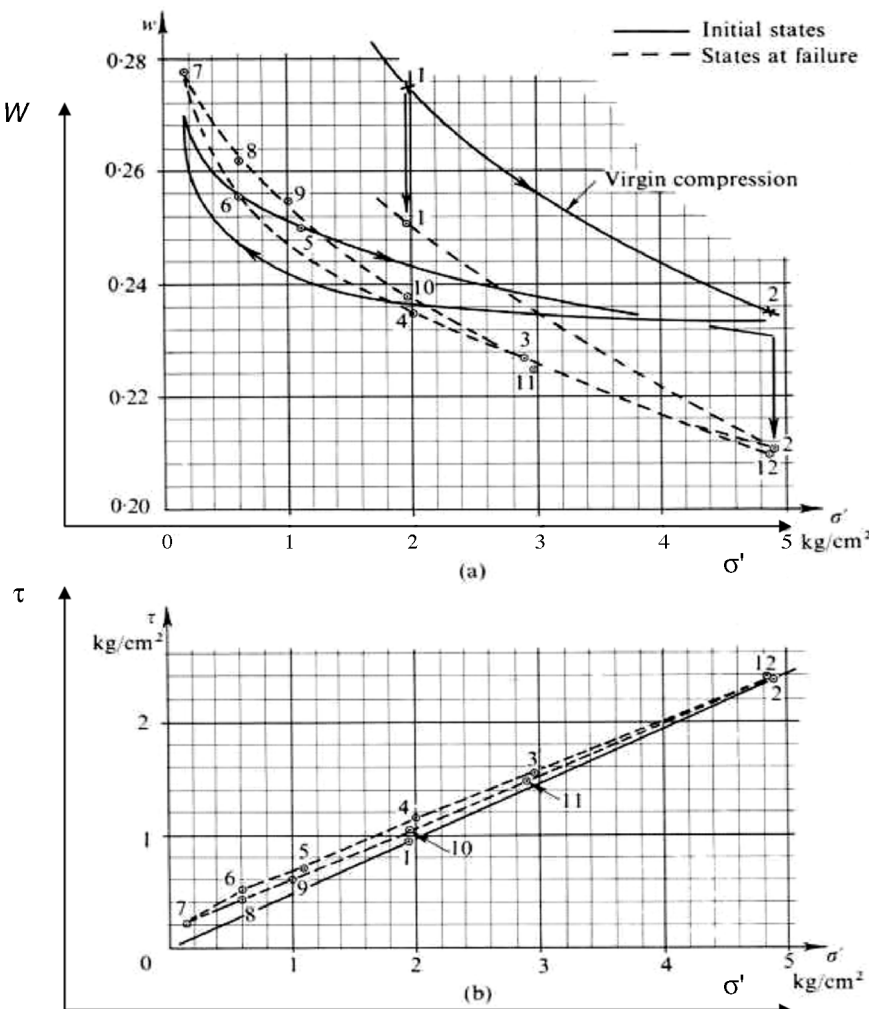
Fig. 25 Hvorslev's (1937) data of compression, swelling and shear strength

Figure 26 led Terzaghi to claim that Hvorslev had found a *true* friction ϕ' of clay smaller than the slope at repose $\phi' < \phi_d$ and a *true* cohesion of clay $c' = c'(w)$ that was a function of the water content w. He claimed that these friction ϕ' and cohesion c' parameters are *true* constants in terms of effective stress components (τ, σ'), for saturated reconstituted reconsolidated clay without natural fabric. Terzaghi thought that the surface chemistry of fine clay mineral grains and dissolved salts in pore water are the basis of adhesion between grains, and of his true cohesion. In Fig. 27 the line BC applies to one value of σ'_e, corresponding to one value of w, or the equivalent void ratio $e = v - 1$. He failed to note that Eqn (10) gives peak strength values of over-consolidated clay only on BC in Fig. 27 but does not apply to lightly consolidated clay to the right of C in Fig. 27 and in particular does not apply at point D where plastic compression occurs
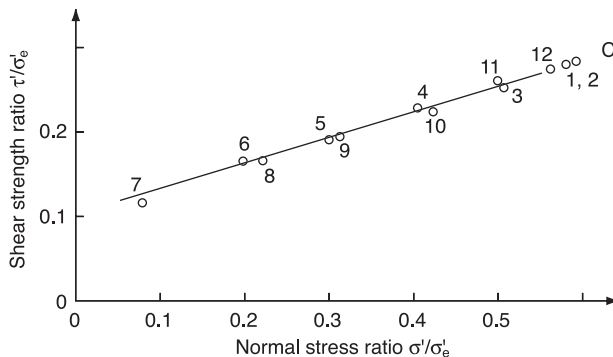
Fig. 26 Hvorslev's (1937) normalized peak strengths

when $\sigma' = \sigma'_e$. If the soil on Hvorslev's thin slip plane had reached a CS failure state, and if he had found the CS water content in that slip plane after failure, then every data point on line BC in Fig. 27 could cluster round the CS point C. If Roscoe (1953) could get the layer of soil that flowed in his Simple Shear Apparatus (SSA) as shown in Fig. 28 to be as thick as the layers of gouge material that are reported in the field then he would get data of soil in the region of failure at the moment of failure; by the CS concept all the data would be at C.

The CS concept explains the undrained apparent cohesion of a soft paste saturated with water as due to internal friction. Schofield and Wroth (1968) describe failure on the left of the Frontispiece when a body of stiff clay disintegrates into lubricated block rubble with a layer of soil paste on areas of contact between blocks in which soil grains are held together by suction. All soil has strength due to friction. In stiff soil there is extra peak strength due to interlocking, but it would be an error to think of friction in fine-grain soil in terms of total stress, and to ignore the effect of volume change in gouge material on thin slip planes. The flow of water for such a volume change takes time. According to the CS concept, when a stiff clay body becomes rubble with cracks and slip planes between blocks, there are layers of soil paste on contact planes at which pore water suction keeps holding blocks together. Schofield and Wroth (1968) wrote about

... a rubble of lubricated blocks, sliding on each other on very thin moist layers of soft, lubricating clay paste. Critical state theory explains the failure mechanism,
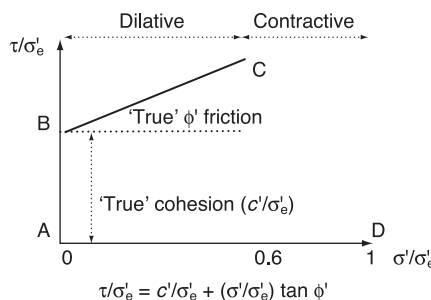
Fig. 27 Hvorslev's 'true' strength of clay soil
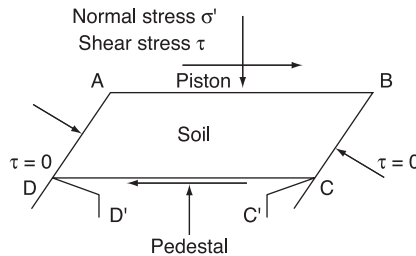
Fig. 28 Roscoe's Simple Shear Apparatus

and also gives us the key to the behaviour of this lubricating clay paste. The soft clay is being severely remolded but it can only soften to the critical state that corresponds with its effective spherical pressure. This pressure, and the corresponding critical state strength, increase with depth in the rubble. The 'friction' concept involves a resistance to relative motion that depends on the effective stress between blocks. We can apply the well established friction calculations to the limiting equilibrium of a slipping rubble only because the strength with which the blocks adhere to each other is proportional to the pressure that has long been effective between them.

The suctions will be whatever is needed to keep CS undrained shear flow in the paste. The ratio of total force normal and tangential to contact areas is the familiar friction force ratio, but this strength will act like glue in resisting cyclic loading and unloading of the contact. Without soil suction, a heap of hard rough grains that stands steady on a vibrating table will sink down to the surface as soon as vibration begins. This will not occur with CS paste at contacts, if cycles of loading and unloading of contact plane areas take less than the time needed for the water content of the CS gouge material on the contact planes to change. Forces between pairs of strong blocks act at a line of contact; *plastic hinges* open with relative rotation of blocks about this line. Stiff clay blocks in rubble are not as strong as rock, and there will be areas rather than lines of contact. The explanation of peak strength points on the straight line BC in Fig. 5(d) may be non-uniform effective stress on Coulomb's slip plane. The contact of blocks on a slip plane may have two distinctly different areas (a) with high effective stress passing through CS soil, and (b) a part of the slip plane with less stress where the stiff clay state points lie to the left of the map of soil behaviour with cracks in dense soil, so the two areas together give a point on line BC.

3.3   CS interpretation of Hvorslev's shear box data

It is most significant that there are no data points on the right side of Fig. 27. If Eqn (10) did apply over the whole range $0 = \sigma'/\sigma'_e = 1$ and if many lines AD, and BE and CF, were plotted against the values of e, they would form (Fig. 29) what we (Roscoe *et al.*, 1958) drew as the Hvorslev surface. We drew a curve ABC in Fig. 29 above the normal compression curve at $\sigma'/\sigma'_e = 1$ on the (e, σ') plane. Figure 29 shows a curved vertical wall, but Hvorslev did not obtain data corresponding to ABC and to this wall. The line BC in Fig. 27 ends at C. It
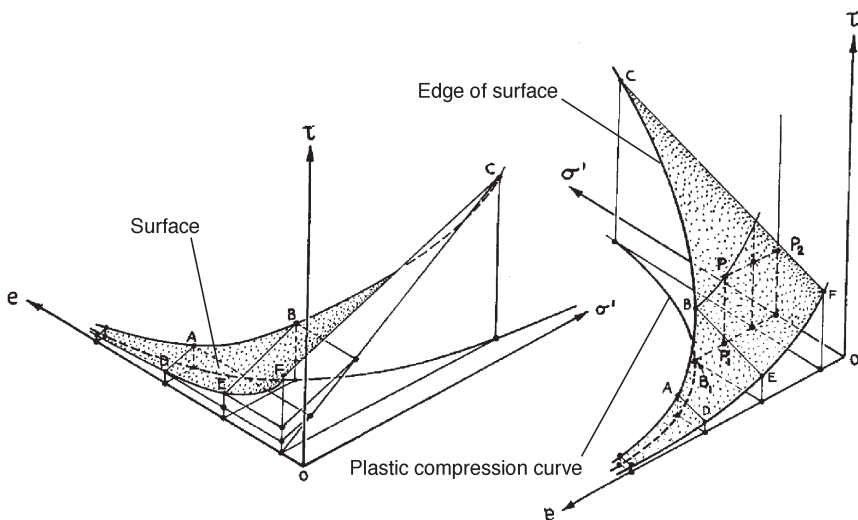
Fig. 29 The Hvorslev surface (Roscoe et al., 1958)

does not extend in the range $0.6 < \sigma'/\sigma'_e$. In Fig. 26 from Hvorslev's doctoral thesis, the data that give the straight line BC in this figure leave a space to the right of C. Hvorslev wrote equations there that obscured the fact that his data fell into a set of ductile and a set of brittle failures as indicated in Fig. 12. The drained tests of heavily over-consolidated stiff clay with $\sigma'/\sigma'_e < 0.6$ to the left of AC in Fig. 24 moved from B to F in Fig. 24. At F the brittle clay failed on a thin slip plane, and gave the data of failure states at points that fitted line BC in Fig. 27. Normally consolidated and lightly over-consolidated specimens with $0.6 < \sigma'/\sigma'_e < 1$ were ductile; they bulged and yielded with water contents that fell from DE to ultimate states on line AC in Fig. 24. In Fig. 27 the normalized state of any test path in the range $0.6 < \sigma'/\sigma'_e < 1$ moved to $0.6 = \sigma'/\sigma'_e$, and the data of the ultimate states lie near to point C. As the lightly over-consolidated soft clay in the area between DE and AC in Fig. 24 yielded, it became denser and reached the double lines AC. It then reached newly disturbed granular material strength values corresponding to the angle of repose $\phi = \phi_d$, as in the soft clay tests of Casagrande and Albert (1932).

A note of caution is needed here. Normally consolidated clay loses water in drained shearing, and tests end at some value $\sigma'/\sigma'_e < 1$. The simple CS hypothesis that has been outlined in Eqns (9) and (10) would require additional information about the value of the lateral effective stresses in the shear box in order to precisely define a CS double line in Fig. 24 or a value of $\sigma'/\sigma'_e = 0.6$ for point C in Fig. 27. A simple CS theory will not apply to all soils, and it should be no surprise that Hvorslev found a significant difference between the ranges of over-consolidation ratios for which the line BC applies, for two different clays. The range for Wiener Tegel V is $0.05 < \sigma'/\sigma'_e < 0.6$ and for Klein Belt Ton is $0.1 < \sigma'/\sigma'_e < 0.85$. However, in neither case did Terzaghi and Hvorslev's extension of their line BC to the right of C in Fig. 27 describe the data of yielding of soft clay. Terzaghi claimed that Hvorslev had verified Coulomb's model of soil strength and found true cohesion

and friction values, but Hvorslev wrote in his thesis that what he had established is that both sand and clay have critical states. He wrote that in the case of cohesive soil a definite, critical void ratio does not exist; any void ratio can become critical if it is produced by a critical consolidation procedure; (the path DEC in Fig. 24 shows such a procedure). Hvorslev was well aware of the plate shapes and small sizes of the grains of clay in the soil he tested, and of the difference between them and the sand that Casagrande had tested, but he still suggested that all soil behaves as shown by the CS soil model in Fig. 11(b). If interlocking is as shown in Fig. 11, soil interlocks at peak strength in zone I in Fig. 12 with Coulomb's failure, but as it shears and contracts in zone C in Fig. 12 it is ductile. Hvorslev plotted his raw data of peak values of (τ, σ') in Fig. 25 for clay that was consolidated to a state shown at point 2, allowed to swell to a state point 7, and reconsolidated to a state point 12. The set of shear box test specimens taken to those points gave peak strengths on a loop forming a dotted curve that lies only slightly above the straight line $\tau = \mu\sigma'$ in Fig. 25, and are only slightly stronger than the straight line in Fig. 25 of fully drained friction values. Rankine's teaching on soil strength, that *friction is the only force which can be relied upon to produce permanent stability*, differs from what Terzaghi taught his students and from how he interpreted his student Hvorslev's research. This re-interpretation by Schofield and Togrol (1966) of Hvorslev's tests confirms Rankine's teaching that engineers using the slip plane model can rely on CS friction ϕ_d but cannot rely on cohesion.

In June 1948, in the foreword to Volume 1 of *Géotechnique*, Terzaghi wrote that the publication of Coulomb's earth pressure theory was a brilliant beginning for soil mechanics but that the number of publications on this soil mechanics subject was '*utterly out of proportion to its practical importance*', as dry, clean cohesionless backfill material is rarely encountered in practice. He noted that when geologists made an inventory of materials that would be encountered in an excavation they paid no attention to factors such as shearing resistance, permeability and compressibility, contrasting structural design using man-made materials with well known properties and earthwork engineering using soil bodies in which material properties vary from point to point. He expressed his hope for advances in a combination of engineering geology and soil mechanics. Clear perception of the uncertainties involved in the fundamental assumptions and intelligently planned and conscientiously executed observations during construction are the basis of geotechnical success. He felt that theory and testing techniques had advanced far beyond immediate practical needs in the years from 1938 to 1948 so that in 1948 '*a well documented case history should be given as much weight as ten ingenious theories and the results of laboratory investigations should not receive too much attention*'. But there were basic questions to be answered about what words such as friction and cohesion mean when the strength of soil is discussed, and *Géotechnique* intended to include papers on this theoretical aspect of soil mechanics as well as papers on case histories.

Volume 2 of *Géotechnique*, published in December 1950, has the proceedings of a conference held at the Institution of Civil Engineers in London on the measurement of the shear strength of soils in relation to practice. Roscoe was one of the participants; all accepted Terzaghi's claim on *true* peak strength cohesion c' and friction $\sigma' \tan \phi'$ in the slip plane model; his claim was that Hvorslev's shear box

test data had validated the slip plane model, and that true cohesion on slip planes in clay depends on the water content of the clay in the region of failure at the moment of failure (although when Hvorslev sampled soil beside the thin slip plane he measured the water content of the clay just before peak strength, not the water content of gouge material on a slip plane after failure). In the conference, Bishop (1950), without explicit reference to Taylor (1948), suggested that (as well as friction and cohesion) the shear stress to cause dilation should be considered, called the *boundary energy correction*; he thought the correction contributed little to shear strength. The research student who measured dilation in Bishop's shear box at Imperial College did find the correction to be small, but his tests only sheared a small layer in the specimen. However, if I am correct in Section 2.1 of this book on *an interlocking soil strength component* in attributing all of Terzaghi and Hvorslev's true cohesion to a significant *boundary energy correction*, then Bishop and Gibson were very wrong. For Roscoe (1950) the outstanding result of the conference was confirmation of Hvorslev's work. He subsequently made each of his students study his translation of Hvorslev's doctoral thesis from German. He rejected the Imperial College shear box test data, and hoped to bring specimens into the same critical states as gouge material on a slip plane in a new research study at Cambridge University with a *simple shear* apparatus (Roscoe, 1953) (Fig. 28) that was intended to find a larger effect with continuous shear flow and uniform density changes in an aggregate of grains. End flaps BC and DA were free to slide and rotate to control specific volumes of soil in his shear box. To help free expansion of dense soil he secured lubricated rubber sheets to the piston at A and B and to the pedestal at C′ and D′. Uniformity of stress within the SSA needs non-zero shear stresses on each face as it rotates. Lubrication on the rotating ends meant the shear stress on the top and bottom faces was not uniform so the SSA was difficult to develop and it was hard to get good SSA data. The process of reinterpretation of published data that has led to this book took many years.

At that London conference, Haefeli (1950) confirmed that water contents of soft clay, before and after shearing at the ETH in Zurich, did lie on lines such as DE and AC in Fig. 24. Ultimate soft clay strengths lay on what he called the α line, at an angle ϕ_s of 'apparent internal friction'. His α line at an angle ϕ_s was the same as line AC at the angle ϕ_d in Figs 4(c) or 11(b). T&P attributed cohesion to the *shearing strength of adsorbed water layers* between grains at contact points, hence a water content decrease explained a cohesion increase. Haefeli was expressing a general belief of the conference delegates in London when he separated soil strength into a sum of friction and cohesion. He assumed that cohesion relates to the energy that is needed to remove water molecules from *the absorbed water films, which surround the individual grains* when he wrote:

> Cohesion may be assumed to be governed by the adhesion of the absorbed water films, which surround the individual grains. The proportional increase of cohesion with the consolidation pressure can thus be explained by the increase in the contact area or, more generally, by the more pronounced influence of the molecular forces.

The test path in Fig. 24 reached the point B and continued to F with drained shearing and failure on a slip plane, but if it were to have returned along the

dashed line to C and if drained shearing had taken place at a point J between C and E, the path would have been from J to K. The same soil that had been at B and had been discussed with words such as friction and cohesion would then be discussed with words such as plastic compression and yielding. CS yielding of soil before failure occurs in small-volume elements containing many grains, in much the same way as the gas laws apply to small volumes of gas containing many gas molecules that all interact with each other. In the CS model an aggregate of solid soil grains is held together only by effective spherical stress and not by any adhesion of one grain with another. Energy stored and work done in distortion of the aggregate of grains does not relate to a particular plane through it.

The *Hvorslev surface* that Roscoe *et al*. (1958) drew (Fig. 29) shows an edge to the Hvorslev surface with a curved vertical wall directly above the curve of normal compression with $\sigma'/\sigma'_e = 1$ on the (σ', e) plane. We were incorrect to draw a surface all the way to that edge since there is no test data in the space to the right of C with $\sigma'/\sigma'_e = 0.6$ in Fig. 27. We should only have drawn lines such as BC in Fig. 29 ending at the CS line in a space with axes (τ, σ', e). The Hvorslev surface relates only to the states on the dry side of CS just before peak strength (Fig. 29). In Figs 12(c) and 12(d), the dotted lines on the dry side of the CS line have stress ratios higher than those at the angle of repose on the wet side of the CS line. They refer to a discontinuous interlocked aggregate with separate blocks slipping relative to each other. In Figs 12(c) and 12(d) the dashed lines on the wet side of the CS line have stress ratios lower than those at the angle of repose. Roscoe *et al*. suggested that on the wet side of the CS line a curved yield surface with cross sections of approximately parabolic form may be determined experimentally from both drained and undrained tests, and that test paths cross this surface and ultimately reach the CS. By the CS concept, if Hvorslev had been able to sample the water content of CS gouge material within the slip plane gouge material after dilation, all data on the dry or wet side of critical states would have accumulated at the end C of the line BC in Fig. 27. In Fig. 29 the curve DEF in the (τ, e) plane shows that τ increases as e and hence water content decreases. If the explanation of the curve DEF is a cohesion that depends on the thickness of the water film, this must apply right across Fig. 27. Since the value of e is constant, the water film thickness is constant, and if we apply the cohesion theory from B to C we should also apply it to the right of C. When the slip plane model was contrasted with the CS model of soil behaviour in the first chapter of this book, the plot of Eqn (2) in Fig. 1(b) was described as a map of behaviour. The CS model explains why behaviour changes at C.

The CS concept does not explain why Hvorslev's slip planes through dense stiff clay in his shear box mobilized strength data that fitted his straight lines in Fig. 26. When Skempton and Petley (1968) studied the development of slip planes and the formation of structural discontinuities in stiff clay they referred to experiments on a slab of clay sheared into two parts. The underside of the slab was placed over the edges of two plates that were made to slip past each other and dragged the slab with them. The upper surface of the slab was observed, and successive discontinuities were seen to develop at various angles to the ultimate slip plane. The lightly stressed soil slabs were in non-uniform stress states far to the left in the Frontispiece. The slip plane passed through what can be described as

discontinuous rubble, and the angle between the direction of the slip plane and the direction of the plane on which the major principal effective stress acted at failure agreed with the Mohr–Coulomb failure criterion calculation when they used Hvorslev's true friction angle. The paper about the progressive development of discontinuities and a slip plane then makes a calculation that requires the region to which it is applied to be continuous. There is an attempt to understand Hvorslev's peak strength data in Fig. 29, and an attempt to understand the data of stable yielding in triaxial tests of reconstituted clay soil in the Frontispiece. CS theory considers scalar invariants of effective stress tensors of stress at points in an aggregate, not vectors of stress on planes through it. It plots the spherical effective pressure p', and the stress ratio q/p', but the Hvorslev surface plots with components of stress σ' normal to a slip plane in Fig. 12(d) and stress ratios τ/σ' in Fig. 12(c). The Frontispiece builds on the 1958 conclusion of Roscoe *et al.*:

> *The main, and perhaps most surprising, conclusion to be drawn from the work outlined above is the remarkable similarity between the behavior of the clays and the cohesionless granular media, and it might be relevant to refer to a comment by Terzaghi (1956) on the mechanical concept of the behavior of clays.*

Hvorslev's analysis of his laboratory tests fitted his test data to a line such as BC in Fig. 5(d) for Coulomb's slip plane, and his data could be explained by combining CS friction with interlocking in a disturbed aggregate of hard grains. Figure 5(d) shows these alternative interpretations of test data in terms of cohesion and friction properties (c, ϕ') or $c = 0$. When Schofield and Wroth (1968) discussed Henkel's (1956) analysis of the long-term stability of retaining walls in stiff fissured London Clay, we applied the CS analysis of disturbed soil to undisturbed soil with cohesion caused by cemented bonds or chemical effects as well as the closeness of grains. For Henkel's set of wall failures in North London, he found that, with a friction angle of $\phi' = 20°$, the c contributing to the stability of the failed ground fell below his expected peak c value. Skempton (1977) proposed that London Clay had time-dependent cohesion. The CS alternative was for time effects to be due to the transient flow of pore water in mechanical disturbance of the aggregate of grains in gouge material near the slip plane. Skempton applied his supposition that the value of c should fall with the passage of time to the calculation of the short-term stand-up of a steeply battered face in the excavation for the foundation of the Bradwell nuclear power station; this supposition was wrong, so the face failed before completion of the work. Schofield and Wroth used $c = 0$, $\phi' = 22°$ to get a CS alternative to Skempton's and Henkel's calculations.

Geotechnical centrifuge testing is a laboratory test method with a longer history than the triaxial test, as will be discussed further below. It re-creates aspects of an actual case of failure with scaled boundary conditions. This method was used in two studies of scaled combinations of consolidation, swelling, cracking and shearing on models made of undisturbed soil in the UMIST centrifuge. One example (Lyndon and Schofield, 1970) tested models of scaled excavations in large undisturbed London Clay samples. Two cut faces of a 10 m excavation into stiff, brown, weathered, fissured, London Clay, steeply battered at different inclinations, failed in test times of 28 and 55 minutes corresponding to 12 and

24 week times for prototype failure, which more or less corresponded to what happened at Bradwell. It was consistent with a time scale factor for softening of the square of the length scale (as in Terzaghi's time factor for consolidation). The other example was Lyndon's (1972) modelling of the 1954 Lodalen landslide with a scaled excavation, slow swelling and long-term failure in large undisturbed samples of Lodalen clay. In both examples the long-term softening in the failure zone depended primarily on the suction of water into the zone, and the time for which a slope will stand before failure is not a matter of time-dependent cohesion. Skempton saw Hvorslev's line BC in Fig. 5(d) as a fundamental truth about the strength of clay. Although he finally accepted that first-time failure of stiff fissured brown London Clay is consistent with soil strength on line AC equal to fully softened CS friction with no cohesion, he did not appreciate the significance of the predicted behaviour of OCC on the wet side of the CS.

4   Limiting stress states and CS

Rankine (1857) began with a clear objective as follows:

> The subject of this paper is the mathematical theory of that kind of stability, which in a mass composed of separate grains, arises wholly from the mutual friction of those grains, and not from any adhesion amongst them.

When he considered the aggregate of clean, rough irregular grains with limiting stress on slip planes he tried to follow Cauchy's method of dealing with a solid body as a continuum, but he kept the concept of a frictional limit to the shear stress on any plane.

4.1   Strain circle, soil stiffness and strength

The treatment of the vector components of stress on slip planes up to here in this book would have been familiar to 18th-century engineers such as Coulomb. All changed after Cauchy (1789–1857). Late 19th- and 20th-century engineers learned about the stress and strain circles that will be developed in this section. For a student who needs to familiarize themselves with the mathematical concepts of stress and strain, a starting point is that properties do not change when samples are moved from place to place and trimmed. This is the principle behind soil sampling and laboratory testing, and it is also behind the concept of strain. Triaxial and simple shear test specimens look different, but the two tests can be shown to be fully equivalent by this principle. The shape changes in Fig. 30 are linked with strain increments in the triaxial and the simple shear tests. In Fig. 30 a square element of a plane body is moved and trimmed in five steps that restore it to the original shape. Step a** is simple shear distortion. Step b* is rotation. Step c* cuts the corners of the specimen, to leave a rectangular shape without displacement or distortion. Step d** distorts the rectangle back to the original square. Step e* rotates it back to the original position. The deformation geometry of the specimen in steps a** and d** resembles the SSA and the triaxial test. These deformations do not involve slip on any discrete plane.

Shearing of a square causes a change of angle γ at each corner. We see in Fig. 30 that this involves distortion (as two sides of a square rotate by angles $\pm\gamma/2$ towards each other in step a**), and body rotation (in step b*). The essential nature of strain is that steps a** and d** show exactly the same phenomenon, but appear different as we adopt different reference axes. A body rotation of the dashed vector diagonal is subtracted from step a** to get step b*, and in step d** an extension strain ε_1 of side 1 of the rectangle and a compression strain ε_2 of side 2 of the rectangle returns the shape to the original square. To understand how change of length and change of direction work in a more general plane strain we examine a strain that involves stretching space by ε_x in the x direction
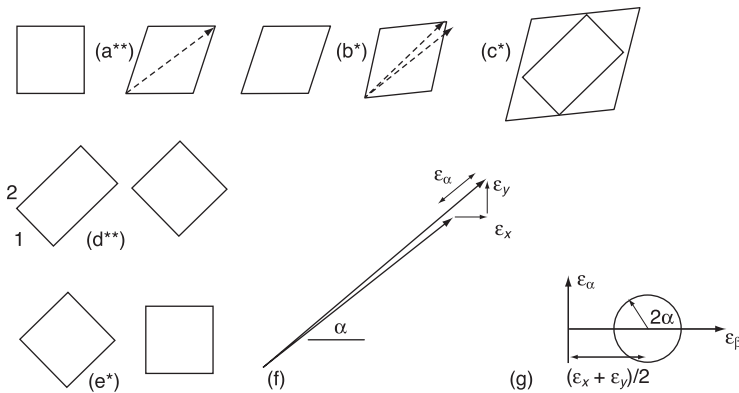
Fig. 30 Distortion (**), rigid body displacement (*) and the strain circle

and ε_y in the orthogonal y direction in Fig. 30. The effect on a unit vector inclined at an angle α to a major strain direction is shown in Fig. 30(f). The unit vector both extends by ε_α and also rotates through ε_β. If the unit vector is seen as having components of length $\sin \alpha$ and $\cos \alpha$ that are each elongated by strains, simple equations relate the strains as follows:

$$\varepsilon_\alpha = \varepsilon_1 \cos^2 \alpha + \varepsilon_2 \sin^2 \alpha \tag{12}$$

$$\varepsilon_\beta = \varepsilon_1 \sin \alpha \cos \alpha - \varepsilon_2 \cos \alpha \sin \alpha \tag{13}$$

Since $\cos 2\alpha = \cos^2 \alpha - \sin \alpha$, and $\sin 2\alpha = 2 \sin \alpha \cos \alpha$, these equations give

$$\varepsilon_\alpha = (\varepsilon_1 + \varepsilon_2)/2 + [(\varepsilon_1 - \varepsilon_2)/2] \cos 2\alpha \tag{14}$$

$$\varepsilon_\beta = [(\varepsilon_1 - \varepsilon_2)/2](\cos \alpha \sin \alpha) \tag{15}$$

This second set of equations show that $(\varepsilon_\alpha, \varepsilon_\beta)$ gives a point on the circle in Fig. 30(g) with centre $(\varepsilon_1 + \varepsilon_2)/2$ and radius $(\varepsilon_1 - \varepsilon_2)/2$. As the angle α in Figs 30(f) and 30(g) rotates from 0 to π, the radius to the point $(\varepsilon_\alpha, \varepsilon_\beta)$ on the circle rotates through 2α. The strain circle allows interpretation of data from a strain gauge rosette that is stuck to a plate. From the data of changes of length in the directions of the gauges in the rosette we can get principal directions of two lines on the plate that elongate without rotation.

A simple starting point with plane stress is shown in Fig. 31 in a triangle KLM with principal stresses (σ_1, σ_2) acting on horizontal and vertical sides ML, KM,
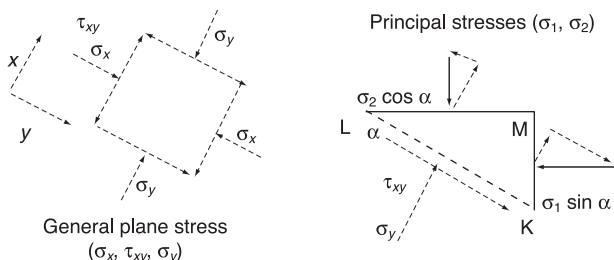
Fig. 31 Plane stress components
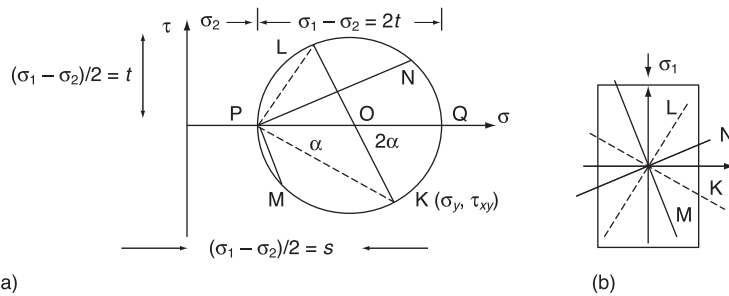
Fig. 32 Plane stress circle. (a) Four plane stress points on a circle. (b) Directions of four planes (K, L, M, N) on which four stress vectors act

and with a general section side LK inclined at an angle α. To the left is a general square plane element with axes (x, y) inclined at the angle α. Normal and shear stress components $(\sigma_x, \sigma_y, \tau_{xy})$ act on the element sides. The side LK of triangle KLM is of unit length, so $KM = \sin \alpha$ and $ML = \cos \alpha$. The stress components $(\sigma'_x, \sigma'_y, \tau_{xy})$ can be found in terms of $(\alpha, \sigma'_1, \sigma'_2)$, or (α, s, t) by the resolution of forces normal to and parallel to LK in Fig. 31 as follows:

$$\sigma_x = \sigma_1 \cos \alpha \cos \alpha + \sigma_2 \sin \alpha \sin \alpha$$

$$= (\sigma_1 + \sigma_2)/2 - [(\sigma_1 - \sigma_2)/2] \cos 2\alpha = s - t \cos 2\alpha \tag{16}$$

$$\sigma_y = \sigma_1 \cos \alpha \cos \alpha + \sigma_2 \sin \alpha \sin \alpha$$

$$= (\sigma_1 + \sigma_2)/2 + [(\sigma_1 - \sigma_2)/2] \cos 2\alpha = s + t \cos 2\alpha \tag{17}$$

$$\tau_{xy} = (\sigma_1 - \sigma_2) \cos \alpha \sin \alpha = [(\sigma_1 - \sigma_2)/2] \sin 2\alpha = t \sin 2\alpha \tag{18}$$

where

$$s = (\sigma_1 + \sigma_2)/2 \quad \text{and} \quad t = (\sigma_1 - \sigma_2)/2 \tag{19}$$

Anticlockwise shear stress and compressive normal stress are plotted as positive quantities in Fig. 32; this convention is adopted in soil mechanics because soil fails in tension, but student engineers are taught the opposite convention in strength of materials lectures on materials such as steel. The components (τ, σ') give the point K. Equations (16) to (19) show that K lies on a stress circle with the centre O at a point $\sigma = s$ and radius t. The fact that this circle cuts the σ axis at the opposite ends of a diameter confirms the assumption in Fig. 31 that there are two principal directions of principal planes on which (σ_1, σ_2) major and minor stresses act. Point P on the circle is called the pole of planes. Parallel to the plane in direction KL in Fig. 31, a general line through P at the angle α cuts the circle at a point K with coordinates (σ, τ) that are the components of stress on that KL plane. Through the pole P in Fig. 32(a) four lines (K, L, M, N) cut the circle at points N, K, M, L, with coordinates representing the stress components on planes in four directions of sections K, L, M and N shown in Fig. 32(b).

Pairs of points such as K and L, or M and N, represent stress components on two orthogonal sections through points in a continuum. The normal stresses σ at these points differ, but the shear stresses τ are equal in magnitude and opposite

in sign, and are called complementary shear stresses. In Fig. 32(b) the major stress σ_1 on the plane test specimen acts vertically on the horizontal plane, and is plotted as point Q. Through Q a line drawn parallel to the plane on which σ_1 acts, intersects the circle at the point P that is called *the pole of planes*. In general, to find components of stress on a plane in a given direction, a line is drawn through this pole P parallel to that direction. It intersects the circle at a point with coordinates of the components of stress. For example in Fig. 32(b), minor stress in the test specimen acts horizontally on the vertical planes, and a vertical line drawn through P cuts and is tangential to the circle at the minor stress point σ_2.

In the early 20th century, transformations from one set of reference axes to another that had been encountered in continuum analysis were met in problems of relativity and electromagnetic theory. Newton had introduced what he called *fluxions* and are now called derivatives in the calculus and physical laws that then became expressed in terms of physical constants, or quantities that are independent of the observer's choice of reference axes. The aspects of the physical world that could be deduced by mathematics became part of what is called applied mathematics and mechanics. The role of experiment was reduced to the determination of physical constants, thought by some to be work for technicians. An overarching new mathematics developed, called tensor analysis, and new engineering textbooks introduced tensor notation. Stress and strain circles now appear antiquated, but a student who understands graphics well enough to solve engineering stressing problems need not understand or be overawed by tensor analysis. For example, the stress circle lets us comment on Coulomb's tests on rock and SSA tests on soil. Figure 33(a) shows a point in a continuum with lines at 45° through it in directions K, M, L and N. In Coulomb's Plate 1 (Fig. 1(c)), of his 1773 Essay the test in his Fig. 2 has a weight hung from a loop of rope round the root of a stubby cantilever. In Fig. 33(b) the vertical plane M bears a uniform shear stress τ. If a clockwise shear stress c_u acts on the vertical plane, equal and opposite shear must act on the horizontal plane. Figure 33(e) shows the difficulty that was bound to occur in
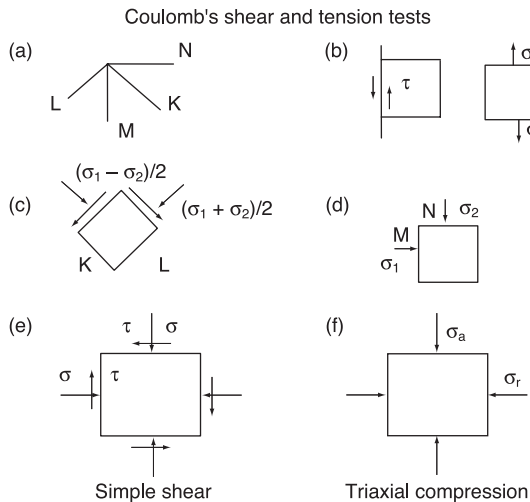
Fig. 33 *Boundary forces in alternative tests*

An increment in spherical stress $\delta p'$ causes δv volumetric strain increment

An increment in shear stress δq causes $\delta \varepsilon$ shear strain increment
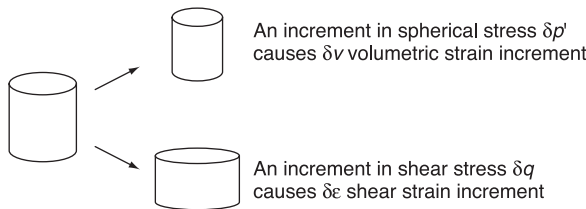
Fig. 34 Bulk and shear stress and strain

Roscoe's SSA (Fig. 28). The rotating end flaps BC and DA (Fig. 28) covered by lubricated rubber sheets did allow expansion but eliminated the shear stress that was needed on them. Hence stress was not uniform in the SSA.

In the late 19th century it was still thought possible that one physical constant might define the elastic properties for isotropic material; as a 20th-century student I was taught about Young's 17th-century elastic modulus E, not about K and G; I thought that elongation of metal in tension depends on a single material property like coiled spring stiffness. I found later that elongation of a bar involves two quite different effects; part is caused by reduction of the metal density, but most is due to shear distortion. Love (1927) still referred to multi-constant and rari-constant theories in the historical introduction to his treatise on the mathematical theory of elasticity. Cartesian tensor analysis (Jeffreys, 1931) showed that two elastic properties, K and G, are needed to define the elastic stress–strain behaviour of an isotropic continuum. In soil mechanics when the Mohr–Coulomb theory was dominant, all laboratory tests aimed to find soil constants. Development of CS theory had to rely on the data of soil laboratory tests where the original purpose was to support the ruling theory. Penman (1953) had published his triaxial test data at the BRE. Bishop and Henkel (1962) had published Imperial College triaxial test data. These publications needed to be reinterpreted. The basic elastic constants K and G for an isotropic elastic continuum (Fig. 34) led to the (p', q) parameters that re-interpreted the data. A spherical stress increment $\delta p'$ divided by the elastic bulk modulus K gives δv, a volumetric strain increment. The increments in deviator stress δq_i divided by the elastic shear modulus G gave elastic shear strain increments $\delta \varepsilon_i$. A truly triaxial test would apply a different pressure $(\sigma'_1, \sigma'_2, \sigma'_3)$ normal to each face of a cubical test specimen, but we do not have cubes of soil to test because we drill vertical holes in ground, press sharp cutting tubes down at the base of the holes, and get more or less undisturbed cylindrical soil samples. These cylindrical samples are sheathed in thin flexible rubber and tested in what is called a triaxial cell, but which in fact applies axial stress $\sigma'_a = \sigma'_1$ and radial stress $\sigma'_r = \sigma'_2 = \sigma'_3$, as we have already seen in Fig. 2. The general stress state in Fig. 35 can be expressed in the following terms:

$$\sigma'_1 = (\sigma'_1 + \sigma'_2 + \sigma'_3)/3 + (\sigma'_1 - \sigma'_2)/3 - (\sigma'_3 - \sigma'_1)/3 = p' + (q_3 - q_2) \quad (20a)$$

$$\sigma'_2 = (\sigma'_1 + \sigma'_2 + \sigma'_3)/3 + (\sigma'_2 - \sigma'_3)/3 - (\sigma'_1 - \sigma'_2)/3 = p' + (q_1 - q_3) \quad (20b)$$

$$\sigma'_3 = (\sigma'_1 + \sigma'_2 + \sigma'_3)/3 + (\sigma'_3 - \sigma'_1)/3 - (\sigma'_2 - \sigma'_3)/3 = p' + (q_2 - q_1) \quad (20c)$$

Equations (20) and Fig. 35 show that a truly triaxial stress $(\sigma'_1, \sigma'_2, \sigma'_3)$ can be decomposed into three general shear components (q_1, q_2, q_3) and a spherical

Spherical p' Three orthogonal shears q_1, q_2, q_3

(a)   (b)   (c)   (d)
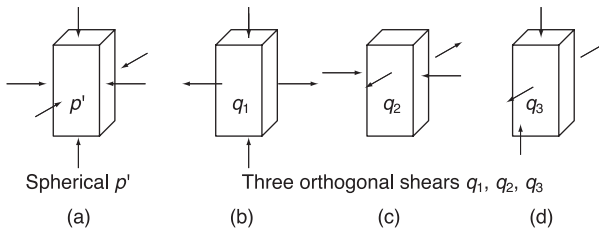
Fig. 35 *Components of truly triaxial stress*

component p'. In gas or fluid that cannot sustain shear stress we think of p' as pressure. Deviator stress involves compression $+q$ acting on one face of a cube, tension $-q$ acting on a face at right angles, and zero pressure on the third face. Their zero sum means that deviator components contribute nothing to the fluid pressure p', as is seen in Eqns (21) and (22):

$$p' = (\sigma'_1 + \sigma'_2 + \sigma'_3)/3 \tag{21}$$

$$q_1 = (\sigma'_2 - \sigma'_3)/3 \tag{22a}$$

$$q_2 = (\sigma'_3 - \sigma'_1)/3 \tag{22b}$$

$$q_3 = (\sigma'_1 - \sigma'_2)/3 \tag{22c}$$

The successive states imposed in drained triaxial compression tests with $\sigma'_1 = \sigma_a$ and $\sigma'_2 = \sigma_3 = \sigma_r$ define a test path. Scalar-invariant parameters (q, p') can be derived from the principal effective stress components:

$$q = [(q_1^2 + q_2^2 + q_3^2)/2]^{1/2} = \sigma'_a - \sigma'_r \tag{23}$$

$$p' = (\sigma'_a + 2\sigma'_r)/3 \tag{24}$$

We have seen earlier in this book that the most important property of a grain aggregate is that a shearing deformation can cause volume change. Isotropic elasticity cannot model this. In an isotropic elastic continuum, spherical stress cannot cause shear distortion, and shear stress cannot cause volume change. If clockwise-turning shear caused dilation in a material, then anticlockwise shear must cause contraction. If a clockwise material were to exist, symmetry would require that an anticlockwise material must also exist, in which anticlockwise turning shear would produce dilation. In order for linear isotropic elastic material to be neither clockwise nor anticlockwise, it must have constant density in shear distortion. In Fig. 14(b) the dilation or contraction of a grain aggregate cannot depend on the shear direction.

This is an appropriate point for a small comment on the parameters plotted in the Frontispiece. A value of q derived from the sum of the squares of shear components as in Eqn (23) must be a positive quantity, but in Fig. 2(a), where $q = \sigma_a - \sigma_r$, the possibility of both positive and negative values of q allows for a difference in behaviour in tests where axial or radial stress is the major stress. This applies in the Frontispiece where stress obliquity $\eta = q/p' = 3(\sigma_a - \sigma_f)/(\sigma_a + 2\sigma_r)$ covers two zones. The top half of the map has $\sigma_a > \sigma_f$ stress obliquity $\eta > 1$ positive and the bottom half has $\sigma_a < \sigma_r$, so $\eta < 1$ is negative. In the case of a stress vector on a plane, the angle of obliquity is always positive, but in the triaxial test the

generalized parameter η has an additional meaning. In Fig. 2(a) the cell pressure can be held constant and, by pushing a plunger down into the cell, the force on the top cap can be increased, but it is possible for the plunger to pull the top cap upwards against the cell pressure and make axial stress less than radial stress. Two further possibilities are that the hanger load will keep the axial stress constant and that stress obliquity will be changed by a change of cell pressure, or that the total axial and radial pressure will both be held constant and that injection of a small quantity of pore water at the pedestal connection will reduce p' and cause the obliquity to change.

Different limiting states are involved when a specimen shears on a slip plane and when it cracks. The cracking that is observed in lightly stressed dense specimens differs in different halves of the map. In the upper half of the Frontispiece, an axial compression causes a test cylinder to split on axial planes, with cracks like the cracks that are seen in the free surface of ground at the top of the slope, and in logs that are split for firewood; in the lower half, either axial relief of stress or radial compression causes cracking on planes perpendicular to the axis of a test cylinder; it can crack into many discs. If a tunnel face carries stresses in both radial directions that are too high it will *spall*, with pieces of rock bursting out of the face along the tunnel axis, and similar spalling is seen when concrete slabs fail with high stresses in the plane of the slab. Tension cracking of concrete is seen in split cylinder specimens. In these tests, instead of standing in a testing machine, specimens are compressed between two lines of contact at the ends of a diameter. Cylinders split apart on the diametric plane. In tests of compacted Teton dam core material tests at Cambridge University, the onset of cracking was detected by an increase in permeability both to water and to air. Unsaturated compacted soil cylinders were subjected to split cylinder tests. To detect cracking they were cling-wrapped to seal the free surface, and an air pressure gradient led to an axial flow of air, which then bubbled through water. The onset of cracking of soil was detected both by a shift in the load deflection line and by a sudden increase in the rate of air bubbling. The cracks were seen in radiographs after tests. No total stress acts normal to a crack surface. In Fig. 2 with no pore water pressure $u = 0$, if the radial stress is zero then $\eta = +3$, or if the axial stress is zero then $\eta = -\frac{3}{2}$, so an upper and a lower line can be drawn in the Frontispiece at these values. An alternative tensile strain criterion for cracking is that, when a crack opens, the grains that will form asperities on either side of the new crack surface move away from each other far enough for the new crack surface to become unlocked. Another possible criterion is a line with $p'_c/p'_{cs} = 1/100$ where p'_c is the mean normal effective pressure at the onset of cracking and p'_{cs} is the CS mean normal effective pressure. The Cambridge test data were scattered, but all were inside such lines on the map.

The OCC model that will be discussed below is within the scope of isotropic plasticity in solid mechanics. To describe granular media with critical states (v, p'), it introduces the parameter $v_\lambda = v + \lambda \ln p'$ and the CS relation (Eqn (10)) is written as $v_\lambda = \Gamma$. During both clockwise and anticlockwise shearing, soil contracts in states in which $v_\lambda > \Gamma$ (called *on the wet side of critical*), and dilates in states in which $v_\lambda < \Gamma$ (called *on the dry side of critical*). OCC is a model for isotropic soft soil on the wet side of the CS during plastic yielding and flow. I

developed analysis of soil test data using (q, p', v) parameters in 1955–1957 at the outset of my research (Schofield, 1960) for the purpose of interpreting the then newly published series of research theses and *Géotechnique* papers on triaxial testing at Imperial College and the triaxial test handbook by Bishop and Henkel (1957). These publications showed stress circles at failure of sets of triaxial test specimens, and retained only one peak stress circle from the data of one specimen at failure, and all other test data had to be discarded. The specimens' specific volumes varied. No set of circles at failure had a very precise failure envelope. The advantage of (q, p') parameters over stress circles was that the new analysis retained data from all stages of one test as points on one test path. The initial portion of any path is not well defined. Initial displacement is needed before the aggregate of grains at the end of a test cylinder is properly in contact with the pedestal and the top cap. The final portion of the path suffers from the distortion of test cylinders at failure. Data from the middle portions of many test paths when correlated to reduce errors due to specific volume variation give more insight into soil behaviour than is given by stress circle envelopes.

Slow tests of saturated cylindrical soil specimens in rubber sheaths in triaxial cells with drainage or pore pressure measurement of pore pressures or suctions to find the effective stress give excellent data, but the Mohr's circle interpretation of the test data is doubtful. Points on either the stress ellipse or circle do correctly represent plane stress components (τ, σ') tangential to, and normal to, lines through a point in a plane body, and engineers can find stress components on inclined lines from the ellipse or circle, but it does not follow that vectors across particular planes matter. The stress tensor and its invariants involve all vector components on all planes. Schofield and Wroth's (1968) criticism of both stress circle and ellipse was that such

> ...*representation of stress imparts no understanding of the inter-relation of stress-increment and strain-increment in elastic theory, that it plays little part in continuum theories, and that the uncritical use of Mohr's circle by workers in soil mechanics has been a major obstacle to the progress of our subject.*

In the Mohr–Coulomb interpretation of data, a stress state is represented by a *stress circle*, and a test path ends with one ultimate stress circle of limiting stress at failure. The test interpretation by a path through a series of points (q, p', v) space exhibits elastic strain and plastic yielding as well as ultimate failure of a test specimen.

The above discussion of stress circles and (q, p') raises a question about Rankine's reaction to discovering that the limiting stress conditions on a plane through a point in soil also apply on a plane in a second direction. Since experience of failure of retaining walls is that a wedge of soil slips as a single slip plane forms, an alternative reaction would have been to deduce that Eqn (2) is wrong, unless failure planes also occur in the second direction. Rankine could have deduced that soil failure also involves strain. Triaxial test specimens can fail in two slip plane directions, but the second direction is never considered when soil is tested in a shear box. Rankine, like Coulomb, did not rely on cohesion. He stated that the permanent stability of earth is due to friction alone, but he failed to question the slip plane concept behind Eqn (2).

4.2 Rankine's soil mechanics

Rankine had already made fundamental contributions to thermodynamics when the University of Glasgow elected him to be Regius Professor of Civil Engineering and Mechanics in 1855. He decided to teach stress from the basis of Cauchy's early 19th-century discovery of the stress tensor as presented by Lamé's *Leçons sur la Théoriè Mathématique de l'Elasticité des Corps*. (Rankine (1858) refers to this most influential mid-19th century French textbook.) The array of numbers needed to define stress at a point exhibits *tensor invariance* under transformation of axes; the physical quantities of this type are *tensors*. While plane stress components (τ, σ') at a point in the mid plane of the shear box in Fig. 1(a) define a physical quantity of a type called the *vector*, the whole stress at the point is a physical quantity of a type that is of a higher order than the vector. Neither quantity changes physically if reference axes are chosen in different directions, but each component in the array that defines each quantity shows an appropriate change as the reference axes change. Cauchy showed that when reference axes (x, y, z) are transformed, the array of stress components on inclined planes in a continuum changes in the same way as the array of numbers that define coordinates of points on an ellipsoid. The plane stress ellipse explains what changes in the numbers are appropriate for the plane stress tensor. Rankine taught his students an interpretation of the plane stress by an ellipse; a more simple interpretation is the stress circle. Stress circle teaching in Berlin by Mohr replaced Rankine's stress ellipse teaching, and became universal (Swain, 1882).

What is now called the Mohr–Coulomb failure criterion, as shown in Fig. 36(a), has a pair of lines DA and BC with $c > 0$ enveloping all plane limiting stress circles. In Fig. 36, where AD and CB show Mohr–Coulomb conditions (Eqn (2)), the failure criterion lines are symmetrical on a (τ, σ') plot, and a stress circle with centre O touches the lines at A and B. In Fig. 36(a), lines PA and PB define the α and β directions in Figs 36(b) and 36(c). Here we must explain why the Frontispiece, reproduced in Fig. 37(b), and the (q, p') plot in Fig. 37(a) are asymmetrical. The asymmetrical pair of lines for the Mohr–Coulomb failure criterion in Fig. 37(a), has states on line EF with $q > 0$ corresponding to axial major stress $\sigma_a > \sigma_r$ and states with $q < 0$ on line E corresponding to $\sigma_a < \sigma_r$ that are states not considered in Fig. 36. Figure 37(a) shows how the curves for the Mohr–Coulomb failure criterion on
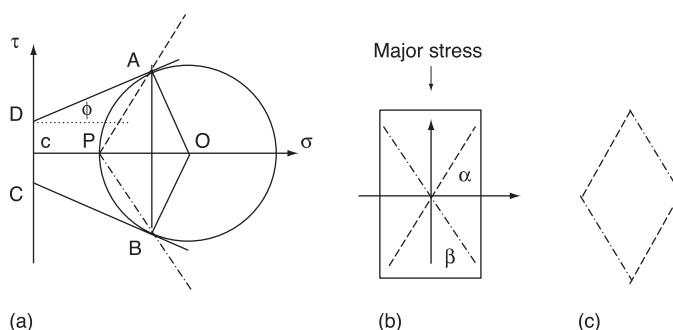
Fig. 36 Mohr–Coulomb theory. (a) Limiting stress at A, B. (b) Directions α, β. (c) Slip lines
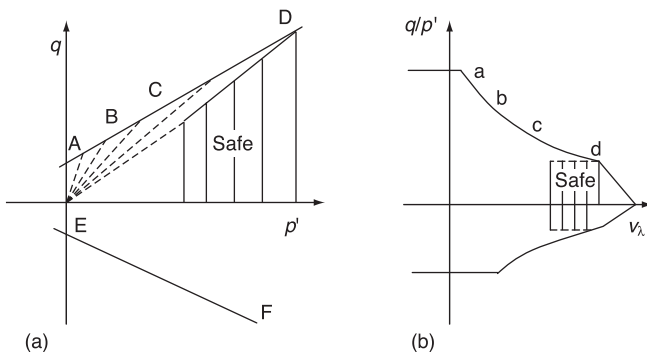
Fig. 37 Mapping of Mohr–Coulomb theory and safe states

slip planes in the Frontispiece can be obtained. At successive points ABCD on the line AD the dashed lines show that as the effective pressure p' increases from A to D, the slope q/p' and stress obliquity decreases. Points abcd in Fig. 37(b) and the curved line through them map the Mohr–Coulomb failure criterion in the Frontispiece. There is uncertainty in Fig. 36(a) as to the value of the intermediate stress. The effect on the parameters used in the Frontispiece and in Fig. 37(a) does not need to be resolved here as the Frontispiece is only a map produced for the purpose of discussion.

Rankine discovered that if Coulomb has a family of parallel lines of limiting stress (as shown as aB, a′B′, in Fig. 1(c)), then limiting stress also applies on a second family of lines in a different direction that Coulomb did not anticipate. The stress circle in Fig. 38(a) represents the plane stress state of the plane soil element at depth z by a wall, as shown in Fig. 38(b) in a vertical slice of ground with self-weight below an inclined unstressed upper plane surface. The faces of a prismatic element in Rankine's *Manual of Civil Engineering* (1874) have pressures on them that are called *conjugate* if the vector of pressure on one face is parallel to the
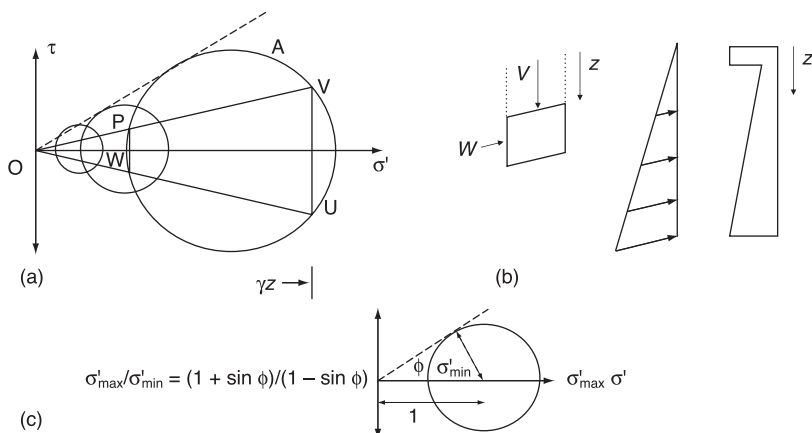
Fig. 38 Conjugate stress and earth pressure. (a) Stress circle. (b) Earth pressure on a wall. (c) Ratio of major and minor stress

other face of the prism. Where he had a stress ellipse our Fig. 38(a) has a stress circle. For a slice through the ground behind a vertical retaining wall, W is the least pressure on the wall. The ground in this minimum *active state* tends to move the wall. The point V on circle A represents the vertical stress on the inclined upper face of the element. The other circles to the left of A represent plane stress states higher up in the vertical slice. The line OV through V parallel to the inclined upper face cuts the circle A in the point P, which is called the pole of planes. Each inclined line drawn through P will cut the stress circle at a point that has coordinates representing the components of the plane stress vector on a line at that inclination in Fig. 38(b). The vertical line PW drawn through P cuts the circle at point W, representing the stress vector components on the vertical face of the soil element in Fig. 38(b). The solid lines DA and BC in Fig. 36(a) are tangential to the stress circle at points D and B and satisfy the Coulomb equation:

$$\pm\tau = c + \sigma' \tan\phi \qquad\qquad\qquad (2\,\mathrm{bis})$$

The faces of the plane prism of soil in Fig. 36(b) are in the vertical and the horizontal direction. The dashed line PA and the chain-dashed line PB are in the conjugate α and β line directions shown in Fig. 36(b) on which limiting stress acts. The stress circle in Fig. 36(a) is drawn with both cohesion and friction in the Mohr–Coulomb equation.

   Rankine (1857) thought that he could solve the plane problem of the stability of earth using a feature of conjugate planes that he had noticed. Figure 38(a) shows three stress circles corresponding to soil states at increasing depths in a slope. Point P is the pole of planes on the largest of these circles. The coordinates of W (Fig. 38(a)) show stress components that act on a plane in the direction PW. The pair of lines OPV and OWU in Fig. 38(a) show that PW is parallel to the τ axis, hence point W in Fig. 38(a) represents the stress components that act on the vertical plane in Fig. 38(b). For a prism with horizontal and vertical faces, the lines OPV and OWU merge with the σ' axis. The stress circle in Fig. 38(c) shows that the ratio of major and minor stress is as given by the equation in that figure. Rankine saw that if the weight of a vertical slice of a slope acted vertically on the inclined base of the slice, then his theory would give him the inclined stress acting on the vertical face of the slice (Fig. 39(b)). At the top of the slice there is zero stress, and stress increases with depth in the slope. He knew the way that the surface slope changed from one slice to the next, and wished to find a family of curved surfaces below the surface such that the base slope of each slice is always conjugate to the vertical direction of the side of the slice. He was on the Glasgow train, preparing his new undergraduate course, when he formulated equations for these surfaces, and quickly wrote a letter to the Secretary of the Royal Society to tell him that he was going to write a paper for the *Philosophical Transactions of the Royal Society*. He thought that he had to deal with the heat equations, with which he was familiar, and could draw a family of curves below the slope like the isothermal curves for conduction of heat in the semi-infinite plane body with an upper surface of general form (Fig. 39(b)). If he had been right, his curves would have been like the isothermals found by graphical methods, but his solution for an upper surface of the general form shown in Fig. 39 in the central part of his paper is wrong. After Rankine's death, Boussinesq (1874)
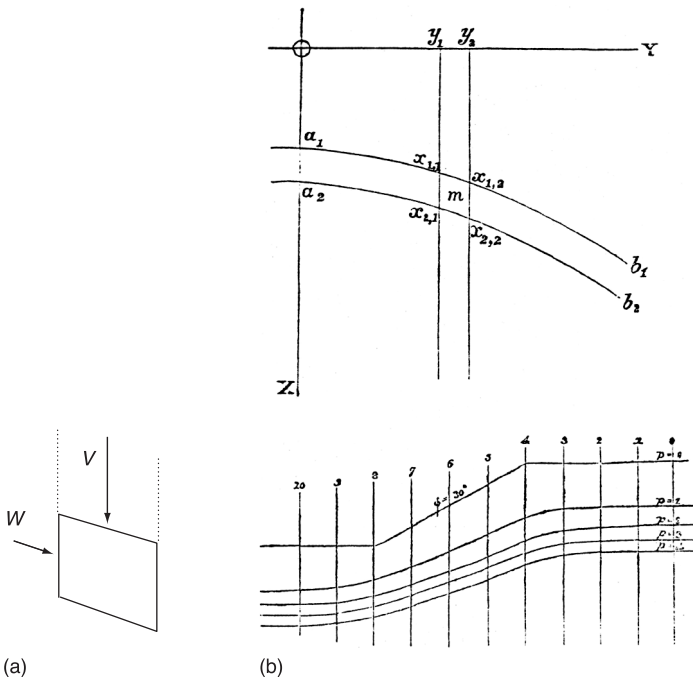
Fig. 39 Rankine's earth pressure analysis. (a) Conjugate stresses. (b) Figs 2 and 4 from Rankine (1857)

pointed out that Rankine should have used the wave equations rather than heat equations. Rankine had useful solutions only for what are now called *Rankine stress states* below an inclined plane surface as shown in Fig. 40. With cohesionless horizontal back-fill, both Coulomb and Rankine found the same lateral force, and agreed that ground can be *at rest* in a range of states between an *active* lower limit and a *passive* upper limit; with the vertical pressure at a depth z in the fill behind the wall as the major stress $\sigma'_{MAX} = \gamma z$ the calculation for a smooth vertical wall from Fig. 38(c) shows that the minor stress is $\sigma'_{MIN} = \gamma z(1 - \sin\phi)(1 + \sin\phi)$.

Correct solutions to the limiting static earth pressure problems with given stresses on the boundaries were given for example by Sokolovsky (1960). He combined the two equations of equilibrium of plane stress with the limiting stress equation to form three equations in three unknowns $(\sigma_x, \sigma_y, \tau_{xy})$. When transformed into two equations in new variables, he could solve the problem by the method of characteristics (see Schofield and Wroth, 1968). All solutions that used the slip plane model neglected strain. Terzaghi (1936) had learned in small-scale earth pressure tests in Turkey and in tests at full scale in the USA that strains affect earth pressures but, as strains did not enter Rankine's earth pressure theory, he concluded that

> *The fundamental assumptions of Rankine's earth pressure theory are incompatible with the known relation between stress and strain in soils, including sand. Therefore the use of this theory should be discontinued.*
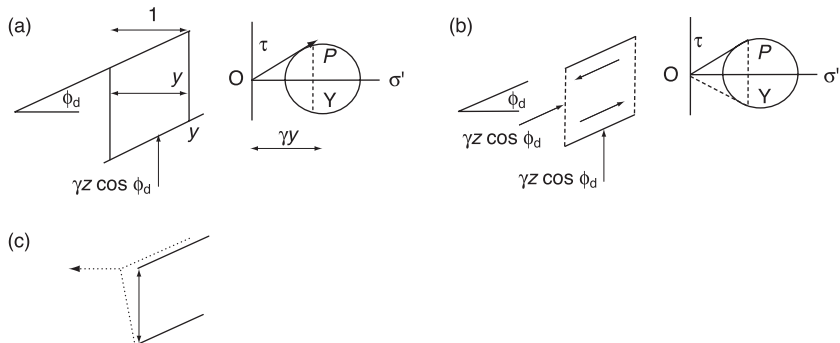
*Fig. 40 Directions of limiting stress in (a) a slope at repose or (b) a shear box.
(c) Perfect dilation in a slope or box if limiting stress directions are slip lines*

Terzaghi correctly noted the importance of strain, and this is seen in tests by
Schofield (1961), but as there is no error in the equilibrium equations the funda-
mental fallacy that has to be corrected must be an error in Eqn (2). If Eqn (2)
were true, the stress boundary conditions would determine the stress throughout
the field, and the strain boundary conditions would not affect stresses. The symmetry
of the stress tensor requires that a limit to stress on a plane in one direction must also
apply to a second plane in another direction. Domains of dependence in solution by
the method of characteristics mean that stresses on boundaries fully determine
limiting stress in a field. If earth pressures involve strain, the strength parameters
(c', ϕ') cannot be constants. The formulation of the OCC model specifies internal
friction of soil in a different way, by a dissipation function.

Rankine wished to analyse a granular material without introducing what he called
the artifice or assumption of Coulomb's slip plane or *wedge of least resistance*.
However, when Rankine assumed that *resistance to displacement by sliding along a
given plane in a loose granular mass is equal to the normal pressure exerted between
the parts of the mass on either side of that plane multiplied by the coefficient of friction*,
he defined internal friction of soil by the same slip plane strength model that
Coulomb had used. Neither Coulomb's limiting stress model nor Rankine's granular
material considered strains. A slip line has constant length. To either side of it a rigid
body is displaced along it with no dimension change. If the two families of lines of
limiting stress in conjugate directions α and β in Fig. 36(b) are also slip lines of
constant length, as mentioned in Section 1.3, then a lattice displacement in Fig.
36(c) will cause a dilatation increment in the plane area enclosed within the lattice.
Parallelograms tend to become squares of larger area. This applies to the slope at
repose in Fig. 40(a) and the simple shear box in Fig. 40(b) that is drawn with the
box base inclined at the slope angle. On the stress circles, point P represents stress
components on a line parallel to the limiting slope in Fig. 40(a) and the base of
the box in Fig. 40(b), and point Y represents limiting stress components on the
conjugate line, shown as a dashed vertical line PY. Lines in conjugate directions
bound the block on the slope in Fig. 40(a). Limiting stress acts on both vertical
and inclined lines in Fig. 40(b), and if both slip line segments have constant
length, then as shown in Fig. 40(c) the vertical line rotates forward with each

material point on the line instantaneously moving horizontally. Hence when the Mohr–Coulomb criterion is extended to consider strains both in the slope at repose and in the shear box, the soil dilates at angle ϕ_d. A principal direction of plastic strain increments cannot be aligned with a principal stress direction in simple flow of the slope. It appears to be the case in landslides that moving material on a slope can rotate as it flows. That type of flow is not associated with a potential function. The Mohr–Coulomb concept returns us to perfect dilation, as in Amontons (1699), Bélidor (1737) and Navier (1819). In Fig. 40(a) no soil mass falls in the Earth's gravity field. No work is done. Energy is not dissipated when the slope fails because a perfectly interlocked Mohr–Coulomb soil does not dissipate energy. We need a different model that does dissipate energy. The deformation of an aggregate of grains is not modelled by the strains associated with the Mohr–Coulomb equation.

Simple tests, made on a table, with screw-top glass bottles half-full of loose sand, will show that perfect dilatancy does not occur in the flow of a heap at the angle of repose. If the voids are filled with air in one bottle and with water in another, and the bottles are slowly rolled along on their sides on the table and tilted to stand on their ends, the sand will form slopes that will be seen to have the same angle of repose ϕ_d in air or below water, confirming the effective stress principles and showing that water is not a lubricant. Sand in each slope at repose will be seen to move generally parallel to the slope, not horizontally, so the evidence from slopes at repose does not support the deduction from Rankine's stress ellipse or from Mohr's stress circle that there is identical behaviour in both the α and β directions with limiting stress and constant slip line length. Experiments on a laboratory table in the Earth's gravity will not have the high effective stress at depth in model slopes that exists at full scale in the field. The geotechnical centrifuge in which the acceleration is increased as the model scale is reduced is an excellent laboratory test apparatus for the study of failure mechanisms rather than constants, but in 1955 this was not understood.

4.3   Skempton's parameters *A* and *B*, and CS values of *c* and ϕ

The Imperial College triaxial tests were discussed in Institution of Civil Engineers meetings and published in *Géotechnique* papers, research theses, and a book by Bishop and Henkel (1957). The results were expressed in terms of the pore pressure coefficients A and B introduced by Skempton (1950, 1954) to describe the response of a triaxial test specimen (Fig. 2(a)) to the change of the cell pressure σ_r and of the axial stress σ_a. He suggested two causes of change in the pore pressure Δu in the test specimen: change in the spherical total stress $p = (\sigma_a + 2\sigma_r)/3$, and change in the deviator stress $\sigma_a - \sigma_r$. His equation can be written as follows:

$$\Delta u = B[\Delta\sigma_3 + A(\Delta\sigma_1 - \Delta\sigma_3)] \tag{25}$$

If partially saturated soil is subjected to an increment of cell pressure $\Delta\sigma_3$, the pore pressure increment will be less than $\Delta\sigma_3$, as small air bubbles in the water compress, but a change of triaxial cell pressure on soil saturated with incompressible water will cause an equal change of pore pressure, so $B = 1$. Skempton

suggested that A was a soil property, and he gave a table of suggested values, with normally consolidated clays having values in the range $+0.5 > A > +1$. A and B were applied in the analysis of slope stability. Figure 1(c) shows in Fig. 8 of Coulombs 1773 Essay the method of slices in which a succession of vertical lines PM, PM$'$ and PM$''$ divide a sliding mass into slices that rest on a slip surface MM$'$M$''$. Part of the weight of soil in each slice is carried by effective stress at the base of the slice, and part is carried by pore water pressure. In order to analyse the change in slope stability caused by a load change, the change in pore pressure on the slip surface must be known. If the triaxial test specimen is regarded as a model of a cylinder of soil at the base of a slice in the field, then the test data of pore pressure changes can be used to predict pore pressures. In earth dam stability calculations it was convenient to introduce a parameter $\bar{B}$:

$$\bar{B} = \Delta u / \Delta \sigma_{\mathrm{a}} = B[1 - (1 - A)(1 - \Delta \sigma_{\mathrm{r}} / \Delta \sigma_{\mathrm{a}})] \tag{26a}$$

If the cell pressure σ_{r} is held constant so that $\Delta \sigma_{\mathrm{r}} = 0$ and the axial stress σ_{a} is changed, this reduces to a simple form:

$$\Delta u = BA \, \Delta \sigma_{\mathrm{a}} = \bar{B} \, \Delta \sigma_{\mathrm{a}} \tag{26b}$$

Triaxial tests in the laboratory could disclose how elements of soil will behave in the ground. Cylinders of soil were subject to axial stress by pressing a plunger into a cell either with or without allowing drainage of pore water. Figures 45 and 46 show Henkel's data for both soft and stiff clay. Figure 46 shows that as axial pressure q is increased on soft clay with constant cell pressure the pore water pressure u_1 is about equal to q so the value $\bar{B} = 1$ is constant. Skempton, referring to a 1947 US War Department report, *Triaxial Shear Research and Pressure Distribution Studies on Soils*, called $\bar{B} = 1$ the *American working hypothesis*. With $\bar{B} = 1$ in a slip circle analysis of the lateral pressure of soft clay on a sheet pile quay wall, a pressure placed on the quay will produce an equal pore pressure at the base of slices, and so not increase effective stress on a slip circle and not generate additional friction. This behaviour of soft ground on the wet side of CS can be contrasted with ground on the dry side where loads on dense soil generate suctions and additional friction in a dense soil body; Casagrande's wrote that such soil '*seems to be bracing itself, to become temporarily more stable*'. The difference between positive and negative pore pressure parameters was seen as a difference between soft and dense clay. Data from the curves in Figs 41 and 42 are tabulated in Fig. 43 for replotting as data points in the space of the variables (p', q, v); $\bar{B}$ is not a unique soil property. The effect is simplified by considering only the value of $\bar{B}_{\mathrm{f}}$ at failure; Roscoe *et al.* were able to relate $\bar{B}_{\mathrm{f}}$ for stiff clay to the over-consolidation ratio.

The CS concepts and the OCC model began with asking how the strength and stiffness of solids could be found from (q, p') plots of triaxial test paths. Figure 35 shows the two different sorts of elastic stiffness that resist volume change and shear deformation of solids. Much as the two elastic constants can be found from triaxial test data, so also if there were two sorts of plastic strength (in volume change and distortion) the data should reveal them. The test paths of
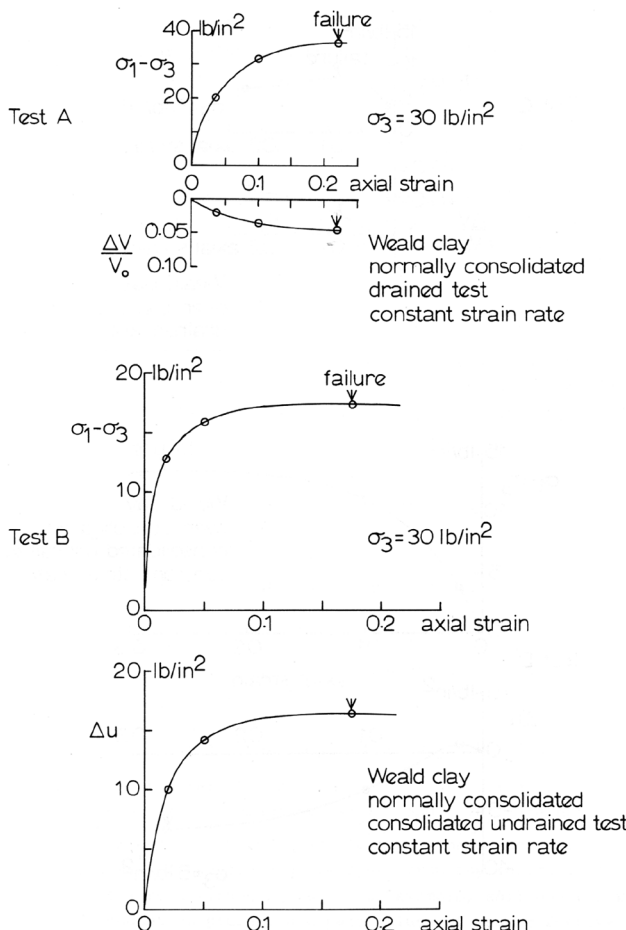
Fig. 41 *Triaxial test data of normally consolidated clay (after Wood, 1976)*

Figs 41 and 42 become paths that approach the CS line (Fig. 43). The CS concept was confirmed by the end points of tests of normally and over-consolidated Weald Clay test data from Imperial College as shown in Fig. 47(b). Parry (1959), a research student of Henkel, confirmed that his own test paths from one side of the CS line or the other side did all approach but did not cross the CS line at the end of each test. The CS line in Fig. 44(a) on the plot of (q, p') from origin 0 and passing through D4 resembles the line of critical porosities AC in Fig. 11(b). The ultimate states in many triaxial tests (Fig. 44) when plotted as v versus $\ln p'$ become a straight line satisfying Eqns (9) and 10 with the CS soil constants M, λ and Γ:

$$q = \mathrm{M}p' \tag{9 bis}$$

$$v + \lambda \ln p' = v_\lambda = \Gamma \tag{10 bis}$$
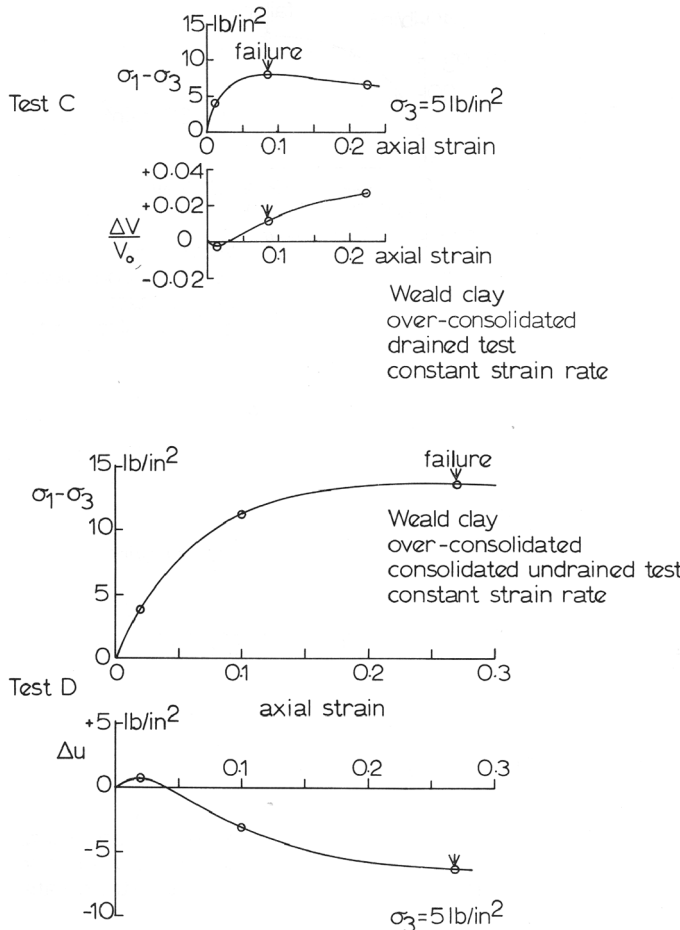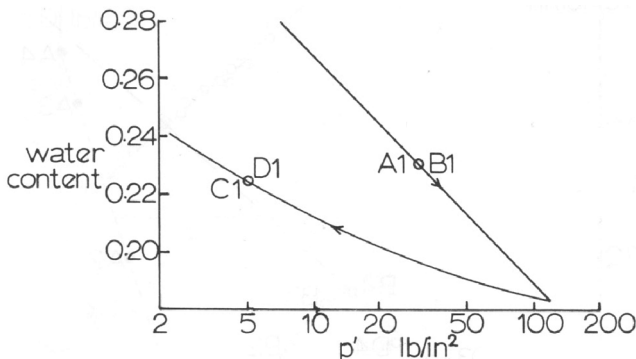
Fig. 42 *Triaxial test data of over-consolidated clay (after Wood, 1976)*

If an undrained triaxial test of saturated disturbed soil at constant water content and specific volume v ultimately reaches the CS, the undrained shear strength c_u of such soil can be determined from these equations as follows:

$$c_u = (\sigma'_a - \sigma'_r)/2 = Mp'_b/2 = \{M\exp[(\Gamma - v)/\lambda]\}/2$$

hence $\quad \ln c_u = \text{const.} - v$ $\hfill$ (27)

I digress at this point to comment how strange the data of test B in Fig. 41 must have been for those who thought of stress in soil in terms of Terzaghi's piston on a spring in a cylinder of water (Fig. 22(d)). The test data show a curve for the axial stress $(\sigma'_1 - \sigma'_3)$ increase equal to the curve for the increase in the pore water pressure Δu. By Terzaghi's effective stress principle, any shear deformation in Fig. 42 that leads to failure of the soil requires a change in effective stress, but if the change of pore pressure u in the cylinder is equal to the change of total pressure on the piston σ_1 there is no change of effective force in the spring. The soil deforms

Weald clay : Equilibrium water-content : pressure
curves for consolidation and swelling under
all-round pressure   (after Henkel, 1959)

Test point	w %	v %	V	q psi	Δu psi	p' psi $= p'_o + q/3 - Δu$
A1	23.2	O	1.64	O	O	30
A2		2	1.617	20	O	36.7
A3		3.5	1.583	32	O	40.7
A4		4.5	1.566	36	O	42 failure
B1	23.2	O	1.64	O	O	30
B2		O	1.64	13	10	24.3
B3		O	1.64	16.5	14	21.5
B4		O	1.64	17.3	16.5	19.3 failure
C1	22.4	O	1.617	O	O	5
C2		0.33	1.612	4	O	6.33
C3		-1.3	1.638	8	O	7.67 failure
C4		-2.7	1.661	6.5	O	7.2
D1	22.4	O	1.617	O	O	5
D2		O	1.617	3.5	1	5.2
D3		O	1.617	12	-3	12
D4		O	1.617	13.5	-6.5	16 failure

G_s= 2.75
v = volumetric strain : compression positive
V = specific volume = 1+e = $1+G_s w$

Fig. 43 *Triaxial test data (after Wood, 1976)*

in Fig. 42 when the spring in Fig. 22(d) does not. Bishop and Henkel (1957) wrote
Eqn (22) in their textbook on triaxial testing and introduced Skempton's pore
pressure parameters without explaining the strange undrained triaxial test of
normally consolidated clay (Fig. 41) with a pore pressure increase that is equal
to the increase in axial stress and a pore pressure parameter value $\bar{B}$ that is

$$\bar{B} = 1 \tag{28}$$

This *American working hypothesis* is not strange if triaxial test paths are plotted in a
space of (q, p', v) parameters. In Fig. 43, triaxial test samples under normal plastic
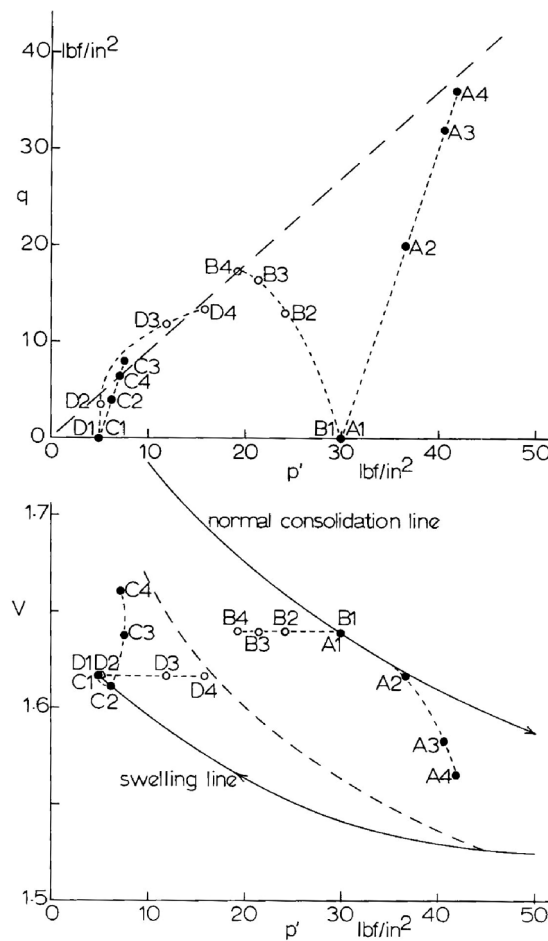
Fig. 44 *Drained and undrained triaxial test paths to the CS (after Wood, 1976)*

compression as the cell pressure σ_r' increases, and pore water drains follow the inclined straight line through point A1, B1. This line is called the NC normal compression line. Triaxial tests of NC specimens have test paths that start from points on this NC line, and the paths will end on the CS curve that is shown by the double lines. A test path will be in an applied loading plane such as is shown in Fig. 45. For example, if a plane with $v =$ const. is drawn through the starting point, the undrained test path must lie in the applied loading plane drawn with a chain-dashed edge in Fig. 45, as follows from

$$q = \sigma_a' - \sigma_r' \qquad (23\,\text{bis})$$

$$p' = (\sigma_a' + 2\sigma_r')/3 \qquad (24\,\text{bis})$$

For a drained triaxial test in which $\sigma_r' =$ const., the applied loading plane has $\Delta q/\Delta p' = 3$, as is shown with a dotted edge in Fig. 45. If the applied loading in a drained triaxial test is controlled so that $p' =$ const. by decreasing the radial
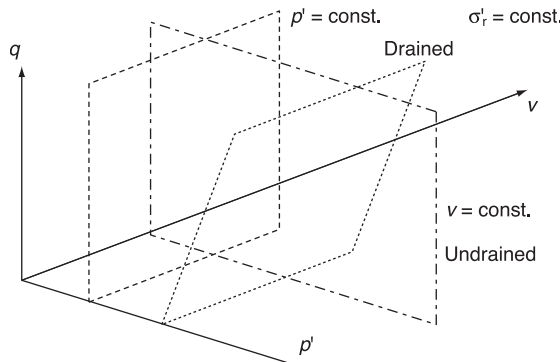
Fig. 45 Triaxial test applied loading planes

pressure as the axial pressure is increased, the applied loading plane will be as shown with a dashed edge in Fig. 45. The CS curve in (q, p', v) space intersects the planes in Fig. 45 at points that represent ultimate states on test paths.

The applied loading planes for $p' = $ const. tests and for tests with an increase of axial total stress and constant triaxial cell pressure are compared in Fig. 46. When applied total loadings get to points shown as 1 or 2, the ultimate effective stress point representing the soil state is C. The parameter $\bar{B}$ at failure as calculated in Eqn (22) in cases 1 and 2, respectively, is $\bar{B} = u_1/q_c$ or u_2/q_c, depending on the choice of applied loading. Since differences of applied loading give different values of $\bar{B}$, it follows that $\bar{B}$ is not a basic material property of soil. If the concept of a unique CS line is correct, then the basic material properties of soil are the parameters that define the CS line. The Conference on Pore Pressure and Suction in Soil in London in 1960 made no mention of the CS concept, published 2 years earlier, or of the use of plots of triaxial test scalar invariants (q, p'), or of any problem with pore pressure parameter A that is clearly not a soil constant. Bishop and Henkel (1962) never mentioned that Roscoe *et al.* (1958) had explained 4 years earlier that it followed from the CS line in Eqn (21) that the plot of $\ln c_u$ versus water content w is linear and that the undrained cohesion of newly disturbed soil paste depends on v, and hence on w (Fig. 47).

The first half of *Critical State Soil Mechanics* (Schofield and Wroth, 1968) led up to a presentation of the OCC model, the second half introduced limiting
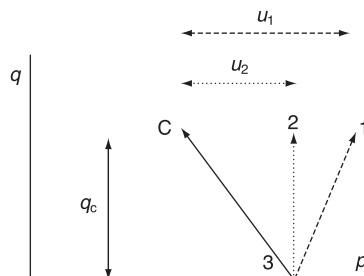
Fig. 46 Pore pressures in two undrained tests
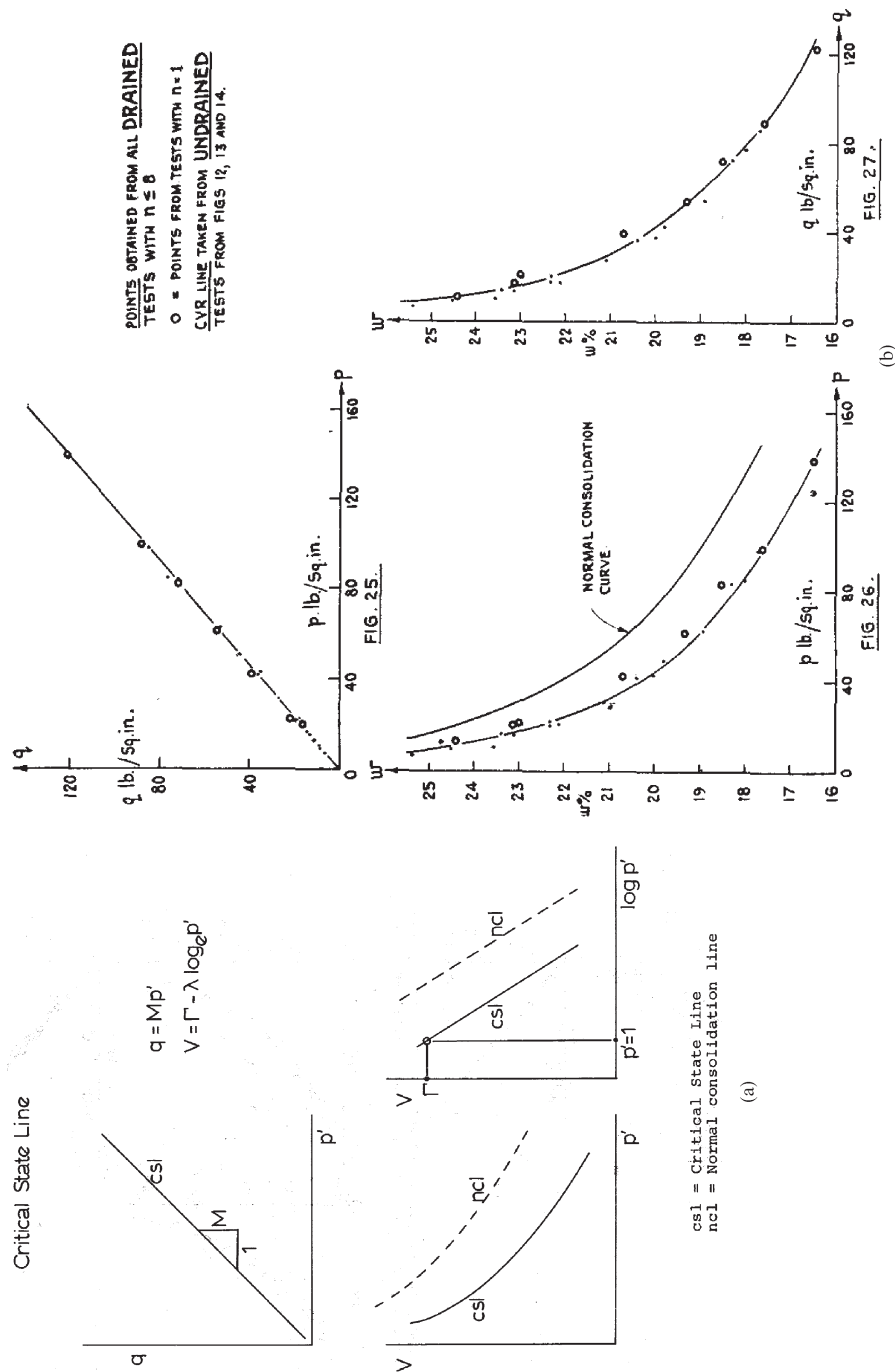
Fig. 47 Critical states of soil ((a) after Wood, 1976; (b) Roscoe et al., 1958)
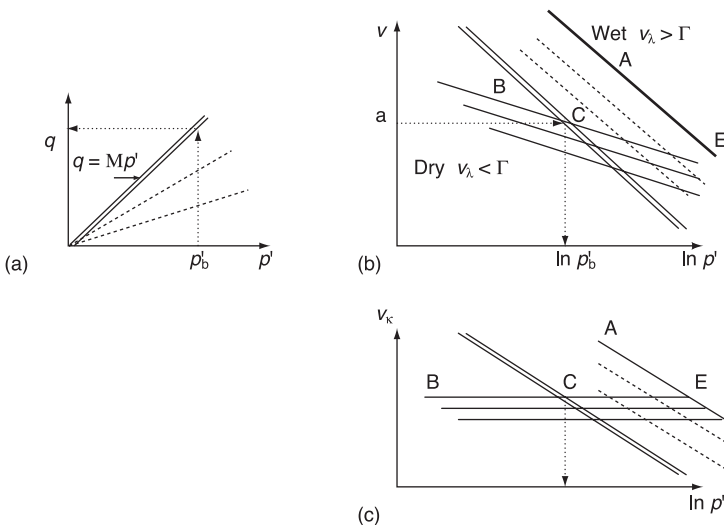
Fig. 48 λ and κ lines $v_\lambda = v + \lambda \ln p'$, $v_\kappa = v + \kappa \ln p'$

stress calculations for geotechnical design. At the outset of that book Wroth and I wrote:

> We wish to emphasize that much of what we are going to write is already incorporated by engineers in their present judgments. The new conceptual models incorporate both the standard Coulomb model and the variations which are commonly considered in practice; the words cohesion and friction, compressibility and consolidation, drained and undrained will be used here as in practice. What is new is the inter-relation of concepts, the capacity to create new types of calculation, and the unification of the bases for judgment.

With hindsight we should have confronted our reader with a basic problem: the words 'problemes de statique' in the title of Coulomb's Essay leave unasked the question of what happens after limiting static equilibrium is reached. A design based on a limiting stress field needs to confirm that the construction materials can dissipate the loading power in associated deformations in any conceivable failure mechanism. In Fig. 48(a) the CS double line has slope M, and friction in the CS flow of soil can dissipate the work done by the loads acting on the construction, but without effective stress there is no friction. Extra strength at peak stress comes from interlocking. The power associated with it is not dissipated. It is safe to rely on ultimate strength on the CS double line with slope M in Fig. 48(a); it is not safe to rely on peak strength.

There are dashed lines with $\eta < M$ in Fig. 48(a) for soil yielding in plastic compression in states on the wet side of the CS double line. In Fig. 48(b) they follow lines parallel to it with slope λ. Elastic swelling and recompression lines like BE have slope κ, and the aggregation on line BE does not change until the soil yields with a plastic volume change and moves to a new elastic κ line. If an aggregate is made to flow at a constant specific volume v (at point a on the v

axis in Fig. 48), the effective spherical pressure must gradually change to the value of p'_b on the p' axis that is found by putting the value of v in Eqn (2), with CS resistance to flow of that aggregate at a point on the double line in Fig. 48(a) as given by Eqn (1). The source of all resistance to flow is the same source that gives frictional strength to a heap of loose grains at repose.

5   Plasticity and original Cam Clay

Stable yielding in ductile mild steel bomb shelters dissipated the energy of collapsed buildings in World War II (WWII). A dissipation function found experimentally for soil led me to equations for stable yielding of an ideal soil, OCC.

5.1   Baker's plastic design of steel frame structures

Plastic design of a structural system ensures that it will safely absorb all the work done in any damage to it. Before coming to more general discussion of plastic design, a particular example will be described that Professor J. F. Baker quoted in his opening lecture on structures to first-year undergraduates in 1948. He had designed a bomb shelter in WWII (Fig. 49(a)) for houses in the UK where a family would sleep under the kitchen table during a night bombing raid. The risk to the family was that a nearby bomb burst could break the brick walls of the house and cause the roof and floors to fall. Wood is weak, and such a table and everyone below it would be crushed. Baker (1954) designed a strong shelter made of mild steel. The members were bolted together in the kitchen, with a steel plate to serve as a table top during the day, and steel mesh sides to prevent rubble from coming in from a collapse of the house in a night raid (Fig. 49(b)). He had already developed an early plastic design method for steel portal frames in his pre-war research, and used this research in the shelter design. I have a friend who, as a boy on the night that the blast of a flying bomb made his family's house collapse, was saved by this type of shelter.

   A portal frame made of three lengths of rolled mild steel angle, AB, BD and DE, is illustrated in Fig. 50. The plastic design finds what limiting vertical and horizontal loads can act safely on the frame. We must know how work is absorbed in it. Coulomb considered the application of a bending moment to a beam with the upper fibres in tension AB and the lower fibres in compression (his Fig. 6 in Fig. 1(c)). He shows plane sections remaining plane, and sketches a curve of fibre stresses that would apply to a material with some curve of stress against strain. Linear elastic bending with plane sections remaining plane will lead to fibre stresses that vary linearly from top to bottom of the beam, shown by the dashed line ac in Fig. 50(f). With ductile mild steel, the full plastic moment is got from the solid lines in Fig. 50(f) with rectangular blocks of tension stress above the neutral axis at b and of compression stress below b. The dashed line of moment M against rotation θ in Fig. 50(a) shows the limiting bending moment M_P for each member of the portal frame. The work dissipated when any *plastic hinge* rotates through an angle θ is $M_P\theta$. The portal frame of height l and span $2l$ in Fig. 50 yields with the plastic hinges that form at A, B, C, D or E

(a)

(b)

(c)
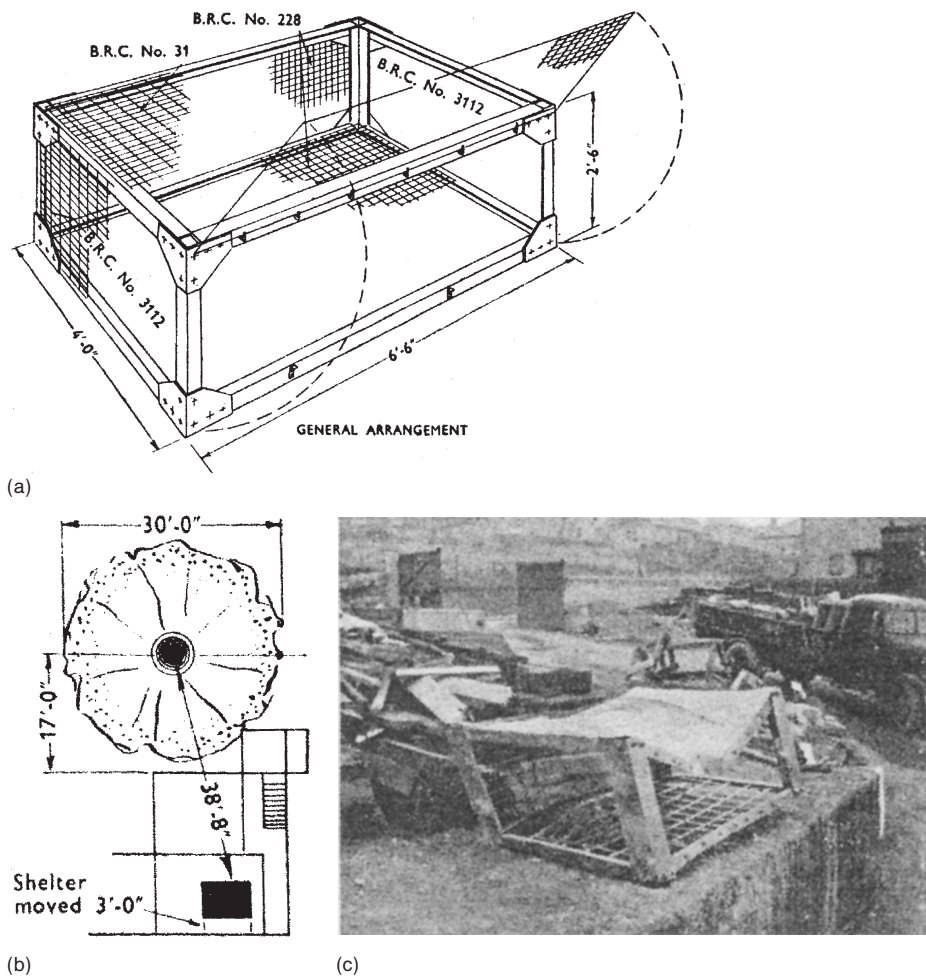
Fig. 49 Bomb Shelter WWII. (a) Details of a bolted ductile mild steel bomb shelter designed by Baker (see Baker, 1954, Civil Engineer in War). (b) Site plan of a WWII 250 kg bomb crater in Falmouth, UK. (c) The collapsed house, and the bomb shelter of the mother and three children who survived the explosion

and turn the structure into one of three dissipative mechanisms; Figs 50(c), 50(d) and 50(e) are, respectively, crushing, swaying and mixed-damage mechanisms in this portal frame. The work done by the applied loads (V, H) in each damage mechanism is the sum of the plastic work in the hinges. Deflections δ give plastic hinge rotations such that in the three cases

(c) $\theta = \delta/l$ at B and D, and $2(\delta/l)$ at C, giving $4M_\mathrm{P}\theta = 4M_\mathrm{P}(\delta/l)$ (29a)

(d) $\theta = \delta/l$ at A, B, C and D, giving $4M_\mathrm{P}\theta = 4M_\mathrm{P}(\delta/l)$ (29b)

(e) $\theta = \delta/l$ at A and E, and $2(\delta/l)$ at C and D,

$$\text{giving } 6M_\mathrm{P}\theta = 6M_\mathrm{P}(\delta/l) \quad (29c)$$
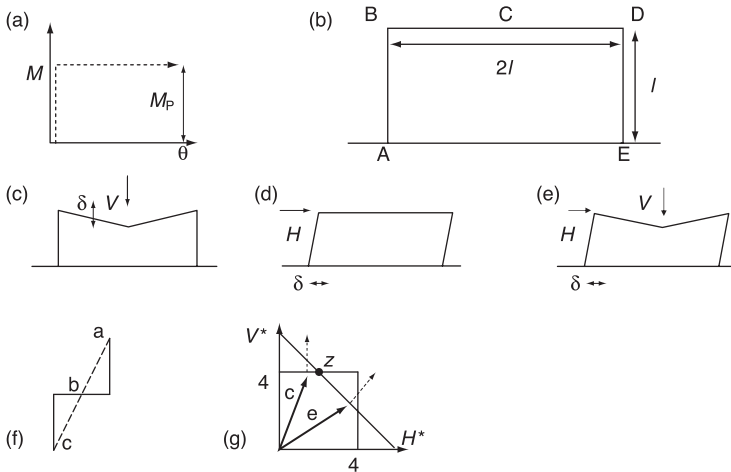
Fig. 50 Portal frame plasticity

The work equations for these three cases are

(c) $V\delta = M_{\rm P} \times 4(\delta/l)$ (30a)

(d) $H\delta = M_{\rm P} \times 4(\delta/l)$ (30b)

(e) $(V + H)\delta = M_{\rm P} \times 6(\delta/l)$ (30c)

Introducing dimensionless generalized stress variables $V^* = V/M_{\rm P} \times 4(l)$, and $H^* = H/M_{\rm P} \times 4(l)$, we get

(c) $V^* = 4$ (31a)

(d) $H^* = 4$ (31b)

(e) $V^* + H^* = 4$ (31c)

In Fig. 50(g) we plot these as three lines, and get the yield locus in (V^*, H^*) for this portal frame. Two bold vectors are sketched within the yield locus for load combinations (V^*, H^*), denoted by the letters c and e. Loading vector c will lead to a crushing mode of the portal frame, and loading vector e will lead to the mixed crushing and swaying mode. This plastic portal frame can absorb the work that will be done on it by the limiting load that can cause each damage mechanism. At the two points where the loading vectors c and e reach the yield locus (Fig. 50(g)), dashed vectors drawn normal to the yield locus show the plastic strain rates. In mode e the failure mechanism gives equal crushing and swaying strain rates, but in mode c there is no sway at all. The yield locus has a distinct corner at the point z, so that in mode c to one side of z the sway load H^* does not move and does no work. To the other side, in mode e, the loads V^* and H^* each have the same movement. The plastic failure mechanism changes at point z. Unlike the elastic deflection of this portal frame, with displacements of loading points gradually changing as loads change, the plastic deflection changes abruptly when the loads pass the corner z.

Baker initially worked on the metal frame structures supporting gasbags in the airships R100 and R101. He moved on to the Steel Structures Research

Committee, taking stress measurements as steel-framed buildings were constructed in London, and making structural analyses. His tests showed that actual stresses bore no relation to the regular stress analyses, but depended on dimensional errors in members, or of their temperatures when in strong sunlight in construction, or on the exact positions and small movements of the foundations. From this research before WWII he knew that ductile mild steel can yield and safely redistribute stress concentrations. He studied bomb damage to buildings in the WWII air raids on London, and his post-war lectures taught students the vital lesson of the significance of structural ductility.

5.2   The associated flow rule and Drucker's stability criterion

The above particular case illustrates general principles shown in Fig. 51, where a generalized load (σ_i, σ_j) acts on a structure. The load was (V^*, H^*) in the case of Baker's portal frame; general (i, j) axes can allow for many independent loads acting on a structure. Plastic displacements $(\delta\varepsilon_i^{\mathrm{p}}, \delta\varepsilon_j^{\mathrm{p}})$ associated with the (σ_i, σ_j) loads are also plotted in the i and j directions. In Baker's frame the bold vector represents the limiting load that brings a structure to the moment of plastic failure, with crushing and swaying movements of V and H. The fan of vectors $(\delta\sigma_i, \delta\sigma_j)$ in Fig. 51 beyond the yield locus represents load increment vectors that cause hardening and flow. In colloquial English, any one of these load increments could be *the last straw*. These words come from the saying that *the last straw breaks the camel's back*. It conjures up the image of a camel that a merchant loads with a great weight (corresponding to load H) at the same time as a camel driver is goading or pulling it (corresponding to load V) to get the poor animal to start moving. The merchant adds a last straw to the load, and the camel collapses, but the collapse mode is determined by the total load (V, H) on the camel and not by the last straw (increment δV). The last straw simply provokes failure in the mode determined by (V, H). In Fig. 50(g) the yield locus has a corner at the point z and a last straw load increment δV to the left of point z will cause the broken back mode of failure in Fig. 50(c), but a last straw to the right causes the mixed mode of Fig. 50(e).

The general rule shown in Fig. 51 is that the dotted vector $(\varepsilon_i^{\mathrm{p}}, \varepsilon_j^{\mathrm{p}})$ of plastic flow normal to the yield locus at (σ_i, σ_j) is associated with the damage mode for (σ_i, σ_j). This is called the *associated flow rule*. For the straight-line segments of the yield locus of the portal frame in Fig. 50(g) this flow rule is evidently valid. The flow
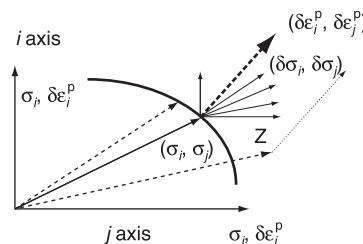
Fig. 51   Yield locus and associated flow

shown as normal to the curved yield locus in Fig. 51 is drawn as if the rule is valid, but it is not self-evident that it must always be valid. The point about a plastic design of a structural system is that the designer makes sure that the rule is valid for that particular system. A load or load increment vector σ or $\delta\sigma$ applied to an elastic body causes *elastic* strain vectors in the direction of these vectors σ or $\delta\sigma$ and proportional to them. The *plastic* strain increment vectors are not in the direction of, or proportional to, either the load or load increment vectors. A limiting load brings the system to some yield point on the locus. The damage mode gives a plastic strain vector in the direction normal to the locus at that point. The amount of plastic strain that will occur during the damage depends on the amount of work that the structure has to absorb in this mode. The plastic design of Baker's shelter ensured that those sheltering in it survived the damage. The desired property of being safe required that all the work done on the shelter was dissipated without the people inside being crushed, and there was no work left over that could lead to uncontrolled momentum. The shelter only deflected 1 ft as it absorbed the work done by a 20 lb/ft^2 ceiling load falling 9 ft in a bombed house.

For Drucker's (1959) stable material, the plastic strain increment $(\delta\varepsilon_i^{\mathrm{p}})$ in Fig. 51 multiplied by a load σ or an outward directed load increment $\delta\sigma$ always has a positive product, ensuring that there is never any energy that the system fails to dissipate or absorb. In Fig. 51 the load vector (σ_i, σ_j) is shown as a bold line. At the yield point a fan of bold load increment vectors $(\delta\sigma_i, \delta\sigma_j)$ is shown directed outward from the locus. If any of these load increments could cause the system to pass some peak load point such that the strength fell (in the way shown in Fig. 10(b) after peak strength at P) then the system would be brittle and not be a desirable ductile safe system. The plastic design ensures ductility and makes sure that the associated flow vector is normal to the locus. The load multiplied by the associated flow vector is always positive if the locus is convex. Any outward-directed load increment vector multiplied by the normal to the locus gives a non-negative product. Any inward-directed load increment vector causes elastic unloading with zero plastic strain increment. Drucker's stability postulate helped me to understand the associated flow rule and the yielding of soil when the OCC model was developed in 1962. Geotechnical engineers are familiar with contours of excess pore water pressure in seepage flow nets, and know that the seepage flow lines are normal to these equipotentials. For the class of system that Drucker postulated, the yield locus is the potential function for plastic flow. At each point on the yield locus the vector of plastic flow is normal to the yield locus.

With this class of structure, engineers can make some simple calculations that bound an exact (but unknown) solution of a problem. The first class of bound comes from a *statically admissible stress field* that distributes stress in all parts of any structure that is under consideration in such a way that the stress everywhere is in equilibrium and nowhere violates the yield condition. This gives a loading vector that may or may not be the failure load but is certainly inside the yield locus. With a convex yield locus we can certainly state that the vector product of the approximate load and the actual plastic flow vector is not greater than the loading power of the actual load and the actual flow vector. That is to say,
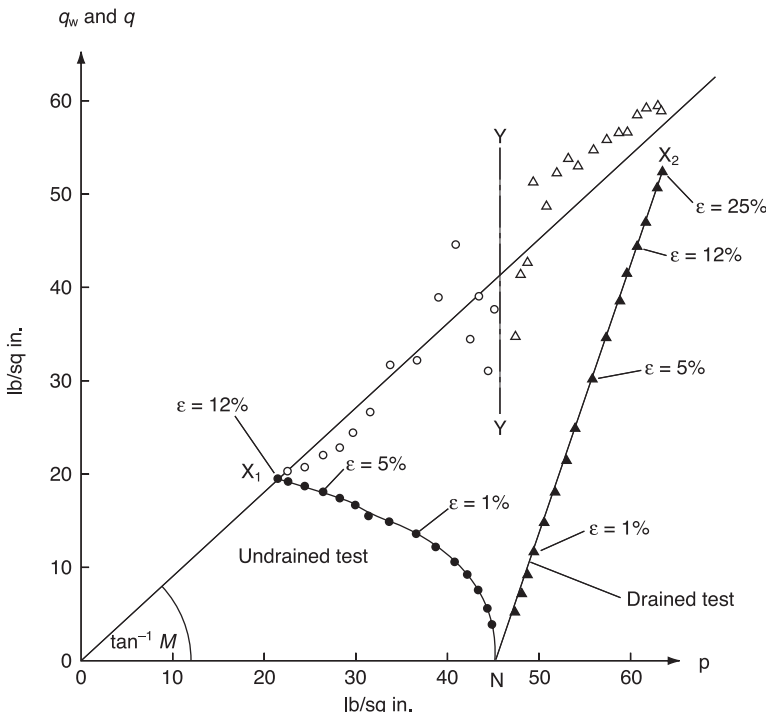
Fig. 52 Thurairajah's (1961) analysis (after Roscoe et al. 1963)

the approximate static load is not powerful enough to cause the damage that must be done in the failure. A second class of bound comes from a *kinematically admissible mechanism*, distributing displacements everywhere in any way such that the displacements everywhere are compatible with damaging movements of the external system that applies loading. It gives a loading vector that will certainly end outside the convex locus such as is shown at Z in Fig. 51. The loading system is powerful enough to do the damage that must be done in the failure, and it certainly violates the yield condition. Each of these two classes of solutions is useful in particular circumstances. For example, rather than working out the moments at beam-to-column connections in a welded or bolted highly redundant steel frame structure, an engineer can find a safe lower bound solution to a collapse load by introducing enough pin joints to eliminate the redundancies; with ductile mild steel an engineer can be sure that the collapse load increases if any pin joint is welded up. The upper-bound solution is appropriate where it is essential to cause plastic flow; an upper-bound calculation would ensure that the system as a whole provides at least enough power to be dissipated in a proposed deformation.

Lecturers who teach simple calculations that are appropriate for ductile mild steel structural components that are welded or strongly bolted together to form stable structural systems should warn students that brick or concrete structures may not be stable in this way, but by a right choice of construction materials and methods an engineer can construct safe systems that are stable in Drucker's

sense. When I had a chance to undertake a final year project in 1950 I made and tested concrete beams in bending. A curve of moment against rotation for my over-reinforced concrete beam had a peak strength like curve d in Fig. 11(a) with crushing of concrete in compression. My under-reinforced beam cracked through the depth of the beam with yield and ductile extension of tensile reinforcement and a curve like f in Fig. 11(a). Such a ductile failure with plastic flow does not result from a law of nature like the gas laws. It is simply a property that Drucker's class of structure gets from right design choices. Application of this lesson in soil mechanics requires care. A portal frame can sway, or be crushed, or fail in a mixed mechanism, but it would be a mistake to think, because plastic compression and shear distortion of a frame appear to be different types of displacement, that there are different types of dissipation In all three different failure mechanisms, work is absorbed by plastic hinge rotation. It would also be a mistake in soil mechanics to think that compression and shear involve different types of power dissipation. In aggregates, some grains will slip past each other and some will slip towards each other, but it is the integrated effect of all grain movements that give the boundary displacements of the whole body. We cannot distinguish power dissipation and grain movements in overall compression from those in overall distortion of an aggregate of grains. Power is dissipated when a stressed aggregate is distorted. The stability and strength of both soft and stiff soil involve work being done in shearing deformation and in volume changes in loose and dense aggregates of soil grains.

5.3   Thurairajah's power dissipation function

The end of Section 2.1 and the beginning of Section 2.2 discussed Roscoe and his co-workers' (1958) *Géotechnique* paper 'On the yielding of soil'. Our Fig. 29 suggested that the peak strength data found from both drained and undrained tests would lie in what we called the Hvorslev surface; this assumed that the power dissipated in a step in test path shear distortion at a state point (e, σ') is the same in both drained and undrained tests. An alternative assumption would have been that at a given state point the aggregate has the same strength in both tests. Our discussion of the work done on soil specimens stated that, if there is a marked inelastic hysteresis in the compressibility of the grain structure, internal work might be absorbed when the average distance between the centres of grains changes, but we anticipated that a detailed study of undrained and drained test data would show that *the work absorbed internally will be independent of the rate of dilatation*.

  I later suggested that, as well as a boundary energy correction, we should consider elastic energy as follows. In any step on a test path there is a difference between the work that can be recovered if the specimen is allowed to swell fully from the state at the start of that step and from the state at the end of that step. I called the difference between these quantities of recoverable work the *elastic energy correction* in order to fit in with the *boundary energy correction* (work $p' \, \delta v$ done in the contraction of a volume by δv in a step on a triaxial test path with constant effective spherical pressure by p'). It was a task for a new student to make a detailed study of the energy balance, step by step along paths of drained

and undrained triaxial tests of saturated reconstituted kaolin clay. Thurairajah (1961), a research student who arrived at Cambridge University in 1958, was given this task. He made triaxial tests of kaolin, and plotted drained and undrained strengths. The solid black points in Fig. 52 are his values of q after both corrections. He calculated power dissipation in successive steps of both drained and undrained triaxial tests, taking account of boundary energy and elastic energy corrections. These corrections to q gave the open-symbol points in Fig. 52. On an undrained test path the fall in the recoverable elastic energy provides a flow of energy into the soil in a step between points on the path. In a drained test there is a boundary energy correction, as above. The sum of the work done by the descending plunger in the triaxial cell plus the energy in each step is the power dissipation. Each open-symbol point is a corrected stress q_W for a step such that when multiplied by the increment of plastic distortion $d\varepsilon$ in that step, $(q_W \, d\varepsilon)$ is equal to the power dissipation.

In 1963 the data of early stages of the tests were unreliable because tests were made at rates that ensured that excess pore pressure in test specimens was low at the time of ultimate failure. In the early stages of tests in Fig. 52 the open points show more scatter for early stages of both drained and undrained tests than at a late stage of a test path. Thurairajah and I discussed this at length. We had no preconceived hypothesis, but it became obvious as we looked at his data that a straight line that fitted the open symbols in Fig. 52, gave a simple function $Mp' \, d\varepsilon$ for the work dissipated in a plastic distortion increment. It confirmed the anticipation of Roscoe *et al.* (1958) that *the work absorbed internally will be independent of the rate of dilatation*. These dissipation data from remoulded kaolin clay tests showed that the soil did not have one kind of plastic strength resisting deformation and a different kind of strength resisting contraction. Our discussion ended as Thurairajah presented his PhD thesis, was examined and returned to Sri Lanka, where he was a professor, and ultimately Vice Chancellor of Jaffna University.

At the beginning of the new academic year 1961–1962, Roscoe was the established lecturer, and I was newly promoted from demonstrator (assistant lecturer) to be a lecturer. Roscoe had sabbatical leave entitlement. Our students had done much research that required his review and publication; he was aware that if he delayed, others might publish their results, but he made an American lecture tour. Calladine (1963), who as an undergraduate had heard Cambridge soil mechanics lectures, had gone to America for post-graduate study of plasticity under Drucker and returned to Cambridge to work on structures, was interested in the CS teaching. He thought that successive yield curves to which the associated flow rule might be found to apply would be given by projecting the elastic swelling curves on the experimentally observed yield surface on the wet side of the CS (CVR in Fig. 53). He got access to test data of plastic strains in drained and undrained triaxial tests, but when he compared the data of plastic strain increments in the tests with predictions from using a yield surface of our 1958 parabolic section he did not find a close fit of strain data to the associated flow rule. Roscoe was in America, and Calladine asked me for a comment. I realized that the set of equations formed by Thurairajah's dissipation function and the associated flow rule could be integrated. I had to discuss all this with Roscoe on his return from America, and also had to ensure that every contribution was recognized in due
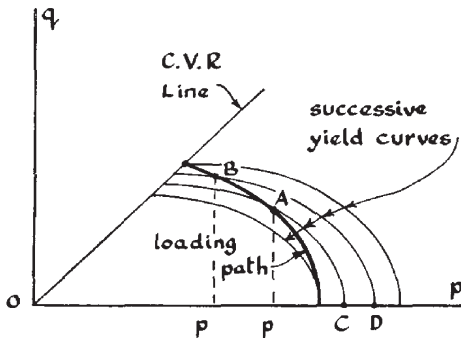
Fig. 6.
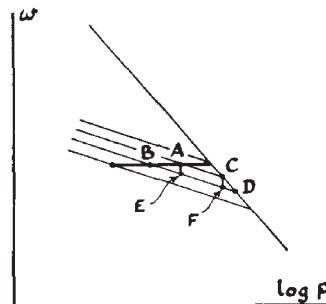
Fig. 7.
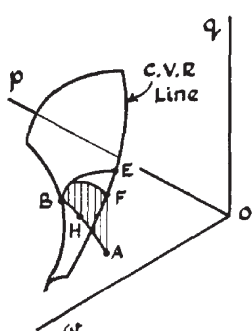
Fig. 4.
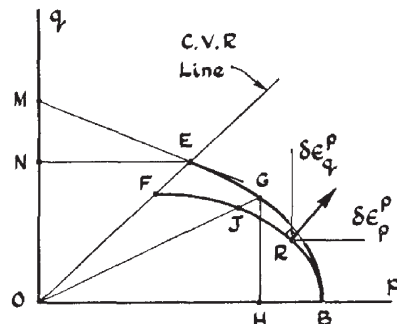
Fig. 5.

Fig. 53 Calladine's (1963) letter

course, which was achieved by the same issue of *Géotechnique* that published Roscoe *et al.* (1963) including a letter by Calladine (1963 and Fig. 53).

5.4   The OCC yield locus

Figure 54 was an illustration in the 1980 Rankine Lecture, and Fig. 55 explains Fig. 54 in more detail. Equation (32) (the first equation in Fig. 54) applies to all states in which Drucker's postulate is satisfied (a positive outward vector product in Fig. 52):

$$dp' \, dv + dq \, d\varepsilon \geq 0 \tag{32}$$

For deformation of soil in states such as the CS point C in Fig. 55, Thurairajah's dissipation function gives Eqn (33) (it is the second equation in Fig. 54):

$$p' \, dv + q \, d\varepsilon = Mp' \, d\varepsilon \tag{33}$$

Equation (34) is found by eliminating the dilatancy $dv/d\varepsilon$ between these two equations:

$$dv/d\varepsilon = -dq/dp' = M - q/p' \tag{34}$$

The integration of Eqn (34) on the wet side of C gives a curve CBD of other stable states as defined by Drucker, including a point B shown in Fig. 55(a).
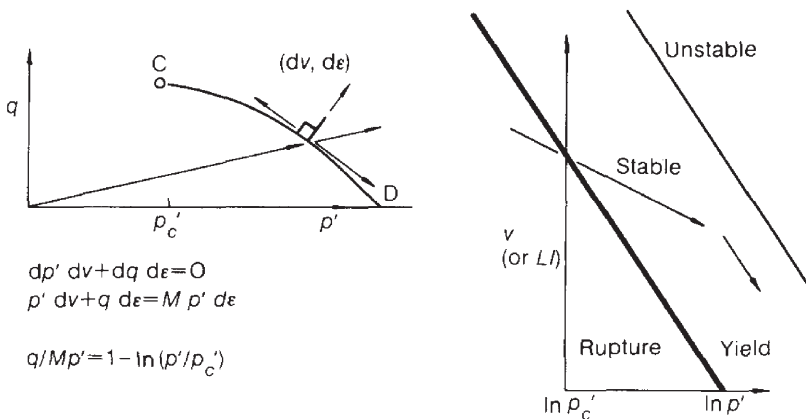
Fig. 54 *Original Cam Clay (Schofield, 1980)*

Point C in Figs 55(a) and 55(b) represents a CS aggregate of grains. Reduction of the deviator stress q on this aggregate at C brings the soil into an elastic state point G in Fig. 55(a), say where the stress ratio $q/p = \eta < M/2.5$. Points like G below the curve CD can be thought of as lying in an elastic wall that has the curved area CDA as a projection on the (q, p') plane. A geotechnical engineer might consider soil in state G to have a factor of safety against failure of 2.5, but in plastic structure design the factor of safety is the proportional increases of all stress components that causes plastic yielding. If we associate with each stress component a plastic strain increment that will occur during yielding, we can ask by how much the vector AG with $q/p = \eta$ can be extended if the aggregate is to remain in a state where it can still absorb all the work that will be done by the stress components that act as it yields. At a state point B in Figs 55(a) and (b) the combination of deviator and spherical stress reaches a limiting value (we have seen such procedures before in Figs 51 and 52). The aggregate is in a
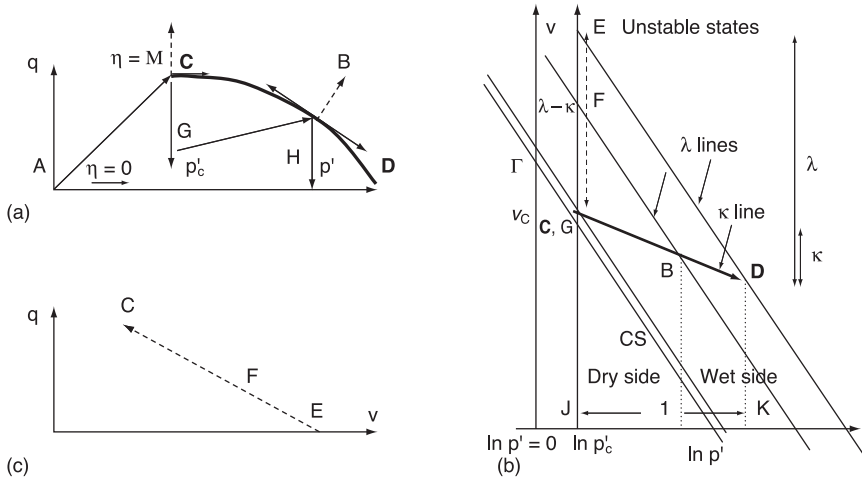
Fig. 55 *Details of OCC*

contractive state where Casagrande supposed that the work done by spherical stress could not be absorbed, and he thought the soil must experience liquefaction as an unstoppable chain reaction. However, I adopted Thurairajah's dissipation function, so the work input from volume contraction $p' \, dv$ plus a work input from deviator loads $q \, d\varepsilon$ are dissipated in plastic power $Mp' \, d\varepsilon$. A plastic volume reduction dv can be stable if it is accompanied by a plastic distortion $d\varepsilon$. If the aggregate is to remain stable by Drucker's stability criterion as we work our way round the curve CD in the manner discussed in Section 2.1, there is a requirement that there must be sufficient plastic distortion of the aggregate to dissipate in friction within it the loading power that will flow into the aggregate as it contracts. Note that the dashed line EFC in Fig. 55(b) has a straight line projection on the q, v plot of Fig. 55(c).

Drucker's stability criterion is an alternative to the stability criterion that Casagrande used, but it is more than that. In much the same way that Professor Baker selected ductile mild steel fabrication with fully bolted connections that can transmit plastic moments in his design of an air raid shelter, geotechnical engineers can ensure a stable state in soil construction at the point B in Fig. 55 by a design process which selects a soil and selects a degree of compaction such that the material is ductile. Optimum compaction for the soil brings it into the zone indicated in the Frontispiece.

Introducing the stress ratio $\eta = q/p'$, by differentiation we can obtain Eqn (35):

$$d\eta = dq/p' - q \, dp'/p^2$$
$$p' \, d\eta/dp' = dq/dp' - q'/p' \tag{35}$$

Combining Eqns (34) and (35) we obtain Eqn (36):

$$d\eta/dp' = M/p' \tag{36}$$

The curve CBD in Fig. 55(a) through the CS point C with coordinates (q, p'_c) is obtained by integrating Eqn (36). Equation (37) is the yield curve for the material that Roscoe and Schofield (1963) called *wet clay*, that I later called *Cam Clay* in my lecture notes, and that in this book I call *OCC*:

$$q/Mp' = 1 - \ln(p'/p'_c) \tag{37}$$

As p' increases in the range $p' > p'_c$ the sketched OCC curve CD on the wet side of the CS line in Fig. 55(a) shows a steady fall of the yield strength $q = Mp'_c$ from the CS strength at C until the strength has fallen to zero at the point D where $\ln(p'/p'_c) = 1$. The power flowing into a contractive soil aggregate causes shear flow to occur with increasing ease, but pressure can increase up to point D without causing the chain reaction that Casagrande predicted in his liquefaction. At C the soil will slip at $\eta = q/p' = M$, but as the pressure increases from C to D the stress ratio for slip falls through the range $M > \eta > 1$, so that the aggregate slips more easily. The zone of stable ductile yielding ends when the effective spherical pressure increase makes the loose aggregate so slippery that it is quite unable to bear both spherical stress and any shear stress.

A proportional loading can increase so that $\eta = q/p' = $ const. The combined spherical stress and shear stress that gives the vector AB ending at B in

Fig. 55(a) then causes anisotropic plastic compression on the path BK in Fig. 55(b). Equation (37) leads to

$$\ln(p'/p_c') = 1 - q/Mp' = 1 - \eta/M = \text{const.} \tag{38}$$

Figure 55(b) shows that the spacing between C and B is $\ln(p'/p_c')$. This spacing remains constant as the aggregate in the state represented by B yields. The increase of stress from G to B in Fig. 55(a) is associated with elastic loading on the path CB, followed by plastic yielding on the path BK (Fig. 55(b)). On the path BK there is yielding and general hardening of the aggregate. When state points are plotted on a base of $\ln p'$, the paths become straight lines with slopes λ and κ. The elastic and plastic compression of OCC in Fig. 55 corresponds in general with Taylor's data of one-dimensional compression of Boston Blue Clay (Taylor, 1948) replotted in Fig. 56.

The OCC model can be worked out by following the geometry of Fig. 55. In Fig. 55(b) the path CD does not extend past the point D at which $\ln(p'/p_c') = 1$ and $q = 0$. The slopes λ and κ of the lines ED and CD gives the spacing between the lines as $\lambda - \kappa$, which, as seen to the right of Fig. 55(b), gives the length EC. There is a family of lines such as FB and ED with slope λ parallel to the CS line. Equation (31) shows that each such line corresponds to a particular value of η so that the length FC is $(\lambda - \kappa)(1 - \eta/M)$. Such lines represent anisotropic plastic compression test paths across the OCC yield surface. It is possible to obtain triaxial test data on drained test paths with increasing axial stress and decreasing cell pressure that keep the spherical effective pressure p' constant. The predicted path by the OCC model will be as sketched as EFC in Fig. 55(b). On that path the prediction is that as the specific volume falls through $\lambda - \kappa$ the value of η/M will rise from 0 to 1 and the value of $1 - \eta/M$ will fall from 1 to 0. In my lectures I gave out a three-dimensional pop-up Cam Clay model to my students, that folded flat in their notes, but could be made to pop up and display the OCC surface generated by straight stress strings, each representing test paths like those of Fig. 55(c). Shibata (1963) (as a research student of Professor Murayama in Kyoto) made such triaxial tests in which the shear strength increased linearly with the reduction of the specific volume in this manner. Figure 48(b) shows what are called κ and λ lines, with the equations

$$v_\kappa = v + \kappa \ln p \tag{39}$$

$$v_\lambda = v + \lambda \ln p \tag{40}$$

For the triaxial test in Fig. 2 where $q = \sigma_a - \sigma_r$ and $p' = (\sigma_a + 2\sigma_r)/3 - u$ we have

$$\sigma_a = \sigma_r + (\sigma_a - \sigma_r) = \sigma_r + q \tag{41}$$

In Fig. 38(c) the ratio of major stress to minor stress is given as

$$\sigma'_{max}/\sigma'_{min} = (1 + \sin\phi_d)/(1 - \sin\phi_d) \tag{42}$$

In Fig. 55(a) the ratio $q/p' = M$ at the CS point C that corresponds to the drained triaxial test and to a slope at repose with major stress parallel to the slope and intermediate stress equal to the minor stress, giving a relationship between M and $\sin\phi_d$:

$$q/p' = M = 3(\sigma_a - \sigma_r)/(\sigma_a + 2\sigma_r) \tag{43}$$

Table 1 London Clay: parameters

λ	0.161
κ	0.062
Γ (at 1 kPa)	2.759
M	0.89

$$M = 6 \sin \phi_d / (3 - \sin \phi) \tag{44}$$

In Fig. 55 the value $v_\lambda = \Gamma$ applies to the CS double line through C, and the value $v_\lambda = \Gamma + (\lambda - \kappa)$ applies to the line of isotropic spherical compression ED through D. The OCC model makes the striking prediction that the spacing of these lines is $\lambda - \kappa$.

In preparation for Tripos examination questions there were example problems for final-year lectures in Lent 1966 of the following type on OCC.

Question

Samples of reconstituted London Clay with the parameters listed in Table 1 follow isotropic compression from a slurry to 500 kPa in a triaxial cell. All pore pressures dissipate. They follow isotropic swelling back to over-compression ratio $p_1'/p_2' = 2$.

There are two samples that are subjected to different stress paths as follows:

(1) Sample A is subjected to a drained axial compression test to failure. Predict the values of q, p' and v at both yield and failure.
(2) Sample B is subjected to undrained axial compression to failure. Predict the values of q and pore pressure at yield and at failure.

Solution

First find how the clay sample's specific volume varies as it is subjected to consolidation and swelling. In Fig. 56, the clay consolidates down the normal compression line (NC) to state 1, where it has an effective confining stress of 500 kPa. The specific volume of the sample v_1 at this point in Fig. 56 is

$$v_1 = \Gamma + \lambda - \kappa - \lambda \ln p_1'$$

$$= 2.759 + 0.161 - 0.062 - 0.161 \times \ln(500) = 1.857$$

Subsequently the soil swells to state 2, where it has an over-compression ratio (OCR) of 2. As the maximum effective confining stress to which it has been subjected it 500 kPa, an OCR of 2 means that

$$p_2' = 500/2 = 250 \text{ kPa}$$

From state 1 to state 2, the soil is elastically swelling on a κ line, and hence at state 2 the specific volume v_2 is given by

$$v_2 = v_1 - \kappa \ln(p_2'/p_1') = 1.857 - 0.062 \times \ln(0.5) = 1.90$$

Both soil samples before the stress paths commence have an OCR of 2, an effective confining stress of 250 kPa and a specific volume of 1.90. This tells us the location of the yield surface in $p'–q$ space. As the maximum effective confining stress to
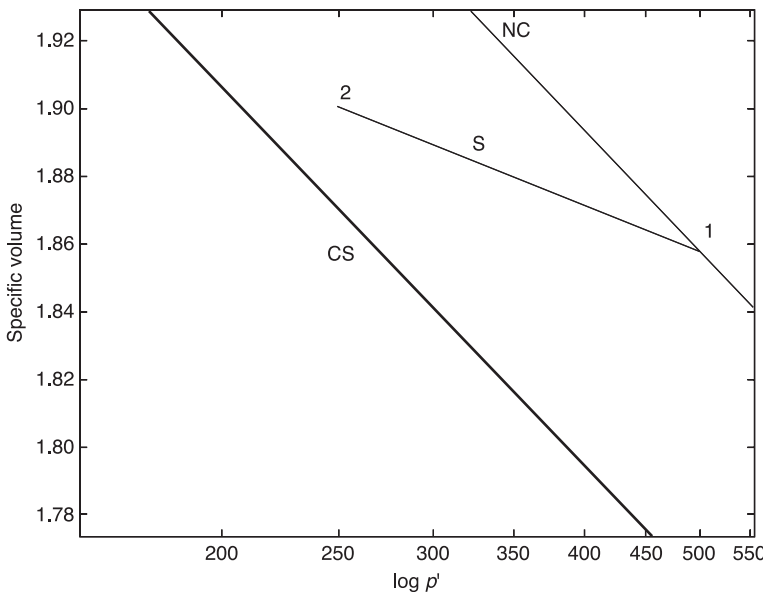
Fig. 56 Example of an OCC normal compression (NC) and swelling (S) lines

which the sample has been subjected is 500 kPa, the yield surface must cross the p' axis at $p' = p'_1 = 500$ kPa, as shown in Fig. 57. The initial state is at point 2 in Fig. 57, and the yield surface shape is found from the equation

$$q/p' = M \ln(p'_c/p')$$
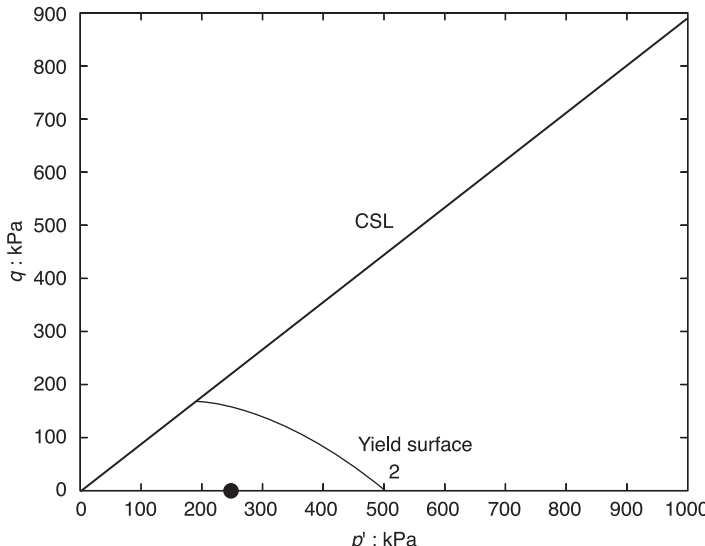
Fig. 57 Example of an OCC CS strength (CSL) line and a yield surface curve

Sample A

Sample A is subjected to drained axial loading with constant cell pressure. We must first plot the total stress path on our p'–q plot. For any increase of 3 kPa in axial load, p' will increase by 1 kPa and q will increase by 3 kPa. The total stress path will slope at 1 in 3 on the p'–q plot, as in the dashed line in Fig. 58. As the test is drained, the effective stress and the total stress changes are identical; the effective stress also follows the dashed line. The sample will yield at point Y in Fig. 58, and reach an ultimate state on the CSL at point U. We find point U as the intersection of the stress path and the CSL, and we find point Y as the intersection of the stress path and the yield surface. At point Y,

$$q/p' = M \ln(500/p') \qquad \text{and} \qquad q = 3 \times (p' - 250)$$

When solved by iteration these equations give $p' = 296$ kPa and $q = 138$ kPa. To find the specific volume we must locate point Y on the $v \ln p'$ plot. As the stress path is within the yield surface, all deformation is elastic and hence corresponds to a κ line in $v - \ln p'$ space, so at point Y the specific volume v_3 is

$$v_3 = v_2 - \kappa \ln(p'_1/p'_2) = 1.90 - 0.062 \times \ln(296/250) = 1.89$$

The ultimate state U is at the intersection of the lines,

$$q = Mp' = 0.89p' \qquad \text{and} \qquad q = 3 \times (p' - 250)$$

giving a point $p' = 355.5$ kPa and $q = 316.4$ kPa. To find the specific volume we must locate point U on the $v \ln p'$ plot (Fig. 56). The sample has yielded. The yield surface has expanded to the new surface shown in Fig. 58. A yield surface in p'–q space corresponds to a κ line in $v - \ln p'$ space, hence we can determine where our new yield surface crosses the p' axis and then calculate our specific
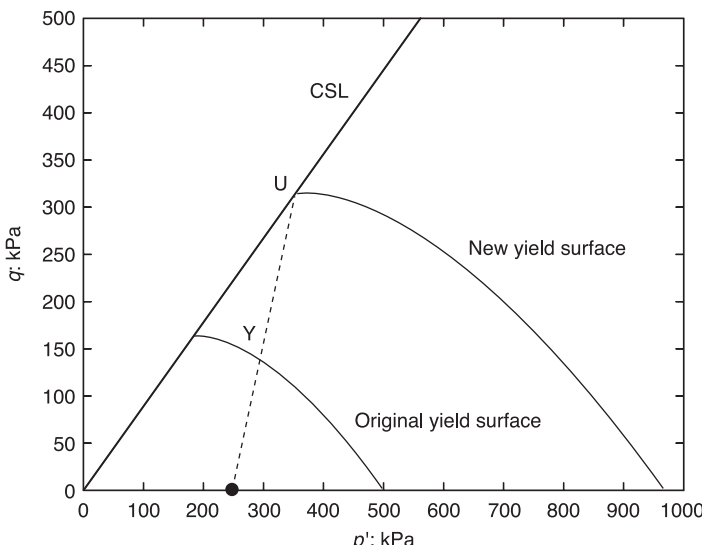
Fig. 58 Example of OCC yielding and hardening in a drained triaxial test

volume from the equation of the κ line crossing the NC line at this effective stress. From the OCC yield surface equation, the yield surface crosses the p' axis at a value p'_c such that

$$q/p' = \mathrm{M}\ln(p'_1/p'_2)$$

hence

$$p'_c = p'\exp(q/\mathrm{M}p') = 355.5 \times \exp(1) = 966\,\mathrm{kPa}$$

A pressure of 966 kPa on the NC line corresponds to a specific volume v_4 of

$$v_4 = \Gamma + \lambda - \kappa - \lambda\ln p' = 2.759 + 0.161 - 0.062 - 0.161 \times \ln(966) = 1.751$$

so at point U the specific volume v_5 is

$$v_5 = v_4 - \kappa\ln(p'_4/p'_3) = 1.751 - 0.062 \times \ln(355.5/966) = 1.813$$

Sample B
Sample B follows the same total stress path as sample A, but as the test is undrained the effective stress path differs. Within the yield surface, the effective confining stress will not change, as all loading will initially be carried as a change in pore pressure rather than effective stress. The stress path shown in Fig. 59 has a yield at point Y of

$$q/p' = \mathrm{M}\ln(500/p') \qquad \text{and} \qquad p' = 250\,\mathrm{kPa}$$

hence $q = 154\,\mathrm{kPa}$. We know that the total stress path has the equation

$$q = 3 \times (p - 250)$$
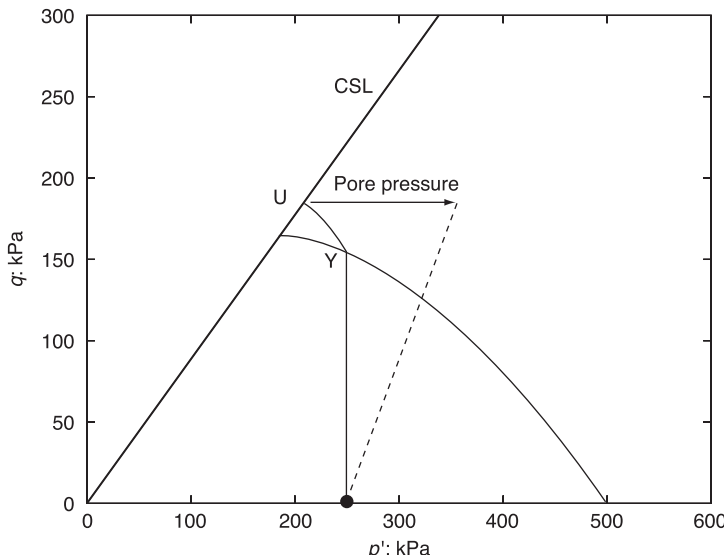
Fig. 59 *Example of OCC yielding in a constant-volume triaxial test*

so $p = 301\,\mathrm{kPa}$, and hence the pore pressure at yield is $51\,\mathrm{kPa}$. Between the yield and ultimate states Y and U, the sample deforms plastically, and hence the effective stress changes. The test is undrained so the specific volume remains constant at $v_2 = 1.90$. Point U is on the CSL, and hence

$$q = Mp' = 0.89p' \qquad \text{and} \qquad v = \Gamma - \lambda \ln p'$$

thus

$$p' = \exp[(\Gamma - v_2)/\lambda] = 207.5\,\mathrm{kPa} \qquad \text{and} \qquad q = 185\,\mathrm{kPa}$$

from the total stress path

$$q = 3 \times (p - 250)$$

so

$$p = 311.5\,\mathrm{kPa}$$

and hence

$$u = 104\,\mathrm{kPa}$$

The advantage of depicting these stress states by points with coordinates (q, p') and not by stress circles is illustrated in Fig. 60, where circles U and U' represent the total and effective stress states at ultimate state, respectively, and similarly circles Y and Y' represent the total and effective stress states at yield. The circles clutter up the figure. Each point on each circle is an accurate representation of the stress on some plane, but it is unimportant if I take a grain aggregate to be an isotropic continuum.

On Roscoe's return from America he began to write up some of the papers planned for his sabbatical leave. We wrote one paper without data that developed the idea of a theoretical model with behaviour that justified calling it *wet clay* for presentation in Wiesbaden (Roscoe and Schofield, 1963) and another paper with experimental data that we sent to *Géotechnique* with the request that a contribution by Calladine should be published in the same issue; the editor, Cooling, said that our model should have a name that might seem less strange to readers, so we used the name *wetter than critical* for it (Roscoe et al., 1963). The Wiesbaden paper stood in its own right with a theoretical model; while Roscoe continued to hope
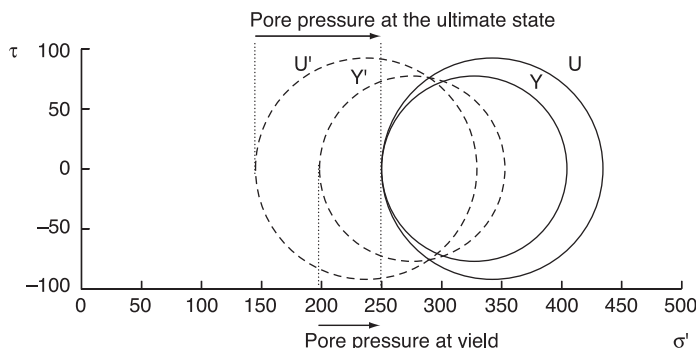
Fig. 60 *Effective and total stress circles for states U and Y*

that new research students would get SSA data that would let him discard all triaxial test data, I did not expect this to happen. I took sabbatical leave as a Fulbright Fellow at Caltech in 1963/1964, and in late 1963 I visited Drucker at Brown University to discuss the corner on the OCC locus; his comment was that a corner could be useful; it need not be altered. But while I spent a year in America, back in Cambridge new students began to compute strain increments on test paths, and when the corner caused a problem they proposed to remove the corner by modifying the dissipation function, and found OCC strains that were excessive on test paths that began from the corner. I sought an explanation of this, as I knew and trusted our 1963 *Géotechnique* paper data.

5.5   Test data, model modification and OCC teaching

Thurairajah's dissipation function had resulted from 3 years of triaxial testing. It was consistent with Taylor's supposition for power dissipation in sand in his shear box. Taylor's dissipation function (Eqn (8)) multiplies the normal stress σ' that is effective on the slip surface by the rate of shear displacement dx/dt and by the coefficient μ. Taylor did not have a second component of dissipation given by a second coefficient of friction multiplied by the rate of dilatation dy/dt; distortion in his shear box is written as dx. In triaxial tests, with a scalar measure ε of the distortion of shape without change of volume v, and with a CS flow rate $d\varepsilon/dt$, the rate of dissipation of energy was found to be $q\, d\varepsilon/dt = Mp'\, d\varepsilon/dt$. In the triaxial test the measure of elastic and plastic change of volume without distortion is dv. I can explain dissipation of frictional power in CS flow as $Mp'\, d\varepsilon/dt$ if I suppose that the elastic energy stored in an average grain depends on p' and that the rate at which a succession of grains are pinched and elastically compressed and quickly released depends on $d\varepsilon/dt$. This energy dissipation concept provides a reasonable alternative to slip plane strength components called cohesion and friction. Thurairajah's function $Mp'\, d\varepsilon = q\, d\varepsilon$ is consistent with power dissipation in the CS, if columns of highly stressed elastic grains buckle in a heap of aggregate at repose with the slope of Fig. 4(a) simply shearing at constant volume. In Fig. 40(a) the work done as the mass of soil descends under gravity is equal to the total work dissipated in each layer parallel to the slope in CS shear under the effective pressure acting on it. The slip plane model has a coefficient of friction $\mu = \tan\phi'$ (Eqns (9) and (2)). In CS flow in a slope at repose, the energy stored in lines of grains and lost in sudden unloading explains the steady energy dissipation process. Additional processes such as high-stress abrasion and crushing may also cause power dissipation, but grain crushing will make dust, and no dust is seen in the time-glass after repeated CS flow at light stress. When a time-glass is made elastic, rounded sand grains are selected that do not crush at light stress. At least part of the friction in CS flow and the limiting stability both in lightly stressed sand in a time-glass and large heaps at repose must be due to dissipation of energy as contacts between highly stressed elastic rounded grains slip. Pore water rapidly damps vibrations of grains in saturated fine soil. Dissipated energy ultimately heats the soil.

Our 1958 hunch that *the work absorbed internally will be independent of the rate of dilatation* meant that dissipation is the same at the CS and in an aggregate

yielding with volume change. The OCC model on the wet side of the CS has contractive soil exhibiting ductile stable plastic yielding, and on the dry side of the CS interlocked soil exhibiting brittle rupture with progressive softening in the thin layer of gouge material forming on the slip surface. I had Taylor's data of tests of sand and Hvorslev's data of tests of clay on the dry side of the CS line. A concept that true cohesion results from electrochemical properties and pore fluids was replaced by the *mechanical concept* that the *behaviour of clays* at peak strength involves interlocking. Any true cohesion would exist on both the dry and the wet side of the CS line or not exist at all. Any argument about true cohesion would end; the OCC model was derived without introducing any cohesion at all. The OCC is not a model of soil behaviour that covers all aspects of cyclic loading and anisotropy. It shows a way to link Casagrande's classification of disturbed soil and Baker's plastic design; it is consistent with treating a disturbed frictional aggregate of interlocked soil grains as a plastic material to which plastic design can be applied. Ducker's stability postulate may not be automatically satisfied by all granular aggregates. The basis of plastic design is the stable dissipation of plastic power. Engineers select construction materials and methods that bring selected soil into safe states so that potentially damaging loading power is dissipated and will not cause harm. Sudden failure on the dry side of the CS indicates that peak strengths are unreliable, but on the wet side of the CS where soil contracts there is a zone of stable yielding and ductile plastic behaviour. Soil states in zone C in Fig. 12 can be stable in Drucker's sense, rather than unstable in the way that Casagrande predicted for the liquefaction of contractive soil.

In any triaxial test data analysis, the value of λ will be known, so v_λ can be calculated at each stage of a test, whether the test is drained or undrained. The stress ratio $\eta = q/p'$ is also easily found, so that the data can be plotted on axes of (η, v_λ) as shown by Schofield and Wroth (1968) in Fig. 61. In a series of tests of water-saturated mixtures of rock flour and kaolin clay to make clay paste specimens with a range of λ value (plasticity index) a test path of a typical sample as shown in Fig. 62 fits the OCC prediction well. Figure 62 also indicates the difficulty in getting test data corresponding to the corner point D in Fig. 55. The cylindrical specimen in a triaxial test has a cylindrical face sheathed in rubber, giving a
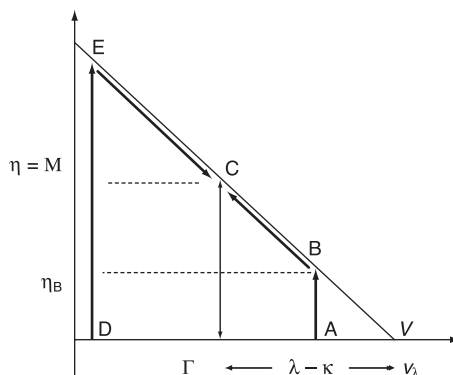
Fig. 61 Finding OCC constants in a (v_λ, η) plot (after Schofield and Wroth, 1968)

$V_\lambda = V_0 + \lambda \ln p'$ curve for mix 2

$q/p' = \eta$

3.18 3.20 3.22 3.24 3.26 3.28 3.30 3.32 3.34

Γ

$\lambda - \kappa$
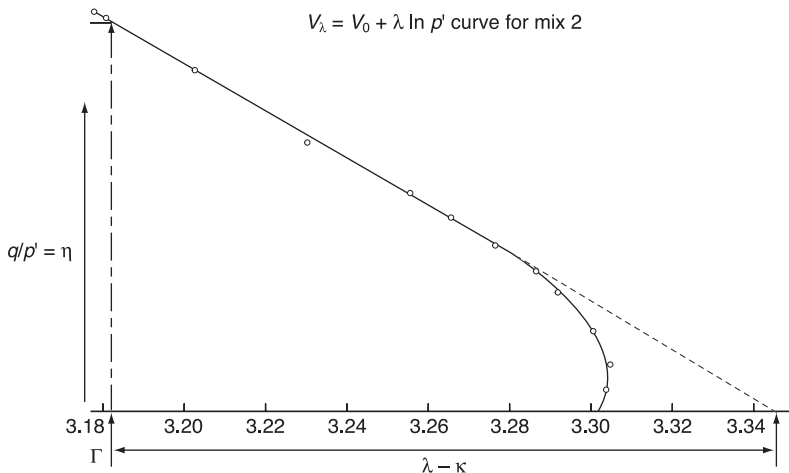
Fig. 62 Test data in a (v_λ, η) plot (Lawrence, 1980)

stress-controlled boundary on which the cell pressure acts uniformly. It stands on a rigid pedestal and has a rigid top plate that can be moved up or down. The specimen is subject to a mixture of stress-controlled and displacement-controlled boundary conditions. If the rigid faces of the top plate and the pedestal are lubricated, the stress will act in the direction of the normal to these surfaces, but it need not be uniform. In Fig. 55(a) when $v_\lambda = \Gamma + \lambda - \kappa$ the predicted yield locus CBD has a corner at C. If an aggregate structure is like a house of cards, then under pure spherical stress it is likely to have volumes within which plate-like grains became parallel in random directions. It will be very slippery and highly plastic in the sense that it will flow to fill the irregular form of a general hole without needing to be forced to flow by local shear stresses. It will not compress homogeneously without distortion but will become heterogeneous. While triaxial test specimens may approach the corner without showing any distortion as a whole, there can be distortion in random volumes that dissipates energy. At the corner D in Fig. 55(a), as we reach the plastic compression point the aggregate will not be able to bear even the least increment of stress obliquity. In states for which Casagrande predicts liquefaction, OCC predicts ductile stable plastic yielding; a soil like Boston Blue Clay when reconstituted and under spherical effective stress is very soft and slippery.

    The introduction of the modified model was justified by a calculation that assumed a specimen after isotropic compression in the triaxial cell must have an initial state at the corner; I doubted that this initial state could be reached. It required an initial path without even the very least amount of stress obliquity. A small over-compression was introduced in the initial stage of sample preparation. I could estimate it when I got the OCC constants (Figs 61 and 62). I used plots of drained or undrained triaxial test data on a graph with the axes (v_λ, η) as in the Frontispiece. Extrapolation of the line ECB on the plot in Fig. 61 gives a point V of virgin compression, and the value of η_B gives the small amount of stress obliquity at the point B at which the yielding began. I have already shown in

Figs 19 and 20 some data that my student (Lawrence, 1980) got later from index tests of a mix of rock flour and kaolin clay; his triaxial test data points in Fig. 62 fit the OCC model in Fig. 61. Calculation of strains on the path ABC in Fig. 61 for the OCC model must follow an initial elastic path between A and B and a plastic path from B to C; I did not have these data on my return from America in 1964, but I expected that if strains were calculated for OCC by this procedure they would fit Roscoe and Burland's (1969) data at least as well as those calculated by the modified theory. Roscoe always raised an objection to the mixture of boundary conditions in the triaxial cell, where the top cap and pedestal control axial displacements, while cell fluid around the sheathed specimen controls radial forces. His objection seemed to me to require the analysis of triaxial test data by the procedures set out in Figs 61 and 62. In the year 1964–1965 after my sabbatical leave, a university lectureship arose, allowing Wroth (who had worked in a London consultancy) to return to Cambridge University. Roscoe then arranged to transfer responsibility for final year lectures before Christmas in 1965 to Wroth, and to me after Christmas in 1966 (Schofield, 1966). Our collaboration in this teaching was the basis of the Schofield and Wroth (1968) book. We included a discussion of stress in a triaxial test specimen under the first increments of cell pressure in Fig. 61 as follows:

> This specimen was initially under virgin compression, but experimentally we can not expect that the stress is an absolutely uniform effective spherical pressure. Any variation of stress through the interior of the specimen must result in mean conditions that give a point A not quite at the very corner V.

I saw the basic significance of OCC to be that a grain aggregate of Rankine's type dissipated frictional work in distortion, and this frictional property gave rational slip plane properties. There cannot be a cohesion that depends on clay minerals and chemistry and is constant from B to C in Fig. 5(d), and then is zero to the right of C. The soil strength theory shown in Fig. 5(c) cannot explain the point C in Fig. 5(d). The apparent cohesion of OCC does not prove that there is adhesion among grains of saturated clay; on the dry side of CS it indicates Taylor's interlocking and pore water suction, and on the wet side it indicates ultimate CS strengths and pore water pressure. Rankine began his 1857 paper by asking what '*kind of stability, in a mass composed of separate grains, arises from the mutual friction of those grains*'. The OCC model showed that if Rankine's aggregate of grains had Drucker's kind of stability it would appear to behave like clay. Many modifications have proved possible, but the yielding of soil with pore water pressures in undrained tests on the wet side of the CS that Roscoe *et al.* (1958) discussed is what is expected in the stable yielding of an aggregate of small grains. The most striking confirmation of OCC as shown in Fig. 63 (Roscoe *et al.*, 1963) quotes a body of data of Thompson (1962) in which test paths with three or four increments of hanger load led to creep until an ultimate pore water pressure was recorded. His data have no points at the predicted corner but fit the OCC yield curve and are quite close to Skempton's (1954) $B' = 1$ straight line path. The modified yield locus normal to the p' axis with no corner implied that an aggregate at the point of plastic compression is insensitive to a slight change of q. If the collapse of an aggregate involves buckling of many columns of stressed grains with local volumes of parallel grains forming, then
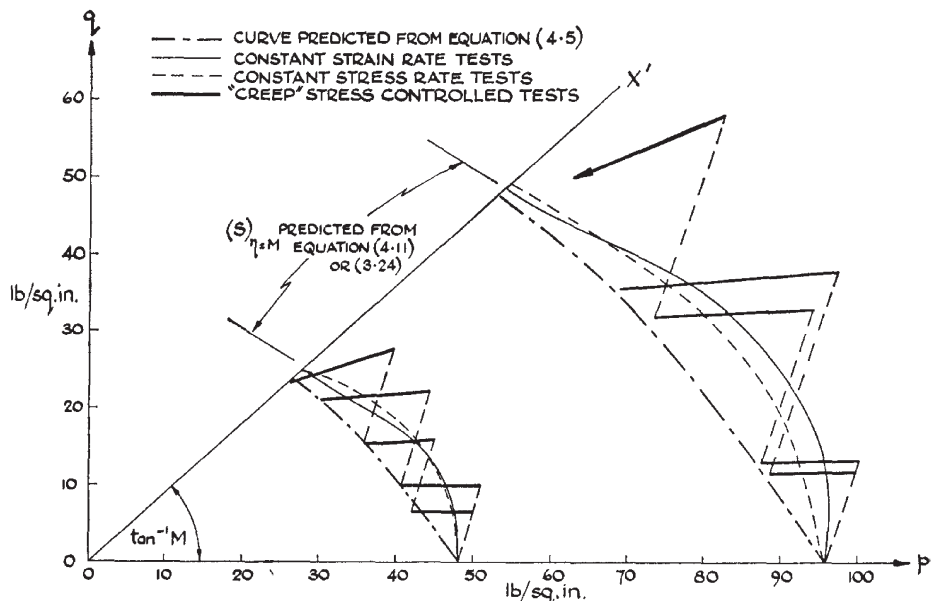
Fig. 63 Thompson's creep data (Roscoe et al., 1963)

isotropic compression of an aggregate in a triaxial cell at point D in Fig. 55(b) is very sensitive to a change of q, and is a poor way to prepare soil samples for triaxial testing. For Rankine's granular aggregate on the wet side of CS with internal friction as defined by an angle of repose but absolutely no cohesion between grains, the OCC model makes a most striking prediction that the space in Fig. 24 between the virgin compression line DHE and the CS line AC is $\lambda - \kappa$, as shown in Fig. 55(b) by the dashed arrowed line ECG; Casagrande and Albert (1932) found a constant spacing Δw from ultimate states after continued shear deformation.

In my final-year undergraduate lectures in early 1966 I contrasted a model with $\kappa = 0$ (that I called Granta Gravel) with a model with $0 < \kappa < \lambda$ (that I called Cam Clay). I chose local names to recognize that our whole group had played roles in the research that led to the model, and to make it clear to students that, although OCC fits experimental data, it is a theoretical model based on mechanics. Plots of v versus $\ln p'$ showed Granta Gravel and Cam Clay as being different, but in later years I introduced plots with $v_\kappa = v + \kappa \ln p'$ and Granta Gravel simply became Cam Clay with $\kappa = 0$. The plastic hardening of OCC is seen to be a shift of state from one κ line to the next. The lecture notes in early 1966 gave a fully three-dimensional yield function for Cam Clay from which general plastic strains could be derived; it became an appendix to our McGraw Hill book in 1968. I left Cambridge University at the end of 1969 to become a professor at UMIST. To introduce CS concepts to practising engineers, I organized courses of lectures with Wroth in UMIST; we once gave our course in Canada.

My handwritten notes in 1966 (now on my internet home page) showed an OCC yield locus in the three-dimensional $(\sigma_1, \sigma_2, \sigma_3)$ principal stress space on the wet

side of CS with Mohr–Coulomb failure surfaces on the dry side. The OCC surface of revolution intersects the six Mohr–Coulomb planes in six short arcs, representing innumerable three-dimensional states. Test paths with elastic and plastic portions that reach these states will generally cause slip plane failures. The only three state points where an OCC test path can reach a CS and can end with steady CS flow are the triaxial compression test points with stress states $\sigma_a = \sigma_1 > \sigma_2 = \sigma_3 = \sigma_r$. It follows that in a triaxial cell it is as difficult to reach ultimate CS flow as it is to reach initial plastic isotropic compression at point D in Fig. 55(b). A further problem arises in primary consolidation of slurry due to the filter cake effect. In any filter press, grains form a cake across the filter, reducing the rate of flow through the drainage boundary. The filter cake layer also is stronger than the slurry, so that only part of the external stress on a sphere causes plastic compression in the centre of the sphere; an attempt to cause spherical plastic compression by applying a spherical total stress increment to a uniform sphere of slurry with a spherical drainage boundary will fail because a spherical shell of filter cake condenses on the drainage boundary, acts in compression and carries some of the external stress. If a piston applies an axial load to a cylinder of slurry with radial drainage, a filter cake forms on the cylindrical wall and supports some of the axial load that is applied by the piston. In both cases the plastic compression process produces a soil body with a hard crust (like a chocolate with a soft centre) and not a uniform body of reconstituted soil. These effects make it hard to say how well or how badly a theoretical model fits test data, by causing uncertainties with reconstituted soil sample preparation. There were further difficulties if we wanted to explain liquefaction and needed experimental data of cyclic shear in an idealized aggregate. An experimental error in 1955 had already shown the need for imperfection in any array of spheres such as is shown in Fig. 8. Wroth as a new research student in 1955 at first tested a perfect aggregate of ball bearings in cyclic shear in Roscoe's SSA, and found that the strength *fell* as the density increased in cyclic shear, which is counter-intuitive. The explanation was that as the number of cycles increased, the ball bearings came into crystalline packing, and dislocations propagated in deformation, as in metal plasticity. Wroth stored the clean spherical ball bearings in oil, but water got into the oil by error, and the ball bearings rusted. He had only just got enough ball bearings to fill the box, and so continued the tests with rusty balls. They showed behaviour that was closer to real soil, with increasing density and *increasing* strength, giving test paths that led to a well-defined CS line. It had been a mistake to try to test a perfect specimen in a perfect shear box. Minor imperfections in close-packed arrays of regular spheres make them behave more like the soil grain aggregates that were the subject of our research. We did not have ideal test apparatus or ideal soil to test in it.

5.6 Laboratory testing and geotechnical design

The test data that have been discussed so far confirm my claim that the Mohr–Coulomb theory has not got a secure basis in experimental mechanics. The significance of OCC remains that it stands in its own right as a consistent CS theoretical model; OCC yield states lie on a line in the Frontispiece map. Attempts to plot the Mohr–Coulomb failure states show the difficulty of reconciling the two

models in the Frontispiece. Imperial College test data as plotted in Fig. 47, Hvorsev's shear box test and Casagrande's index test data validated the CS concept. The OCC model is easily modified, and papers proliferated as new students explored new model modifications or used new test apparatus. When data were published showing that the CS concept did not apply to every soil, this did not mean that the CS concept was invalid. If engineers are willing to question old theories it can help them to explain soil behaviour in the laboratory. The OCC model needs modification to include load cycles and anisotropy, but it does explain plastic volume change in soft ground and pore pressures. It is one of a succession of changes of concepts of soil strength in which components in successive centuries have been as follows:

- **18th century:** strength = friction + cohesion. Friction observed in slopes at repose was thought to be due to interlocking, not power dissipation, and cohesion measured in direct tension was thought to be the same as cementation strength in shear.
- **19th century:** strength = sliding friction (not interlocking) + cohesion. Friction was thought to dissipate power in slip on sliding surfaces, and clay chemistry causes plots of shear box test data to have an intercept that is called cohesion.
- **20th century CS theory:** strength = CS friction as in a slope at repose due to power dissipation in stressed-aggregate distortion + interlocking with zero cohesion.

Both Coulomb and Rankine took cohesion as zero in newly disturbed soil. In a CS view, aggregated hard grains are held together only by the effective spherical stress p' and not by adhesion of one grain to another. Taylor's interlocking gives apparent cohesion to soil, and adds a peak on top of CS strength without increasing power dissipation or improving safety. If a soil has a reliable aggregate of hard grains, the internal *friction* as measured at the CS is a reliable strength component. It determines the drained angle of repose. Taylor did not study cyclic loading, but small-amplitude shear strain cycles on lightly loaded dense sand generally cause contraction. It was a steady increase of the shear strain that caused the positive interlocking shown in Fig. 9(a). The rapid undrained shear strength c_u is the internal friction in an aggregate in states on the sloping line ACH of critical porosities in Fig. 18(b); the undrained shear strength that makes saturated soil paste seem to be a perfectly plastic body with constant cohesion is due to friction, not cohesion.

To state that CS concepts offer a basis for geotechnical engineers to continue to solve geotechnical problems, observe ground in the field and use plastic design methods is not to propose a rejection of all the soil mechanics thinking set out in T&P, which is indeed a good book. Milton wrote in the *Areopagitica* that

> *A good book is the precious life blood of a master spirit, embalmed and treasured up on purpose to a life beyond life.*

Milton was writing 150 years before the French *Descriptions de L'Egypte*, and 350 years before the opening of Tutankhamun's tomb in the Valley of the Kings there, so I do not read in this quotation all that is now associated with mummification, but rather the sense that T&P is a book to be treasured by the reader.

6 Geotechnical plastic design

The ductile mild steel structure of the Empire State Building (ESB) absorbed the impact of a B-25 bomber in 1945; less ductile structures exhibited progressive failure. Geotechnical engineers can study ductile or brittle failures by model tests with soil under appropriate stress in a centrifuge.

6.1 The place of plastic analysis in design

The OCC model shows that a type of plastic analysis that is helpful with structures also helps us understand the classification and the selection or rejection of soils as construction materials, and the problems of liquefaction and of dilation. I am sure that our teaching, like Baker's structural teaching, should be based on plastic design theory and on approximate methods of analysis by upper and lower bounds. Whether structures are made of reinforced concrete or mild steel or soil, they will not have a disproportionate response to a small load increment or be at risk of progressive collapse if they can dissipate enough energy in potential failure mechanism. The value of alternative load paths within a structure and of continuity and ductility, which was evident in bomb-damaged London, was also evident on 28 July 1945 in New York when an Army Air Force B-25 bomber crashed into the ESB between floors 79 and 80 in dense fog. The ESB was built in 1930 with a 60 000 ton mild steel frame structure. The crew and some civilians were killed, but the energy of the crash was absorbed locally in plastic deformation. The B-25 started a fire but it did not penetrate into the core of the ESB. Newspaper photographs in 1945 showed a plane embedded in the ESB (the tail portion stuck out 80 floors above the street) not a collapsed ESB. There was a difference between an aircraft structure and the ESB structure. The men flying the aircraft accepted that they were in a structure that could not itself dissipate the energy of all potential failure mechanisms. The ESB was New York's icon, where people could expect engineers who built structures for public use to make them *as safe as houses* (and more safe than aircraft). But if the tests to determine soil constants and computer calculations in the design and construction of civil engineering structures, geotechnical or others, are compared with the material testing and design calculations and flight testing required for aircraft, it is doubtful if our structures are as safe as commercial aircraft.

Elastic structural analysis as used in the ESB design finds a distribution of stress in equilibrium with the applied loads on the redundant frame structure, and finds elastic strains compatible with the displacement imposed on it. An error in the dimensions of a redundant structure that is within allowed construction tolerances, or a foundation settlement, can cause strains that greatly increase the local maximum elastic stress, but an understanding of the associated plastic flow rule

of the theory of plasticity in structural design reassures engineers that it does not matter that the elastic analysis is not precise; it can be proved to be a safe lower bound to the actual plastic collapse load of a fully connected ductile steel structure. An elastic analysis that finds a stress distribution that does not cause yielding anywhere in the structure in static equilibrium with an applied load is a *statically admissible lower bound* to the actual plastic collapse load; an analysis that assumes a failure mechanism and calculates an applied load that is powerful enough to move it gives a *kinematically admissible upper bound*. After research on design of steel frame structures before WWII, plastic design methods of steel frame structures (Baker *et al*., 1956) were validated by bomb and blast damage to all manner of structures in WWII. Baker *et al*. claimed that the whole basis of elastic design was faulty *and the path which designers had been following for nearly a century was nothing more than a blind alley*. The value of ductility as a basis for steel structure design was a lesson learned after WWII both in the UK and in the USA (Beedle, 1968). The lesson did not continue to be taught, as is seen by contrasting the safe ductile yielding of Baker's bomb damage shelter in 1941 with the brittle failure and disproportionate bomb damage in the Oklahoma Federal Center failure in 1985 and in the 2001 collapse of the Word Trade Center towers. After a large amount of fuel spilled across open-plan floors, fire affected the upper parts of both towers, but not their lower parts, and their final collapse might not have been so rapid if a plastic design had considered failure mechanisms such as are shown in Fig. 50, and had led to strong floors that could continue dissipating energy during large deformations and strong floor-to-column connections capable of surviving large displacements. Baker prefaced the printed version of his introduction to a conference on the settlement of structures with a spoken comment that, while he valued kind remarks that some geotechnical engineers made about him, he wondered if they appreciated that his work aimed to reduce the need for their work. He had observed steel frames during construction and seen causes of damage including dimensional error in lengths of members, thermal strains, and errors in locating foundations that are more serious than differential settlement of ground. If a building frame could accept damage before being clad or given a brittle plaster finish, the builder would not need a geotechnical engineer!

Masonry *stone skeletons* are flexible and can accommodate differential settlement, but no energy is dissipated in structural strains; the rotation of a masonry hinge can be seen, in soil mechanics terms, as interlocking, which does not dissipate energy. Baker's plastic design of mild steel structures involves the selection of materials in which energy is dissipated. The construction of full-strength connections in redundant structures ensures the redistribution of unsuspected stress concentrations. The ductile yielding of mild steel safely redistributes stress concentrations that would initiate fracture in stronger but more brittle steel. The metallic bonds between iron atoms and the slip of dislocations in the crystal structure allow mild steel to yield with constant volume. The strengthening of alloy steel can be based on the locking of dislocations by alloy atoms, but steel can become brittle as it is strengthened. Geotechnical engineers use soil classification tests to help them select construction materials that are able to dissipate work when disturbed; compaction strengthens and hardens them. Soil behaviour when disturbed will depend on the effective

pressure in the aggregate of soil grains and the packing density. Soil is a ductile plastic material that is as reliable as mild steel if it is not over-compacted. It is most tough and ductile as a plastic material at the CS effective pressure, but is brittle when over-compacted and lightly stressed. It will flow as debris in a catastrophic failure if, when in states shown as Herrick's liquefaction states in the Frontispiece, it is fractured into rubble and subjected to a high hydraulic gradient.

6.2   Lessons from the geotechnical centrifuge

When Sokolovsky (1960) sets up stress field equations for solution by the method of characteristics he refers to Pokrovsky's centrifuge with a whole model at an N-scale model factor in a uniform acceleration field N time's the Earth's gravity. Experiments on models at reduced scale gave masons an understanding of static equilibrium and of the mechanisms of deformation in a stone skeleton, but small models cannot test rock. Mining of the slopes of an open-pit mine for ore extraction has been studied in the Earth's gravity with a model pit so large that it filled a room, with all dimensions and the rock fissures equally reduced in scale, and a frame built over the model, giving access to the model for excavation of the open-pit by hand; that model was made from weak plaster blocks of strength reduced by the scale factor of the model dimensions so it was possible to make that model demonstrate the crushing of weak rock. The value of that reduced-stress model depended on the accuracy with which failure of the weak plaster represented a scaled-down failure of the rock. In a reduced-scale model at increased accelera-tion in a centrifuge, each FE of real rock is subject to the real stress. It was not possible at that time to excavate a pit while a test package was in centrifuge flight. When modified constitutive models for soil were introduced into FE numer-ical models of boundary value problems, new physical data were needed from different tests of laboratory specimens. The geotechnical centrifuge offered a new way to test disturbed soil under all appropriate boundary conditions. Effects due to anisotropy and cyclic loading in soil occur in each small-model FE. Each stage of a centrifuge model test satisfies equilibrium and compatibility in soil elements that can be thought of as 10 000 laboratory test specimens. The state of the reconstituted soil slurry in each of them is initialized and then follows a test path with exactly the stress and the strain history that is ideal for laboratory tests. Many new items of laboratory test equipment would need to be built in order for each of those elements to be taken through appropriate test paths. In the small tank that Casagrande struck with a hammer in his liquefaction experi-ment the stresses were low. His later suggestion that even dense sand under high pressure could liquefy was not based on a laboratory model test under high stress.

  Pokrovsky's centrifuge model contains many elements, each under an appro-priate stress; some at very low stress near the ground surface and some at a depth in the model where stress is high. As thousands of elements of reconstituted soil, each of about the same size as a small triaxial test specimen, come under different stress, every element provides the right boundary conditions for neigh-bouring elements in the centrifuge, and each element of reconstituted soil in the model follows a path in a small-scale model test at increased acceleration. If a set of similar models at different scales show similar behaviour, the scaling laws

will be confirmed by what is called *modelling of models*. In the First International Conference on Soil Mechanics at Harvard University, Terzaghi said that '*the possibilities for successful mathematical treatment of problems involving soils are very low*'. In the proceedings of Terzaghi's first international conference at Harvard University, Pokrovsky (Pokrovsky and Feodorov, 1936) showed the data of centrifuge model tests giving earth pressures in the ground below a full-scale plate load test. Terzaghi derided '*the utter futility of small scale models*' (regarding published '*well documented case histories*' as the only data of use to geotechnical engineers). He failed to acknowledge that Pokrovsky's paper did show that a centrifuge test series could model plate loading tests and get the same data as full-scale field trials with more accuracy and less cost and delay than was incurred in the field.

In a discussion of the actual lateral pressure of the earthwork, Sir Benjamin Baker (1881) wrote that if a man says he has no experience of failure of works of his own construction, '*that merely proves that his experience has not been extensive*'. An engineer needs to be able, without putting a client to too great an expense, to gain '*experience of failure of works of his own construction*'. Wherever trial construction is considered, centrifuge model tests should also be considered. If we can validate the techniques of geotechnical centrifuge model tests, our data can change engineering theory and practice. A contract from engineers in practice for geotechnical centrifuge testing can provide the experience of failure now, in an orderly way, that the chaos of WWII provided for Baker's generation, that gave him the opportunity to introduce the plastic design of steel structures to engineers in practice. Geotechnical centrifuge model testing can show liquefaction to students, or can give us experience with which to check plastic design teaching based on CS concepts. Engineers can solve problems at model scale of events that at full scale are uncontrollable. We can learn how to get a new class of data from repeatable strong earthquakes on small centrifuge models. I presented a plan for geotechnical centrifuge development at a meeting of the British Geotechnical Society that would be costly and take time. UK Science Research Council (SRC) funds were committed to other projects; a small centrifuge development was supported, but a large centrifuge in Cambridge needed other funding (Schofield, 1995). I recruited a research student, who got access to a large British Aerospace centrifuge in Luton, left over from earlier British rocket research, and took Cambridge models in a strong box for testing there (Avgerhinos and Schofield, 1969). I went in 1969 to be Professor of Civil Engineering at UMIST. Rowe was then a Professor at Manchester University, and we both built centrifuge facilities.

The UK Building Research Station (BRS) funded model tests at UMIST of failures of raised Thames levees. Whatever Thames Tidal Flood Barrier was built, the existing levees A shown in section in Fig. 64(a) as built on the marsh soil B would have to be raised on the seaward side of the barrier. The BRS made a cofferdam on the seaward side of a coastal levee, and filled it with water that seeped through cracks. They saw that the landward slope had sloughed away, causing a breach. This full-scale test had explained failures in the 1953 tidal floods that occurred just before overtopping. But the BRS were concerned about a failure in Dartford creek where the lock keeper had gone out and walked along the levee by his house on the night of the flood. The levee by his house failed that night, and blocks of levee of as much as 50 tons were washed onto the marsh layer A in

Fig. 64(a). If he had seen that overtopping was imminent he would not have let his family stay in the house where they all died. The BRS thought that there may have been a new kind of failure, with rising water pressures in layer C altering the pore pressures within the levee and causing failure on a slip surface. Any proposal to raise the Thames levees faced the risk of this kind of failure. A full-scale trial could not be made without great cost and public alarm, and the BRS wanted to study such an event in confidence in tests of centrifuge models. The outcome of the tests (Hird, 1974) was a simple explanation of the Dartford levee movement. As soon as uplift pressure in the underlying sand layer C was equal to the weight of layer A, the marsh was uplifted. The failure state with a flow of water up through tensile cracks or pipes in layer A was to the left of the Frontispiece. The BRS learned what they needed. To observe transient pore pressures in soft clay below model levees we spent some BRS money giving Druck Ltd their first contract developing a novel solid-state pore pressure transducer (PPT). It ensured that the model reached equilibrium safely without failure before the storm surge tide was applied to the model. This PPT was to play a crucial role in all later centrifuge studies, making it possible to study liquefaction in model earthquakes.

In 1973 I thought that Pokrovsky (Pokrovsky and Feodorov, 1936) had published no more centrifuge papers after the one written for the first ISSMFE Conference at Harvard University, and wondered if this was due to a fundamental difficulty, perhaps with Coriolis effects in rotating models. Contact with Russia was difficult, but at the 7th International Society of Soil Mechanics and Foundation Engineering (ISSMFE) Conference in 1973 in Moscow its Chamber of Commerce had a trade exhibition. Hoping to provoke a centrifuge discussion there, I hired a space to exhibit a display of posters describing work in Cambridge and Manchester. Soviet engineers then got permission for an exchange of information with foreigners in a meeting at the end of the conference at the Hydroproject, which had a very powerful centrifuge. I met and was given books by Pokrovsky and Feodorov, and by Malushitsky. The books showed that Pokrovsky had modelled nuclear weapon craters and had led the development of centrifugal modelling in the USSR (Schofield, 1998b). It explained why his work was classified at the height of the Cold War. The Test Ban Treaty prevented US full-scale tests from resolving uncertainty about liquefaction in large weapon craters. All contact was difficult, but when I understood what Soviet centrifuge model tests had achieved by 1973 I could also see that we were not only separated from the Soviets by military secrecy; there was a theoretical gap between us. Resource development in Siberia and Soviet far-eastern lands and defence needs meant that their engineers dealt with permafrost, so Soviet soil mechanics was based on creep, with model tests at different scales to find the exponent of a power law for creep that best fitted the observed scaling of time. Our effectively stressed aggregate of soil grains was an elastic–plastic body with time effects due to consolidation. I based soil mechanics on a theory of plasticity with time effects being due to primary consolidation, which made centrifuge models look better to me than to them. I got their books translated into English, but I could find a publisher only for the translation of Malushitsky (1981); there is still no published translation of the other books into English.

Malushitsky describes his test facility at the Kiev Projekt Institute between 1966 and 1970, the procedures and soil types, observations, and systematic check of

accuracy by modelling existing waste heaps of overburden soil in open-cast mines for sulphur and for coal in the eastern Ukraine. He tested methods of forming heaps, the effect of foundation weakness, and the construction of waste heaps on hydraulic tailings lagoon areas with large movement of hydraulic wastes in the foundation, and he integrated his model tests into the mine waste management:

> *Making use of the recommendations cited above, the first mine in the Kuzbass (the 'Krasnogor') deposited without accident, during the course of one year, on old hydraulic waste-heaps, more than one million cubic metres of solid, hard overburden without occupying any new land, and reduced the mileage of dump trucks by 1.5 times.*

When excavators had to undermine existing heaps, the slopes seen to stand up safely were much steeper than would be allowed by a soil mechanics calculation. Model tests provided the chief engineer of the 'Krasnogor' mine with data that he needed to ensure safe working, so that

> *…over a period of two years undercutting of the slopes of internal waste-heaps was carried out at the 'Krasnogor' mine which made possible a reduction in the volume of re-excavated material by 4.2 million cubic metres.*

This example suggested to me that it was possible for a geotechnical centrifuge facility to model problems connected with toxic and nuclear waste. The scale factor for the mass of waste is N^3. A model test of the movement of $10\,g$ of toxic waste in a plume at a scale of $N = 300$ would correspond to a full-scale test using $300^3 \times 10\,g = 27$ tonnes of toxic waste. The seepage flow in the model in 1 week of continuous operation scaled up by a factor of N^2 would correspond to $300^2 \times 1\,week = 500$ years. Models made safely in a laboratory glove box with actual soils and toxic waste from a very hazardous site and tested in a dedicated facility would give data that could not be obtained in the field. I proposed a European facility, but that was not funded. Roscoe died in a motor accident in 1970 while I was at UMIST. In Cambridge, a 10 m beam centrifuge planned by Roscoe was built by Wroth but not commissioned. The SRC had no funds for centrifuge development. When I returned to Cambridge University in 1974 I had to fund work on the centrifuge by a succession of contracts. In Schofield (1980) I described how, with swinging platforms fitted to the beam, work was done on a wide variety of contracts. Successive models were tested by a group of university staff and research students. Funds for the continued development of equipment and instrumentation were earned from industry by the centre under my direction from 1974 to 1998. The basic research that led to OCC was going to undermine confidence in the Mohr–Coulomb model, but centrifuge development would let engineers in practice use model tests to gain new experience when the time came to apply new theories as they were developed.
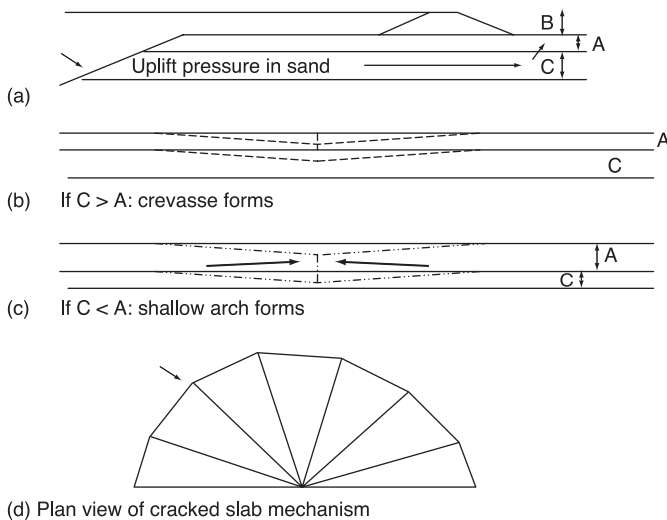
6.3   Herrick's liquefaction in models

There is more to be found by laboratory testing about a geotechnical problem than values of c or ϕ or other soil constants for use in a computation. A centrifuge model test can reveal a failure mechanism and the displacement mechanism

before failure. When the USACE Waterways Experimental Station (WES) gave me a contract for research into *environmental problems of liquefaction* they asked me to model every example of liquefaction that I thought possible, and I began with Mississippi levee tests. From the start of the 19th century, the US federal government had tasked the USACE with maintaining navigation in what was to become a system of over 20 000 miles of US waterways. The floods in the mid-19th century established the need for the USACE also to be tasked with flood control of the river through the Mississippi River Commission, formed in 1871. The work involved levees and floodways, channel improvement and stabilization, and tributary control. The Civil War had impoverished the South, and the USACE got a new task after a flood in 1927 when Roosevelt's New Deal addressed the poverty of the South. About the same time as the Tennessee Valley Authority was set to work, the USACE was to complete a project by which the highest flood of record in every tributary of the Mississippi could be safely routed to the Gulf of Mexico. The system of federal levees and river control structures had to survive erosion that would occur at every bend as the river meanders through the Lower Mississippi Valley. The USACE built a large hydraulic model in Vicksburg in the WES grounds to study every river bend.

Soil selection for levee construction used Casagrande's classification system. He also gave advice on the risk of liquefaction of river banks. In places on the flood way the federal levees are miles apart, in between which private levees protect private interests, but a USACE general (who is in command in a flood fight) takes control of the river and all tributaries and decides what land will be flooded (after the flood the federal government makes compensation payments). The soil in the Lower Mississippi Valley came down the river, transported as sediment and deposited across the width of the valley. In a naturally formed meander the river forms a shallow point bar deposit of sand on the inside of a bend and cuts deeply into the outer bank. Each flood deposits silt over the sand bar, and as the river meanders in the Lower Mississippi Valley, a typical vertical profile of ground will show (Figs 64(b) and 64(c)) the point bar sand deposit (layer C in the figures) in the face of the river bank below a crust of stiff silt soil of variable thickness (layer A). When the river is at the flood stage, tree tops stand above the brown water, but if engineers on the levee see the trees sink into the flood they know that their levee is in danger. The river is eroding the point bar sand C and undermining the stiff crust of soil A. If the erosion progresses, it may open a crevasse, breaching the main-stem levee. They must build a set-back levee behind the potential breach quickly to prevent the river flooding out of control. Prediction of the likely locations of such breaches allows the USACE to have construction plant available in the right location. Casagrande predicted that Hazen's liquefaction event would be likely to occur if the overburden A was thick, causing the effective pressure on the point bar sand C to be high. A review of the records of actual crevasses found the opposite to be true; I was asked if centrifuge model tests could explain why, and I found that models could show me the reason.

Our Cambridge Mississippi tests (Padfield, 1978) considered a bend where the main levee stands far back from the river. To model erosion by the river of the exposed face of layer C our centrifuge model in an 850 mm diameter tub had layers A and C (Fig. 64(a)), resting on a little platform below water. A water

(a)

(b)   If C > A: crevasse forms

(c)   If C < A: shallow arch forms

(d) Plan view of cracked slab mechanism

Fig. 64 River bank failures. (a) Section. (b, c) Elevation. (d) Plan view of cracked slab mechanism of the Mississippi River crevasses

tank above the tub had a short pipe down into layer C and, when the model was in equilibrium, air pressure applied to the tank caused a flow of water to erode the sand layer C into the test river. Soil could flow away below the platform on which the model rested. The centrifuge was fitted with swinging platforms so that soil and water could swing up into the testing position. The test took place under water out of sight, as it does at full scale, but after a test the tub swung down and we could drain the river and inspect the under water failure. The outcome was that the collapse mechanism of layer A above the site of erosion depended on the ratio A/C. Figure 64(c) shows the case where A was thicker than C. As A cracked, arching forces between segments spanned across the erosion site, which kept the effective stresses in a cone of plastic failure so that slab A remained intact as it descended, and acted as an articulated mattress, preventing further loss by erosion of layer C. If A was thinner than C the segments of cone descended past the level of the interface between A and C. All arching thrust was lost. Once the stress moved to the dry side of the CS the soil in slab A was no longer a ductile plastic material. Slabs of A and underlying point bar sand C all flowed into the river, leaving a semi-circular crevasse in the bank. A WES engineer who saw photographs of the model failures flew me along the river in a light aircraft to see semi-circular liquefaction crevasses in the field, just as our models had showed. I had no knowledge before the tests that this is the actual mechanism of failure. A model test at reduced scale and increased acceleration is an excellent way of testing models made with granular aggregates because their behaviour mechanisms depend on the pressure and packing density.

The alarm that high effective overburden pressure could cause Hazen's liquefaction of deeply buried sand below levees protecting low-lying parts of New Orleans, and result in crevasses and floods, seemed to have been mistaken. Model liquefaction was in states to the left of the Frontispiece. A general lesson

from the Thames and Mississippi model tests about river bank system geometry is shown in Fig. 64:

(1) **B > A**. If a river bank is higher than the layer on which it rests, a river at the flood stage may cause uplift pressure failure. A possible safety measure would be to cut through A to form open pools behind the levees to relieve uplift pressure in C. The river would flood the land slowly and safely without catastrophic sudden uplift failure of A or displacement of the levee.

(2) **C > A**. If an underlying point bar sand deposit is thicker than the overburden layer, the overburden cannot arch across an erosion cavity as a plastic slab and stop erosion. An articulated mattress on the exposed face of C would provide a possible safety measure. Levee engineers can learn a rule, like the geometrical rules of masons, that thin overburden is dangerous. Layer A must be thicker than any underlying sand layer (B < A) and thicker than the height of any levee that is built upon it (C < A).

A different concern arose in the last quarter of the 20th century when oil and gas were found below the North Sea bed between Britain and Norway. The sea there is about 100 m deep. In order to achieve early production, oil companies had to order offshore structures 'off the drawing-board' before a single such structure had been placed on the deep North Sea bed. One project, to supply Britain with gas from the Norwegian Frigg field, had a steel jacket structure for drilling the wells and production of gas in this northern field, and a pipeline that ran via a concrete manifold structure to the south. The steel structure was accidentally ruined during installation. The company kept the project on time by using their manifold structure on the northern site. When installed in September 1975 in 96 m of water it became CDP1 (Concrete Drilling Platform 1) at Frigg. The prestressed concrete tower structure had a central shaft that extended 30 m above sea level to a steel deck. It rested on an annular raft, of 101 m external diameter and 54.4 m internal diameter, on dense sand. The raft did not have a skirt, as at that early date the value of a skirt was not realized (later concrete rafts had steel skirts that penetrated the sea bed round them). Casagrande's 1975 advice that '*even dense sand, if heavily loaded, can experience actual liquefaction*' led the designer to reduce the effective stress on the sand as far as possible, hoping to lower the liquefaction risk. The sand state was far on the dry side of the CS line. In due course, storm waves rocking the exposed tower of CDP1 were seen to be larger than had been expected further south. The edges of the lightly loaded raft were intermittently pulled up and pressed down on the sea bed, causing pumping and erosion. Lacasse *et al.* (1991) wrote that

> *Videotapes of an underwater survey in September 1976 showed sand flowing from the underside of the base through the rabbit holes. The sand flow was described as a 'breathing' process with a rhythm close to the wave period.*

The word *breathing* suggests an image of a man taking a nap with a handkerchief over his face that rises and falls in rhythm as he snores; Herrick's image of Julia is more picturesque. Casagrande's advice that even a dense sand bed can liquefy under high stress led the CDP1 designer away from the *wet side of the CS* towards the *dry side of the CS*. His maximum vertical stress was as low as possible, with a

triangular stress distribution across the base under the design moment. The pressure at the edge of the slab cycled from zero to a maximum pressure, but when the storm wave heights at Frigg applied moments that were greater than the design values, the effective pressure could not become negative. The moment lifted first one edge of the slab and then the other off the dense sand, and caused pumping. The ground loss caused cracks in the concrete. The cameras at Frigg saw medium to fine very dense sand being pumped out from below the raft under zero effective stress. The structure cracked when the loss of sand undermined the base. The loss of sand by pumping might stop if a drained loading berm were placed round the base; settlement damage might be made good by grouting. Model tests were discussed but not proceeded with.

For Casagrande in 1936 nothing could stop a sand flowing once it has changed into a flow structure. The chain-dashed arrow from B to C in Fig. 18(a) shows fully drained shear and deformation at constant effective pressure p_1 that brings soil to a safe porosity n_0. In his 1975 theory the definite critical porosity for sand changes to the CS double curve in Fig. 12 and the double line AH in Fig. 18(b). Hvorslev had stated in 1937 that his experiments showed that Casagrande's 1936 void ratio does not exist in the case of fine-grained soil, and that any void ratio can become critical if it is produced by a critical consolidation procedure, as in Fig. 18(b), where critical porosity decreases as effective pressure increases. The CS concept applies both to sand and to silt and clay. With a CS line AH in Fig. 18(b) crossing compression lines AB and FH, in Fig. 18(b) a chain-dashed arrow from B towards C leads to drained shearing deformation at the constant effective pressure p_1 in a CS state at C, but now a solid arrow from B to K leads to undrained shearing with effective pressure p_1 decreased only until the CS at K is reached with flow with a constant positive pore water pressure $u = p'_B - p'_K$, where p'_B is the pressure at B and p'_K is the pressure at K.

The final set of tests that I will discuss here relate to brittle embankment dams. The Lower San Fernando Dam was constructed by hydraulic filling above Burbank; it failed on 9 February 1971 during the San Fernando earthquake with high pore pressures that led to a slip of the upstream face similar to the slip in the Fort Peck Dam. In the mid-West and the Mississippi valley where water is plentiful, Army Engineers could build their dams with pumped hydraulic fill; in the mountains, water is scarce, and the Bureau of Reclamation or the Los Angeles Division of Water and Power had to use earth-moving and compaction plant to build dams. A number of such dams had been built in California before anyone raised the question of whether an embankment built of granular aggregates without any clay was at risk of liquefaction in earthquakes. Older embankment dams that had survived previous Californian earthquakes had been built with clay soil. However, in the western states in general where water is too scarce for hydraulic fill construction and no plastic clay is available, agencies such as Bureau of Reclamation and the Los Angeles Division of Water and Power used machines to excavate, haul and heavily compact non-plastic fine silt soil to build embankment dams such as the Teton Dam in northern Idaho and the Baldwin Hills Reservoir in Los Angeles. The foundation movement of dam sites under the weight of water and soil causes brittle soil to crack. Both dams failed, with cracks in dense brittle soil near zero effective stress in the zone on the dry side of

the CS line in the Frontispiece where liquefaction of cracked rubble is plotted, with high hydraulic gradients. The engineers for both dams placed great emphasis on achieving high density, but a less compact, more ductile, soil body would have been a better barrier to water flow. Both dams failed with near-vertical faces to a channel through which the water flowed. It was a tribute to the level of compaction that had been achieved that the faces stood while the entire contents of the dam flowed past, but if less heavily compacted, such soil deforms with smaller cracks. They flood with water when the dam fills. A small crack could self-heal, and a dam could remain watertight.

I got support for a set of centrifuge tests at the University of California in Davis and also at Cambridge University for centrifuge model tests made with Teton Dam core material. I reported the results to the Bureau of Reclamation. A slab of compacted soil formed a model of a section of the dam core, with a vertical crack at right angles to the dam. A window against the crack face let it be observed as water flowed through the narrow crack. Soil grains eroded from the face fell down and filled the bottom of the crack. The erosion formed a void that migrated upwards to the surface. There was a graded filter layer downstream that fell into the rising void and plugged it, so the crack did not turn into a pipe. The vertical face of a crack in compacted Teton Dam core material was observed while seepage water flowed along the crack. My report showed loose soil sloughing off the crack face, filling the crack with mud and causing a void to slowly migrate upwards to the surface while mud slowly plugged the crack. A graded filter layer rested on the upper surface, and the essential requirement of the layer was that it was thick enough to fall into any void that arrived and plug it. Any faults in the rock below the Teton Dam were due to move when the dam was filled, and there was no possibility of predicting precisely where foundation movement would occur. What was needed was construction that was not too stiff, leading to cracks that were not too large, and filling that was not too fast, leading to plugging of cracks, and graded filter layers to fill migrating voids. The Teton Dam was the last in a series of Bureau of Reclamation dams that successively were compacted harder, with soil states moving further to the left in the Frontispiece. It failed with a crack face to the full height of the dam. It was filled more rapidly than the others to get an earlier return on investment. There was no time for cracks to heal (Muhunthan and Schofield (2000)).

The Seed *et al.* (1976) account of the Teton Dam failure began with an FE analysis of the compacted embankment that found a low stress in the cut-off trench below the dam as built. He superposed the pore water pressure transmitted through the flow net on filling the dam, on top of the FE total stress. Where the sum was negative it was said that the effective stress fell to zero and the soil cracked, but simple superposition no longer applied with those boundary conditions. Total stresses changed during filling, and should have been recalculated with no strain parallel to the underlying rock faces. Cracks, pipes or channels have often been encountered and led to failure. The lesson that should have been learned was the value of ductility and of measures to ensure that internal erosion leads to self-healing. The Los Angeles Division of Water and Power engineer Proctor built a heavily compacted embankment that formed the Baldwin Hills Reservoir. A novel drainage system below that reservoir was intended to detect

leaks, and the data did reveal them, but no action was taken. The dam failed while I was a Fulbright Fellow at Caltech (1963–1964). When I visited the dam just after failure I was struck by the excellence of Proctor's compaction. The vertical faces of the very narrow vertical cleft in the embankment through which the entire contents of the dam had flowed had not fallen. That very strong over-compacted soil made a poor dam was also evident in photographs of the Teton Dam failure, showing the great torrent at failure rushing past high vertical faces of over-compacted soil.

Hazen's suggestion that a hydraulic-fill dam had been liquefied by a shock has been represented by points in the Frontispiece on the wet side of the CS. Casagrande's 1936 theory refers to soil looser than a critical porosity in Fig. 18(a); his 1975 paper refers to unpublished studies for the USACE at the time of the Franklin Falls Dam, to which Taylor (1948) also referred, with an inclined CS line like ACH in Fig. 18(b) replacing the constant critical porosity line CE in Fig. 18(a). In 1936, soil below the constant porosity critical line was supposed not to be at risk of liquefaction but if soil was in a safe state, pressure reduction might allow swelling into a state with a risk, as shown by the bold inclined arrow **Z** in Fig. 18(a). In contrast, in 1975 contractive soil above the CS line was supposed to be at risk of liquefaction, and Casagrande warned that even dense sand might be taken into a state where it is at risk by a pressure increase as shown by the bold inclined arrow **Z** in Fig. 18(b). This 1975 paper led to concern that deeply buried sand and gravel layers laid down at the end of the last glacial period may cause widespread liquefaction risk and to much expense in construction. In my centrifuge models of examples of liquefaction I never achieved Hazen's liquefaction. I cannot say that it will not be achieved in other centrifuge models, but I have based the Frontispiece on the failures that I achieved. Various triaxial tests have been reported as evidence for Hazen's liquefaction, where a test path approached the CS from the wet side and ended in unstable failure. I regard such failures as instabilities that apply to the specimens with the boundary conditions tested rather than as evidence that soil at the same state in an embankment will liquefy. This section has discussed some cases on which I have based the Frontispiece entry on Herrick's liquefaction. Better model tests would be needed to make a better entry.

6.4 Geotechnical centrifuge developments

In my 1980 Rankine Lecture and in a lecture in St Louis (Schofield, 1982), I reported that centrifuge studies had led me to review Casagrande's definition of liquefaction. Model earthquake tests in Cambridge gave our students test data from which they got a new understanding of pore water pressures (Schofield and Lee, 1988). In the Bumpy Road system that we used for some years, the earthquake actuation energy came from the massive centrifuge arm; later, it proved possible to retain the modelling equipment and simply replace the supply of stored angular momentum by a flywheel. The earthquake actuator applies earthquake waves at predetermined frequency for a predetermined time in which an acquisition system stores pore pressure, acceleration and displacement data from solid state transducers in a flash memory for retrieval after the test. This type of test has transformed the position in earthquake engineering research. Where previously

no one thought we had a basis from which to comment on Casagrande's liquefac-
tion and critical voids, after we could analyse our own test data at Cambridge
University, and other centrifuge workers had similar direct experience, we all
had a new authority to make comments. The new geotechnical centrifuges have
created a new opportunity for laboratory workers. Both disturbed and undis-
turbed soil specimens can now be subjected to laboratory tests that produce
data with a direct relevance to works and observations in the field. A great
many computer programs are available which require soil to be characterized by
parameters describing one or other aspect of a constitutive model (many of
which models claim descent from CS concepts or Cam Clay). Engineers who
observed soil behaviour in the laboratory used merely to determine values to be
given to the parameters used in the computation. Triaxial test equipment does
not impose all the conditions that are relevant to failure; now we observe
behaviour mechanisms.

A new opportunity to make tests in geotechnical centrifuges on models that
represent a complete dam or segment or a foundation system as a whole allows
us to find a value of one or other parameter which covers integrated effects through
a unit of construction. In the application of plastic design to steel structures, the
role of stress and strain in the analysis are played by the bending moment applied
to a rolled steel member in Fig. 50(a) and the plastic hinge rotation. This example
can be extended in the study of jack-up spud fixity, where a structural analyst who
regards foundations as elastic spring hinges needs to know when the fixity became
non-linear. To study the behaviour of offshore jack-up platforms in a centrifuge
with a mobile model, a soil sea bed layer was placed as a carpet around the
circumference of the 2 m drum in Cambridge and accelerated to 300g. It offered
identical conditions at 20 different locations at which the model was deployed,
and the platform was subject to cyclic loading that modelled the wind and wave
forces on a platform in a storm (Tsukamoto, 1995). At the outset of the model
tests there were no data of fixity of jack-up spuds when loaded at full scale to
incipient failure in a storm. The data of foundation fixity found by the end of
the tests enabled an oil company to validate the new programme that they
wished to introduce for selection of rigs for use on North Sea sites. Much greater
danger and cost and uncertainty of environmental conditions would have been
involved if an attempt had been made to get similar data from platforms deployed
in the field.

The money for the development of centrifuges and of modelling technique was
earned on contracts. When the government stopped spending departments such as
Transport or the Environment from placing contracts for university research, it
was harder to get, but it remained possible to find money for research on offshore
structures for the exploration and production of oil and gas. I was told that oil
companies wanted to buy research within a market where there were several
competing research organizations that all reached international standards. It
was essential both to encourage and assist all those that wanted to compete with
me and also to try to remain pre-eminent in the field and win the best contracts.
At the time of the Stockholm ISSMFE conference in 1981 when President de
Mello first formed Technical Committees (TCs) on various topics he agreed that
one of the first should be TC2 on centrifuges. It was possible to internationalize

the topic with a variety of committee members and a succession of specialist conferences that produced many papers from many centres in ISSMFE TC2 conference volumes that lifted the shroud of military secrecy from the topic and created wide academic and commercial activity in a centrifuge model testing market.

Cambridge University was unwilling at that time to have their name associated with trade, but I was allowed to set up a company, Andrew N Schofield & Associates Limited (ANS&A), earn money on ANS&A contracts, fund successive students, and continue equipment development in Cambridge. In one typical study the *bearing capacity factors* that Terzaghi had based on fragments from the theory of plasticity were replaced by yield locus concepts and studies of structure–foundation interaction that we validated by experiments (Dean *et al.*, 1993). Each such study led to a PhD thesis by a research student. There was also the possibility of earning money by manufacturing test equipment and instrumentation in Cambridge for the new test facilities that began to be built. In France, LCPC specified their facility at Nantes after reading all the published information, and visiting and drawing help from our experience in Cambridge, but got a French aerospace firm, Acutronic, to build their centrifuge. When I spoke at the Nantes opening, Acutronic asked for ANS&A cooperation to help them to sell centrifuges to other centres, so I formed a second company, Centrifuge Instrumentation and Equipment Ltd (CIEL), for this purpose. Potential users visited Cambridge, and were offered training for their workers and planning and provision of test equipment for their facilities (Schofield and Taylor, 1988). ANS&A was particularly closely involved with the US army centrifuge at the WES (Ledbetter *et al.*, 1994). With each development the risk of accidents was comparable to risks that there would have been with research students and technicians using light aircraft. Contact with professional engineers meant that all involved in Cambridge learned to work responsibly. People that were funded by ANS&A to work in the Cambridge facility went on to build and work in new centres in other countries. In 20 years, new effective stress modelling techniques became well known. Cambridge University had become better organized for its involvement in trade on my retirement in 1998, so I liquidated ANS&A and CIEL, and passed over goodwill and assets. Many of the 175 PhD theses in the Cambridge soil mechanics group over the past 50 years involved cooperation with engineers in geotechnical process and construction that continues today.

6.5   Conclusions

Any student civil engineer who learned the principles of soil mechanics in T&P and found that *il put les entendre les principles et s'en server* (it was possible to understand the principles and to follow them) will know from their own experience what great benefit the teaching at Harvard gave to 20th century civil engineering education. To conclude this book I must explain my confidence in proposing to change some principles of that education. Goodman (1999) describes Terzaghi as 'the Artist as engineer'. My translation of Coulomb's words *un Artiste un pue instruit* as 'a builder without higher education' equated artisan and builder. The front cover of this book shows a novel structure made 600 years ago, costing a

King's ransom, and requiring 14th century builders (each of whom Coulomb or Goodman could describe as *un Artiste* or an Artist) to adopt a building plan that was accepted and trusted a century later by artisans who never met the authors of the plan. I suggested in the second paragraph of Section 1.2 that their confident design methods were based on education that included model testing. The same properties of soil grain aggregates that lie behind the simple OCC equation (shown on the front cover) also lie behind the success of geotechnical centrifuge model tests. Aggregates are not perfectly scaled in models. No one yet knows exactly how sand grains interact with each other in a slope at repose such as is shown on the back cover. In any model the aggregate of individual soil grains depends on lines of highly stressed grains to transmit forces. Each grain has experienced many previous unstable events. When lines buckle each grain moves in ways that are affected by the weights of grains, by the energy released in buckling, and by the local geometry of grains. Whatever is happening among those grains the success of centrifuge tests confirms that Critical State teaching places 'the theory of earth pressure on a true foundation' (in Reynolds' words).

I have explained in the pages of this book that a true cohesion governed by the adhesion of absorbed water films around soil grains is not proved to be applicable in the Mohr–Coulomb equation, and it is not proved that (on the wet side of the CS) contractive soil liquefies. If there were any true cohesion on the dry side of the CS line, it would also be seen on the wet side, but the OCC model for Rankine's aggregate of grains with no adhesion works there. Figure 63 shows plastic compression and yielding with CS friction as predicted by the OCC model fitting the data of equilibrium after creep. The CS concept and the OCC model give a better insight into soil behaviour than the Mohr–Coulomb hypothesis (Schofield, 2000). Geotechnical engineers should prepare themselves to work within a civil engineering industry that knows that there are fundamental errors in the soil mechanics that Terzaghi and Casagrande at Harvard University, and Skempton and Bishop at Imperial College, and their colleagues, taught their students.

Amontons observed a sliding friction force independent of the slip plane contact area, and only dependent on σ', with a coefficient of friction μ of about one-third for well-lubricated surfaces. He formulated the asperity theory that Coulomb learned, from Professor Bossut in the Mézières engineering school and from Bélidor's engineering textbook. This theory was still taught in Paris at the École Polytechnique in the 19th century using the edition of Bélidor revised by Navier. This 18th-century asperity theory can only apply to resistance to an initial motion, not to steady sliding. Coulomb also learned from the physics textbook of Musschenbroek that a component of strength due to cohesion or adhesion acts when a solid body separates into two parts, either in tension or shear. He questioned these theories and his experiments found these theories were not true. Intact rock strength in tension did give a safe approximate value for rock strength in shear, but as a designer he made the prudent assumption that all soil is newly disturbed with no cohesion. Gouge material on a slip surface may dilate and reach CS strength and density with quite small slip displacements.

Casagrande envisaged a critical porosity such that loose grains at higher than critical porosity will show a decrease of volume. Taylor made experiments on dense sand in which he rediscovered Amontons' interlocking on the dry side of

the CS. Terzaghi did not notice that the dense clay shear box test data of his research student Hvorslev showed that there was a critical effective pressure such that there true cohesion and friction did not apply when a higher effective pressure acted. The OCC model of the behaviour of contractive aggregate represents what is observed in the yielding and plastic compression of soft silt and clay. Terzaghi suggested that newly disturbed reconstituted clay has a true cohesion that depends on the closeness of clay grains to each other, and a true friction that is less than the angle of repose of a heap of loose grains. His supposed cohesion on the dry side of the CS was not a true soil constant for a given porosity, but was an effect due to interlocking that applied up to and not above a critical effective pressure.

Thurairajah's analysis of his triaxial test data showed that the energy dissipated in the distortion of a stressed grain aggregate depends on the effective pressure (energy stored in grains is lost when a grain slips) and on the magnitude of the distortion increment. An isotropic grain aggregate with this dissipation function has states that are stable by Drucker's criterion. The plastic yielding of the aggregate in these states interposes states of ductile plastic compression shown in Fig. 55 between the line of critical states and the line of unstable isotropic compression under spherical effective pressure that replaces Casagrande's liquefied states. CS soil mechanics teaching follows Coulomb and Rankine. The OCC model shows soil aggregate behaving in the way that was found at Harvard University and in Vienna, with interlocking instability localized into a distinct slip plane on the dry side of the CS and with stable yielding on the wet side. The process of education and research that Terzaghi envisaged, and his Harvard soil mechanics teaching on 'true' cohesion and friction, and the teaching there by Casagrande on liquefaction, must be reappraised. This should lead to new laboratory tests and new observations in the field. Terzaghi spoke in his Conference at Harvard University of the need for geotechnical engineers to be *well grounded in mechanics*.

The work on CS concepts and the OCC model has made it clear that soil mechanics research needed continuity over much more than 50 years, rather than the very brief periods of Harvard and MIT research. Plastic design is an essential part of a well-grounded education. In their textbook, Schofield and Wroth explained the use of the undrained cohesion and drained friction parameters c_u and ϕ_d in plastic design based on disturbed soil strength rather than on peak strengths of undisturbed soil samples. Plastic design by student engineers based on CS strength can follow the principles of Coulomb and Rankine with a safety factor of 1.25. Model tests give insight into appropriate deformation mechanisms. The Frontispiece shows the importance of the effective pressure in the behaviour of a granular aggregate. If model tests at reduced scale are to be relied on, they require increased acceleration. The research effort and investment in geotechnical centrifuge modelling at Cambridge University has resulted in model test facilities and expertise that are within reach of every geotechnical engineer throughout the world.

Goodman (1999) wrote that, after investigation of ground conditions for the design of construction works, Terzaghi was constantly vigilant to detect nuances in new information from a site about ground conditions; he needed equal vigilance to realize the significance of new theories of soil behaviour, and new mathematical

formulation and experimental validation of ways to solve problems; strain compatibility equations had to be introduced if Eqns (9) and (10) replaced Eqn (2). To Terzaghi, the possibility of the successful mathematical treatment of problems involving soils appeared very limited, and small-scale model tests were 'utterly futile', but time has passed since Terzaghi recommended a shift of the centre of gravity of research from the study and the laboratory into the construction camp. Laboratory geotechnical centrifuge modelling, digital modelling by numerical methods, and field observational methods are all available as research methods that can correct soil mechanics errors. Small model tests in advance of construction and observations during it have proved useful in the development of understanding of the geotechnical processes in which engineers are involved. In early stages of design, much smaller amounts of soil are available for testing than are accessible when construction begins; if unexpected problems arise, large blocks of undisturbed soil can be obtained and tested in a geotechnical centrifuge. The creation of centrifuge test facilities, and publications of the ISSMGE TC2, provide the possibility of such tests giving new physical insights to engineers who face the challenge of geotechnical engineering in the 21st century. Soil mechanics knowledge learned by civil engineers during 300 years must not be forgotten, but engineers must review the changes in basic thinking on soil strength in the past 300 years, not changing every plastic design calculation that came down to us from Coulomb and Rankine but making a rational choice of the soil properties to be used in them. Any engineer should bring structural material into a tough and ductile state as far as is possible. A plastic analysis on a CS basis will emphasize the benefits of ductility in geotechnical structures. *True cohesion* now has significance only in respect of the historic misinterpretation of Hvorslev's data. Rankine (1874) wrote:

> *Earthwork gives way by the slipping or sliding of its parts on each other; and its stability arises from resistance to the tendency to slip. In solid rock, that resistance arises from the elastic stress of the material, when subjected to a shearing force; but in a mass of earth, as commonly understood, it arises partly from the friction between the grains, and partly from their mutual adhesion; which latter force is considerable in some kinds of earth, such as clay, especially when moist.*

> *But the adhesion of earth is gradually destroyed by the action of air and moisture, and of the changes of the weather, and of alternate frost and thaw; so that its* friction is the only force which can be relied upon to produce permanent stability... *The temporary additional stability, however, which is produced by adhesion, is useful in the execution of earthwork, by enabling the side of a cutting to stand for a time with a vertical face for a certain depth below its upper edge. That depth is greater the greater the adhesion of the earth as compared with its heaviness; but diminished by excessive wetness.*

References

Amontons, G. (1699) De la résistance causée dans les machines, tant la frottements des parties qui les composent, que le roideur des Corde qu'on employe, et la maniere de calculer l'un et l'autre. *Histoire de l'Académie Royale des Sciences*, **206** (published 1702).

Avgerhinos, P. J. and Schofield, A. N. (1969) Drawdown failures of centrifuged models. In *Proceedings of the 7th International Conference of the SMFE*, Vol. 2, pp. 59–64.

Baker, B. (1881) The actual lateral pressure of earthworks. *Minutes of the Proceedings, Institution of Civil Engineers*, Vol. 3, pp. 140–186.

Baker, J. F. (1954) Plasticity as a factor in the design of war-time structures. *Civil Engineer in War*, **3**, Institution of Civil Engineers.

Baker, J. F., Horne, M. R. and Heyman, J. (1956) *The Steel Skeleton*, Vols I and II. *Elastic and Plastic Behaviour and Design*. Cambridge University Press, Cambridge.

Beedle, L. S. (1968) *Engineering Plasticity*. Cambridge University Press, Cambridge.

Bélidor, B. F. de (1737) *Architecture Hydraulique*. Jombert, Paris.

Bishop, A. W. (1954) The use of pore pressure coefficients in practice. *Géotechnique*, **4**, 148–152.

Bishop, A. W. and Henkel, D. J. (1957) *The Measurement of Soil Properties in the Triaxial Test*, 1st edn. Edward Arnold, London.

Bishop, A. W. and Henkel, D. J. (1962) *The Measurement of Soil Properties in the Triaxial Test*, 2nd edn. Edward Arnold, London.

Bossut, M. l'Abbé (1772) *Du Frottement. Traité Elementaire de Méchanique Statique*, I. Paris.

Boussinesq, J. (1874) *Annales des Pont et Chaussées: Memoires et Documents*, 5 Série, Vol. VII, 2nd Semestre, pp. 169–187.

Bowden, F. P. and Tabor, D. (1973) *Friction: An Introduction to Tribology*. Heinemann, London.

Calladine, C. R. (1963) Correspondence. *Géotechnique*, **13**, 250–255.

Casagrande, A. (1936) Characteristics of cohesionless soils affecting the stability of slopes and earth fills. *Journal of the Boston Society of Civil Engineers*, **23**, 13–32.

Casagrande, A. (1975) Liquefaction and cyclic deformation of sands, a critical review. In: *Proceedings of the 5th Pan-American Conference on Soil Mechanics and Foundation Engineering, Buenos Aires*. Reprinted as Harvard Soil Mechanics Series, No. 88, 27pp (1976).

Casagrande, A. and Albert, S. G. (1932) *Research on the shearing resistance of soils*. Published by the authors, Cambridge, Mass.

Coulomb, C. A. (1773) Essai sur une application des regeles de maximis et minimis a quelques problemes de statique, relatifs a l'architecture. *Mémoires de Mathématique et de Physique*, **7**, 343–382.

Coulomb, C. A. (1781) Theorie des machines simples. *Mémoires de Mathématique et de Physique*, **10**, 161–332.

Couplet, P. (1726) De la poussée des terres contre leurs revestmens, etude la force des revestemens qu'on leur doit oppser. *Histoire de l'Académie Royale des Sciences*.

Cundall, P. A. and Strack, O. D. L. (1979) A discrete numerical model for granular assemblies. *Géotechnique*, **29**, 47–65.

Dean, E. T. R., James, R. G., Schofield, A. N., Tan, F. S. C. and Tsukamoto, Y. (1993) The bearing capacity of conical footings on sand in relation to the behaviour of spudcan footings of jackups. In: *Predictive soil mechanics*. Thomas Telford, London, (eds) Houlsby, G. T. and Schofield, A. N., pp. 230–254.

Drucker, D. C. (1959) A definition of stable inelastic material. Transactions of the ASME. *Journal of Applied Mechanics*, **26:1**, 101–106.

Feynman, R. P., Leighton, R. B and Sands, M. (1965) *The Feynman Lectures on Physics*. Addison-Wesley (at Caltech I heard Feynman deliver early lectures of this course in 1963).

Florin, V. A. and Ivanov, P. L. (1961) Liquefaction of saturated sandy soils. In: *Proceedings of the 5th International Conference of the ISSMFE, Paris*, Vol. 1, pp. 107–111.

Goodman, R. E. (1999) *Karl Terzaghi: the engineer as artist*. ASCE Press, Reston, Virginia.

Haefeli, R. (1950) Investigation and measurements of the shear strengths of saturated cohesive soils. *Géotechnique*, **2**, 186–208.

Haigh, S. K. (2002) Effects of earthquake-induced liquefaction on pile foundations in sloping ground. PhD thesis, University of Cambridge.

Hazen, A. (1920) Hydraulic-fill dams. *Transactions of the ASCE*, 1713–1745.

Henkel, D. J. (1956) Discussion. *Proceedings of the Institution of Civil Engineers*, *Part II*, **5**, 230–233.

Heyman, J. (1995) *The Stone Skeleton*. Cambridge University Press.

Heyman, J. (1972) *Coulomb's Memoir on Statics: An Essay in the History of Civil Engineering*. Cambridge University Press, Cambridge (reprinted 1999, Imperial College Press, London).

Hird, C. C. (1974) Centrifugal model tests of flood embankments. PhD thesis, University of Manchester.

Hvorslev, M. J. (1937) Uber die Festigkeitseigenshaften gestörter bindiger Böden. *Ingenior-videnskabelige Skrifter*, *A*, **45**.

Jeffreys, H. (1931) *Cartesian Tensors*. Cambridge University Press, pp. 248–250.

Lacasse, S., Goulois, A., Robberstad, L., Andersen, E. and Boisard, P. (1991) The foundation of the Frigg CDP1 structure: a case study. *22nd Offshore Technology Conference, OTC 6512, Houston, Texas*, pp. 125–131.

Lawrence, D. M. (1980) Some properties associated with kaolinite soils. MPhil thesis, University of Cambridge.

Ledbetter, R. H., Steedman, R. S., Schofield, A. N., Corte, J. F., Perdriat, J., Nicolas-Font, J. and Voss, H. M. (1994) US Army's engineering centrifuge: design. In: *Centrifuge 94*. Balkema, Rotterdam, (eds) Leung, C. F., Lee, F. H. and Tau, T. S., pp. 63–68.

Lee, F. H. and Schofield, A. N. (1988) Centrifuge modelling of sand embankments and islands in earthquakes. *Géotechnique*, **38**, 45–58.

Leslie, J. (1804) *An Experimental Inquiry into the Nature and Propagation of Heat*. London.

Love, A. E. H. (1927) *A treatise on the mathematical theory of elasticity (4th edn)*. Cambridge University Press.

Lyndon, A. (1972) Centrifugal model test of a natural clay slope failure. PhD thesis, University of Manchester.

Lyndon, A. and Schofield, A. N. (1970) Centrifugal model test of a short-term failure in London Clay. *Géotechnique*, **20**, 440–442.

Malushitsky, Yu. N. (1981) *The Centrifugal Model Testing of Waste Heap Embankments*, translated from Russian. Cambridge University Press, Cambridge.

Merriman, T. (1939) Communication in a War Department Corps of Engineers, US Army Report on the slide of a portion of the upstream face of the Fort Peck Dam, Fort Peck, Mont. US Government. Printing Office, Washington.

Muhunthan, B. and Schofield, A. N. (2000) Liquefaction and Dam Failures. In: *Slope Stability 2000*, Geotechnical Special Publication No. 101, Proceedings of sessions of Geo-Denver 2000, ASCE Press, Reston, Virginia.

Musschenbroek, P. Van (1729) *Physicae Experimentales, et Geometricae, . . . Dissertationes*. Leyden.

Navier, C.-L. M. H. (1819) *Architecture Hydraulique*. Firmin Didot, Paris (new edition of Bélidor, 1737).

Padfield, C. J. (1978) The stability of river banks and flood embankments. PhD thesis, University of Cambridge.

Parry, R. H. G. (1959) Correspondence on 'On the yielding of soils'. *Géotechnique*, **8**, 184–186.

Penman, A. D. M. (1953) Shear characteristics of a saturated silt, measured in triaxial compression. *Géotechnique*, **3**, 312–328.

Pokrovsky, G. I. and Feodorov, I. S. (1936) Studies of soil pressures and deformations by means of a centrifuge. In: *Proceedings of the 1st International Conference of the ISSMFE, Harvard*, Vol. I, p. 70.

Rankine, W. J. M. (1857) On the stability of loose earth. *Philosophical Transactions of the Royal Society*, **47**, 9–27.

Rankine, W. J. M. (1858) *A Manual of Applied Mechanics*. Charles Griffin, London.

Rankine, W. J. M. (1874) *A Manual of Civil Engineering*, 10th edn. Charles Griffin, London.

Reynolds, O. (1885) On the dilatancy of media composed of rigid particles in contact. With experimental illustrations. *The London, Edinburgh and Dublin Philosophical Magazine and Journal of Science*, Vol. XX, 5th Series, pp. 469–481.

Reynolds, O. (1902) *On an Inversion of Ideas as to the Structure of the Universe. Rede Lecture*. Cambridge University Press, Cambridge.

Roscoe, K. H. (1950) Proceedings of the Conference on the measurement of shear strength of soils in relation to practice. Closing session discussion. *Géotechnique*, Vol. II, No. 2.

Roscoe, K. H. (1953) An apparatus for the application of simple shear to samples. In: *Proceedings of the 3rd International Conference of the ISSMFE, Zurich*, Vol. 1, pp. 186–191.

Roscoe, K. H. and Burland, J. B. (1969) On the generalized stress-strain behaviour of 'wet' clay. In: *Engineering Plasticity*. Cambridge University Press, Cambridge, (eds) Heyman, J. and Leckie, F. A.

Roscoe, K. H. and Schofield, A. N. (1963) Mechanical behaviour of an idealised 'wet-clay'. In: *Proceedings of the European Conference on SMFE, Wiesbaden*, pp. 47–54.

Roscoe, K. H., Schofield, A. N. and Wroth, C. P. (1958) On the yielding of soils. *Géotechnique*, **8**, 22–53.

Roscoe, K. H., Schofield, A. N. and Thurairajah, A. H. (1963) Yielding of soils in states wetter than critical. *Géotechnique*, **13**, 211–240.

Schofield, A. N. (1957) TRL Overseas Bulletins, No. 3. *Lime stabilisation of nodular clayey pea-laterite in Nyasaland*, No. 4. *The use of aerial photographs in road construction in Nyasaland*, No. 5. *Nyasaland laterites and their indications on aerial photographs*.

Schofield, A. N. (1960) The development of lateral force during the displacement of soil by the vertical face of a rotating model foundation. PhD thesis, University of Cambridge.

Schofield, A. N. (1961) The development of lateral force of sand against the vertical face of a rotating model foundation. In: *Proceedings of the 5th International Conference of the ISSMFE, Paris*, Vol. 1, pp. 479–484.

Schofield, A. N. (1966) Archiving Cambridge teaching. A facsimile of my 1966 notes for the Lent term (available at http://www2.eng.cam.ac.uk/˜ans).

Schofield, A. N. (1980) Cambridge geotechnical centrifuge operations. Rankine Lecture. *Géotechnique*, **30**, 225–268.

Schofield, A. N. (1982) Dynamic and earthquake geotechnical centrifuge modeling. In: *Proceedings of an International Conference on Recent Advances in Geotechnical Earthquake Engineering and Soil Dynamics, University of Missouri at Rolla, Rolla*, Vol. 3, pp. 1081–1100.

Schofield, A. N. (1995) Foreword. In: Taylor, R. N. (ed.), *Geotechnical Centrifuge Technology*. Chapman and Hall, London.

Schofield, A. N. (1998a) The Mohr Coulomb error. *Ground Engineering*, **31**, 30–32.

Schofield, A. N. (1998b) Centrifuge development can correct soil mechanics errors. In: *Centrifuge 98*, Balkema, Rotterdam, pp. 923–929.

Schofield, A. N. (1998c) The Mohr Coulomb error. *Colloque*, *Mechanique et Scientifique*, *Jubil. Scientifique de Pierre Habib*, 19 May.

Schofield, A. N. (1999) A note on Taylor's interlocking and Terzaghi's true cohesion error. *Geotechnical News*, Dec., 56–58.

Schofield, A. N. (2000) Behaviour of a soil paste continuum. In: *Developments in Theoretical Geo-mechanics*, *The John Booker Memorial Symposium*, Balkema, Rotterdam, pp. 253–266.

Schofield, A. N. (2001) Re-appraisal of Terzaghi's soil mechanics. Special lecture. In: *15th International Conference on Soil Mechanics and Geotechnical Engineering Conference*, *Istanbul*.

Schofield, A. N. and Taylor, R. N. (1988) Development of standard geotechnical centrifuge operations. In: *Centrifuge 88*. Balkema, Rotterdam, (ed.) Corté, J-F., pp. 29–32.

Schofield, A. N. and Togrol, E. (1966) Casagrande's concept of critical density, Hvorslev's equation for shear strength, and the Cambridge concept of critical states of soil. *Bulletin of the Technical University of Istanbul*, **16**, pp. 39–56.

Schofield, A. N. and Wroth, C. P. (1968) *Critical State Soil Mechanics*. McGraw Hill, Maidenhead. (See http://www-civ.eng.cam.ac.uk/geotech_new/geotech.htm)

Seed, H. B., Leps, T. M., Duncan, J. M. and Bieber, R. E. (1976) *Hydraulic fracturing and its possible role in the Teton Dam failure*. Appendix D of Report to U.S. Dept. of the Interior and State of Idaho on Failure of Teton Dam by Independent Panel to Review the Cause of Teton Dam Failure, December, pp. D1–D39.

Shibata, T. (1963) On the volume changes of normally-consolidated clays. In: *Disaster Prevention Research Institute Annuals*. Kyoto University, Kyoto, pp. 128–134 (in Japanese).

Skempton, A. W. (1950) *Pore Pressure and Suction in Soils*. Butterworth, London.

Skempton, A. W. (1954) The pore-pressure coefficients A and B. *Géotechnique*, **4**, 143–147.

Skempton, A. W. (1977) Slope stability of cuttings in brown London clay. In: *Proceedings of the 9th International Conference of Soil Mechanics and Foundation Engineering, Tokyo*, pp. 261–270.

Skempton, A. W. and Northey, R. D. (1953) The sensitivity of clays. *Géotechnique*, **3**, 30–53.

Skempton, A. W. and Petley, D. J. (1968) The strength along structural discontinuities in stiff clays. In: *Proceedings of Geotech. Conf., Oslo*, Vol. 2, pp. 29–46.

Sokolovsky, V. V. (1960) *Statics of Soil Media*. Butterworth, London.

Swain, G. F. (1882) Mohr's graphical theory of earth pressure. *Journal of the Franklin Institute*, **64**, 241–251.

Taylor, D. W. (1948) *Fundamentals of Soil Mechanics*. John Wiley, New York.

Terzaghi, K. (1936) A fundamental fallacy in Earth pressure computations. *Journal of the Boston Society of Civil Engineers*, **23**, 13–32.

Terzaghi, K. (1943) *Theoretical Soil Mechanics*. John Wiley, New York.

Terzaghi, K. (1956) Correspondence on the 'Physico-chemical analysis of the compressibility of pure clays' by G. H. Bolt. *Géotechnique*, **6**, 191–192.

Terzaghi, K. and Peck, R. B. (1948) *Soil mechanics in Engineering Practice*. John Wiley, New York.

Thompson, W. J. (1962) Some deformation characteristics of Cambridge Gault clay. PhD thesis, University of Cambridge.

Thurairajah, A. H. (1961) Some properties of kaolin and of sand. PhD thesis, University of Cambridge.

Tsukamoto, Y. (1995) Drum centrifuge tests of three-leg jack-ups on sand. PhD thesis, University of Cambridge.

Wood, D. M. (1976) Shear testing of soil. In: *Offshore soil mechanics*. George, P. and Wood, D. M. (eds). University of Cambridge Engineering Department and Lloyds Register of Shipping. Figs 41–44 with permission of the author.

Index

Note: page numbers in *italics* refer to Figures.